



University of Kentucky
UKnowledge

Theses and Dissertations--Microbiology,
Immunology, and Molecular Genetics

Microbiology, Immunology, and Molecular
Genetics


2017

THERAPEUTIC POTENTIAL OF TARGETING REACTIVE OXYGEN SPECIES (ROS) STRESS IN MYELODYSPLASTIC SYNDROME (MDS)

Karine Z. Oben

University of Kentucky, nkz86@yahoo.com

Author ORCID Identifier:

 <http://orcid.org/0000-0003-0195-7253>

Digital Object Identifier: <https://doi.org/10.13023/ETD.2017.011>

[Right click to open a feedback form in a new tab to let us know how this document benefits you.](#)

Recommended Citation

Oben, Karine Z., "THERAPEUTIC POTENTIAL OF TARGETING REACTIVE OXYGEN SPECIES (ROS) STRESS IN MYELODYSPLASTIC SYNDROME (MDS)" (2017). *Theses and Dissertations--Microbiology, Immunology, and Molecular Genetics*. 12.

https://uknowledge.uky.edu/microbio_etds/12

This Doctoral Dissertation is brought to you for free and open access by the Microbiology, Immunology, and Molecular Genetics at UKnowledge. It has been accepted for inclusion in Theses and Dissertations--Microbiology, Immunology, and Molecular Genetics by an authorized administrator of UKnowledge. For more information, please contact UKnowledge@lsv.uky.edu.

STUDENT AGREEMENT:

I represent that my thesis or dissertation and abstract are my original work. Proper attribution has been given to all outside sources. I understand that I am solely responsible for obtaining any needed copyright permissions. I have obtained needed written permission statement(s) from the owner(s) of each third-party copyrighted matter to be included in my work, allowing electronic distribution (if such use is not permitted by the fair use doctrine) which will be submitted to UKnowledge as Additional File.

I hereby grant to The University of Kentucky and its agents the irrevocable, non-exclusive, and royalty-free license to archive and make accessible my work in whole or in part in all forms of media, now or hereafter known. I agree that the document mentioned above may be made available immediately for worldwide access unless an embargo applies.

I retain all other ownership rights to the copyright of my work. I also retain the right to use in future works (such as articles or books) all or part of my work. I understand that I am free to register the copyright to my work.

REVIEW, APPROVAL AND ACCEPTANCE

The document mentioned above has been reviewed and accepted by the student's advisor, on behalf of the advisory committee, and by the Director of Graduate Studies (DGS), on behalf of the program; we verify that this is the final, approved version of the student's thesis including all changes required by the advisory committee. The undersigned agree to abide by the statements above.

Karine Z. Oben, Student

Dr. Subbarao Bondada, Major Professor

Dr. Ken Fields, Director of Graduate Studies

THERAPEUTIC POTENTIAL OF TARGETING REACTIVE OXYGEN SPECIES
(ROS) STRESS IN MYELODYSPLASTIC SYNDROME (MDS)

DISSERTATION

A dissertation submitted in partial fulfillment of the requirements for the degree of
Doctor of Philosophy in the College of Medicine at the University of Kentucky

By

Karine Zinkeng Oben

Lexington, Kentucky

Director: Subbarao Bondada

Lexington, Kentucky

Copyright © Karine Zinkeng Oben 2017

ABSTRACT OF DISSERTATION

THERAPEUTIC POTENTIAL OF TARGETING REACTIVE OXYGEN SPECIES (ROS) STRESS IN MYELODYSPLASTIC SYNDROME (MDS)

Myelodysplastic syndromes (MDS) are a diverse group of clonal hematologic disorders characterized by ineffective blood cell production (hematopoiesis), dysplastic (abnormal) cell morphology in one or more hematopoietic lineages, and progression to acute myeloid leukemia (AML). The response rate to current FDA approved therapies is low and not durable. Just about 50% of MDS patients respond to these drug therapies and a majority of responders relapse within 2-3 years. Hence there is a compelling need to investigate new therapy options.

We investigated the anticancer potential and possible underlying molecular mechanisms of action of a plant-derived compound, Withaferin A (WFA) in MDS. We utilized the MDS-L cell line model to test the efficacy of WFA both *in vitro* and *in vivo*. WFA exhibited potent but selective cytotoxicity to MDS-L cells as seen by a dose-dependent decrease in cell viability of these cells when treated with WFA whereas WFA had no apparent significant effect on the viability of normal primary human bone marrow cells. In addition, WFA significantly reduced engraftment of MDS-L cells in a xenotransplantation model. Through the use of microarray gene expression analysis, we identified that reactive oxygen species (ROS)-activated JNK/AP-1 signaling is a major pathway mediating apoptosis of MDS-L cells by WFA. Increase in ROS plays a central role in the cytotoxicity of WFA in MDS-L cells. Consistent with the finding that increase in ROS plays a central role in mediating WFA cytotoxicity in MDS-L cells, WFA did not increase ROS levels in normal bone marrow cells.

Taken together, these results suggest that pharmacologic manipulation of redox biology could be exploited to selectively target malignant cells while sparing normal cells in MDS.

KEYWORDS: Myelodysplastic syndrome (MDS), MDS-L cells, Withaferin A (WFA), reactive oxygen species (ROS), JNK signaling

Karine Zinkeng Oben

Student's Signature

Date

THERAPEUTIC POTENTIAL OF TARGETING REACTIVE OXYGEN SPECIES
(ROS) STRESS IN MYELODYSPLASTIC SYNDROME (MDS)

By

Karine Zinkeng Oben

Subbarao Bondada

Director of Dissertation

Ken Fields

Director of Graduate Studies

Date

I dedicate this dissertation to God Almighty and my loving family

ACKNOWLEDGEMENTS

It is often said an opportunity is the first step to success. I want to express my sincere gratitude to my PhD mentor Dr. Subbarao Bondada, first and foremost for giving me the opportunity to work with him and for his patience and guidance through a mostly challenging process. My deepest thanks to my advisory committee members: Dr. Alan Kaplan, Dr. Brett Spear, Dr. Donald Cohen and Dr. Ying Liang for their invaluable guidance, feedback and encouragement throughout my dissertation work. Special thanks to Dr. Daret St. Clair for not only agreeing to be my external examiner but also for providing feedback and ideas on my projects.

My deepest thanks to the current and past members of the lab: Ms. Sara Alhakeem, Ms. Mary Kathryn Mckenna, Ms. Beth Gachuki, Dr. Sunil Nooti, and Dr. Latha Muniappan. I could not have asked for a better group of people to work with closely. You all provided an environment in which I could think out loud without fear of judgement. I would never have gone through this program without your relentless support and willingness to help me. You have become family and I can only pray that God blesses you all abundantly. For Latha who passed to glory too soon, I pray that God may rest her gentle soul in peace.

I am truly indebted to Dr. Greg Bauman and Ms. Jennifer Strange in the flow cytometry facility for their kindness and devotion. Many thanks also go to the Combs Research Building family for providing a friendly work environment. I would also like to thank the Department of Microbiology, Immunology and Molecular Genetics family for providing a friendly environment. I extend sincere gratitude to Dr. Jason Anthony Brandon for selflessly helping to perform intravenous tail vein injections for animal experiments. Special thanks go to Dr. Beth A Garvy and Ms. Kate Fresca (mother to all MIMG graduate students) for always going the extra mile to make the graduate student experience as smooth as possible.

Support from my friends, Dr. Yvonne Fondufe-Mittendorf, Grant Jones, Maria Dixon, Marti Ward, Teresa Noel, Hye-in Jing and Smita Joshi has been invaluable. It has been a huge honor, privilege and blessing to be surrounded by such beautiful people whom I could always count on.

I would not have completed graduate school without the support from my family. I want to thank my family in Cameroon: my dad Martin Zinkeng, mom Justine Zinkeng, siblings Javis, Bleris, Stephanie and Michael, my only surviving grandparent Agnes Mbeboh and all of my extended family. You have loved me unconditionally and cheered me on even through the unacceptable long periods

of silence when I avoided communication with you all. I love you all and thank you for your patience during all these years. I am grateful to my dear brothers George, Venant, Anye, Penn and Leonard, who saw my pains and struggles firsthand. Thank you for your love and support especially during frustrating times. You always endeavored to put a smile on my face. I will remain forever grateful. I am equally indebted to my second family - my in-laws especially mummy Rose Oben and Barbra Fobi. Your love and encouragement mean the world to me.

Most importantly, I want to thank the other half of me, my husband Walter N Oben. These past years have been admittedly challenging for us but your love, support, understanding, positive attitude and gentle spirit pushed us through. Your commitment and pride in my success gave me strength.

Above all else, I am grateful to God Almighty who made it all possible.

TABLE OF CONTENTS

ACKNOWLEDGEMENTS.....	iii
LIST OF TABLES	viii
LIST OF FIGURES	ix
CHAPTER ONE.....	1
INTRODUCTION.....	1
CLINICAL FEATURES, PATHOGENESIS AND DIAGNOSIS OF MDS	2
EPIDEMIOLOGY, INCIDENCE AND PROGNOSIS OF MDS.....	7
WITHAFERIN A (WFA).....	10
REACTIVE OXYGEN SPECIES (ROS)	12
EFFECTS OF ROS.....	14
ROS AND CELL CYCLE PROGRESSION	16
ROS AND JNK-MEDIATED APOPTOTIC SIGNALAING.....	17
ROS IN CANCER	20
STUDY MODEL AND OBJECTIVES	21
CHAPTER 2	23
MATERIALS & METHODS.....	23
2a) Cell Culture	23
2b) Reagents	24
2c) MTT and Trypan Blue Dye Exclusion Cell Viability Assays.....	25
2d) Effect of WFA on MDS-L Engraftment in vivo	25
2e) Staining and identification of bone marrow stem cells	27
2f) Annexin-V Apoptosis Assay.....	27
2g) NF- κ B Nuclear Translocation by Immunocytofluorescence	28
2h) Immunoblotting	28
2i) Affymetrix Microarray Analysis.....	30
2j) Quantitative Real-Time PCR (qRT-PCR)	31
2k) Mitochondrial Membrane Potential by JC-1	33
2l) ROS Measurement	33
2m) AP-1 Luciferase Assay	34
2n) Cell Cycle Analyses.....	35
2o) Statistical Analysis	35

CHAPTER 3	36
WFA has a potent but selective anti-proliferative effect on MDS-L cells <i>in vitro</i> and <i>in vivo</i>	36
3a) WFA effectively decreased viability of MDS-L cells in vitro.....	37
3b) WFA inhibited bone marrow engraftment of MDS-L cells in NSGS mice38	
3c) Cytotoxicity of WFA is selective to malignant cells.....	40
Summary.....	58
CHAPTER FOUR	59
Signaling pathways involved in WFA-induced apoptosis in MDS-L cells.....	59
4a) WFA significantly altered expression of genes linked to cell death and survival, cell growth and proliferation, cell cycle regulation and cancer	60
4b) WFA induced apoptosis of MDS-L cells.....	61
4c) WFA activated JNK MAPK signaling in MDS-L cells.....	62
4d) WFA arrested MDS-L cells at S and G2/M cell cycle phases	65
Summary.....	99
CHAPTER FIVE	100
Selective WFA-induced cytotoxicity to MDS-L cells is primarily mediated by increased ROS production	100
5a) JNK signaling plays a significant role in WFA apoptosis of MDS-L cells by WFA treatment.....	100
5b) WFA activated JNK signaling by increasing ROS production	101
5c) Inhibition of ROS production completely protected MDS-L cells from cytotoxicity by WFA treatment	102
Summary.....	122
CHAPTER SIX.....	123
Discussion.....	123
6a) Molecular mechanisms mediating apoptosis of MDS-L cells by WFA .	126
6b) Oxidative stress is a feasible biochemical alteration that can be exploited for selective treatment in MDS.....	129
6c) Model of cytotoxicity mechanisms of WFA in MDS.....	130
6d) Conclusion.....	131
APPENDIX A:.....	135
Licence permission from Nature Publishing Group to re-use figure from Leukemia.....	135

APPENDIX B:	139
COMPOSITION OF POLYACRYLAMIDE GELS.....	139
APPENDIX C:	141
LIST OF ABBREVIATIONS	141
References	145
VITA	155

LIST OF TABLES

Table 1.1 Morphologic abnormalities in myelodysplastic syndromes	2
Table 1.2 Chromosomal abnormalities presumptive of MDS.....	5
Table 1.3 Peripheral blood and bone marrow findings in MDS.....	6
Table 1.4 Three most common features of MDS.....	7
Table 1.5 Radical and non-radical oxygen metabolites produced at high concentrations in a living cell	14
Table 2.1 List of qRT-PCR Primers	32

LIST OF FIGURES

Figure 1.1 Hematopoietic Cell Hierarchy and Lineages	3
Figure 1.2 Structure of Withaferin A	12
Figure 1.3 Redox regulation of ASK1 activation	20
Figure 3.1 WFA significantly decreased the viability of MDS-L cells <i>in vitro</i>	41
Figure 3.2 WFA is substantially more cytotoxic to MDS-L cells compared to lenalidomide	43
Figure 3.3 Drug replenishment every 24 h is required to observe lenalidomide-induced cytotoxicity of MDS-L cells	45
Figure 3.4 The combined cytotoxic effects of WFA and lenalidomide are neither additive nor synergistic	47
Figure 3.5 WFA significantly decreased the viability of KG1 cells <i>in vitro</i>	48
Figure 3.6 Toxicity from combining radiation and WFA treatment is prevented by delaying WFA treatment	49
Figure 3.7 WFA significantly reduced engraftment of MDS-L cells in the bone marrow of NSGS mice	50
Figure 3.8 WFA treatment does not cause mouse bone marrow Suppression	54
Figure 3.9 WFA induced apoptosis of human primary MDS and AML bone marrow cells	55
Figure 3.10 WFA had no significant effect on the viability of normal primary bone marrow cells	57
Figure 4.1 Cytotoxic effects of WFA in MDS-L cells are independent of NF- κ B activation	67
Figure 4.2 Biological functions and/or diseases most significantly affected by WFA treatment in MDS-L cells	69
Figure 4.3 Heatmap of top 20 WFA regulated genes by fold change	72
Figure 4.4 Genes differentially regulated by WFA are linked to apoptosis Induction	73

Figure 4.5 WFA decreased mitochondrial membrane potential in MDS-L cells	75
Figure 4.6 WFA stimulated activation of caspase-3.....	78
Figure 4.7 WFA induced apoptosis of MDS-L cells	79
Figure 4.8 Up-regulated mRNA expression of BAG3 in MDS-L cells treated with WFA.....	81
Figure 4.9 WFA increased mRNA but not protein expression of RGS2 or p38 MAPK activation in MDS-L cells	82
Figure 4.10 Schematic representation of ROS mediated JNK/AP-1 signaling.....	84
Figure 4.11 WFA enhanced mRNA expression of c-Jun and FosB.....	85
Figure 4.12 WFA treatment increased ROS production in MDS-L cells	87
Figure 4.13 JNK MAPK signaling cascade is activated by WFA in MDS-L cells	89
Figure 4.14 WFA triggered AP-1 transcriptional activity in MDS-L cells	91
Figure 4.15 Induction of cell cycle arrest in WFA-treated MDS-L cells	94
Figure 4.16 mRNA and protein expression of cyclin A and CDK2 decrease with WFA treatment	95
Figure 4.17 mRNA and protein expression of cyclin B and CDK decrease with WFA treatment	97
Figure 5.1 JNK-IN-8 effectively inhibits JNK activation by WFA	103
Figure 5.2 Inhibition of JNK activity suppresses transcription of BIM induced by WFA.....	104
Figure 5.3 JNK activation contributes to p21 transcription in WFA-treated MDS-L cells	106
Figure 5.4 JNK-IN-8 substantially abrogates caspase-3 activation induced by WFA in MDS-L cells	108
Figure 5.5 SP600125 inhibits WFA-induced JNK activity	109

Figure 5.6 SP600125 suppresses activation of caspase-3 by WFA	110
Figure 5.7 WFA-induced JNK activation is inhibited by NAC.....	111
Figure 5.8 NAC inhibits JNK activity in WFA-treated MDS-L cells.....	112
Figure 5.9 WFA-induced AP-1 transcription is inhibited by NAC	113
Figure 5.10 Inhibition of ROS blocked BIM transcription in WFA-treated MDS-L cells	114
Figure 5.11 NAC abrogated WFA-induced p21 transcription.....	116
Figure 5.12 ROS inhibition completely abolished WFA-induced caspase-3 activation	118
Figure 5.13 NAC protects MDS-L cells from apoptosis by WFA Treatment	119
Figure 5.14 WFA does not increase ROS in normal primary bone marrow cells	121
Figure 6.1 Cytotoxicity mechanisms of WFA in MDS	134

CHAPTER ONE

INTRODUCTION

Myelodysplastic syndromes (MDS) are a diverse group of clonal hematologic disorders characterized by ineffective blood cell production (hematopoiesis), dysplastic (abnormal) cell morphology in one or more hematopoietic lineages, and progression to acute myeloid leukemia (AML)^{1,2}. Ineffective hematopoiesis leads to peripheral cytopenias such as anemia, neutropenia and thrombocytopenia³; anemia being the most commonly observed. In fact, more than 80% of MDS diagnosis are due to anemia-related symptoms which can manifest as fatigue, exercise intolerance, dizziness, cognitive impairment or an altered sense of well-being^{3,4}. Although less common, infection, easy bruising and bleeding are other clinical manifestations of MDS that can prompt hematologic evaluation and diagnosis³. The peculiar clinical phenotype of anemia in MDS is that it is chronic and worsens with time⁴. As a result, most MDS patients become transfusion dependent over the course of the disease⁵. Increased number and frequency of transfusions decreases overall quality of life and has been associated with a proportional increase in mortality. Organ complications from transfusion-related iron overload are thought to be related to the observed decrease in overall survival in transfusion dependent MDS patients^{4,5}.

CLINICAL FEATURES, PATHOGENESIS AND DIAGNOSIS OF MDS

Characteristic abnormal cell morphologies that can occur in MDS are outlined in Table 1.1. MDS diagnosis heavily relies on these characteristic morphologic changes³.

Table 1.1: Morphologic abnormalities in myelodysplastic syndromes

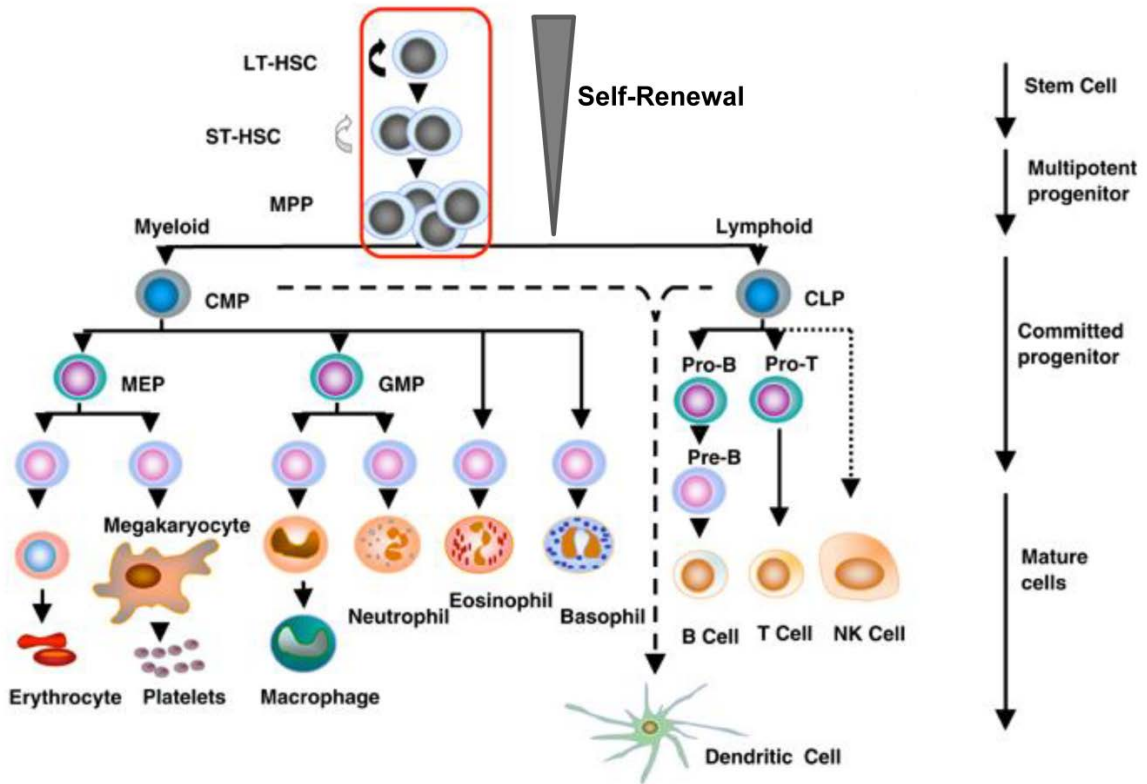
Lineage	Peripheral blood	Bone marrow
Erythroid	Ovalmacrocytes	Megaloblastoid erythropoiesis
	Elliptocytes	Nuclear budding
	Acanthocytes	Ringed sideroblasts
	Stomatocytes	Internuclear bridging
	Teardrops	Karyorrhexis
	Nucleated erythrocytes	Nuclear fragments
	Basophilic stippling	Cytoplasmic vacuolization
Myeloid	Pseudo Pelger-Huet anomaly	Multinucleation
	Auer rods	Defective granulation
	Hypogranulation	Maturation arrest at myelocyte stage
	Nuclear sticks	Increase in monocytoid forms
	Hypersegmentation	Abnormal localization of immature precursors
	Ringed-shaped nuclei	
Megakaryocyte	Giant platelets	Micromegakaryocytes
	Hypogranular or agranular platelets	Large mononuclear forms
		Hypogranulation
		Multiple small nuclei

Adapted from List AF, Sandberg AA, Doll DC. Myelodysplastic Syndromes. Wintrobe's Clinical Hematology, 12th edition, Greer JP (Ed), Lippincott Williams & Wilkins, Baltimore 2008.

The pathogenesis of MDS is not clearly understood but the presence of some healthy cells and involvement of both myeloid and lymphoid hematopoietic

cell lineages suggest that it is a clonal stem cell disease⁶. Hematopoietic cell hierarchy and lineages are illustrated in Figure 1.1. Observed hematopoietic cell defects in MDS span the gamut from reduced (erythrocyte, neutrophil, thrombocyte, CD4 T cell and NK cell) or increased (thrombocyte and CD8 T cell) numbers to defective function (phagocytosis, bactericidal activity, adhesion and chemotaxis of granulocytes, and antibody production by B cells)³.

Figure 1.1: Hematopoietic Cell Hierarchy and Lineages



Hematopoietic Stem Cell (HSC), Long-term repopulating HSC (LT-HSC), Short-term repopulating HSC (ST-HSC), Multipotent Progenitor (MPP), CMP Common Myeloid Progenitor (CMP), Common Lymphoid Progenitor (CLP), Megakaryocyte/Erythroid Progenitor (MEP), Granulocyte–Macrophage Progenitor (GMP).

Adapted from Larsson J and Karlsson S. The role of Smad signaling in hematopoiesis. *Oncogene* (2005) 24, 5676–5692

Some recent elegant studies have demonstrated the clonality and stem cell origin in MDS by integrating cellular hierarchy and cancer genetics. Mutations implicated in MDS occur in the stem cell compartment (founder clones) and new mutations are acquired with disease progression to AML (daughter subclones)^{7,8}. The malignant cells are clonally derived since all mutations found in founder clones were also present in the daughter subclones^{7,8}. These studies suggest that like most cancers, MDS pathogenesis involves a stepwise acquisition of driver mutations through multiple cycles of mutation. Greater than 90% of MDS cases are associated with one or more driver mutations and prognosis significantly worsens with increase in driver mutations^{3,9}. Genes involved in DNA methylation (*DNMT3A*, *TET2*, *IDH1/2*), chromatin modification (*EZH2*, *ASXL1*), transcriptional regulation (*EVI1*, *RUNX1*, *GATA2*) and RNA splicing (*SF3B1*, *U2AF1*, *SRSF2* and *ZRSR2*) are among the most commonly mutated genes⁹. Several cytogenetic abnormalities observed in MDS are outlined in Table 1.2 and are abnormalities used for presumptive diagnosis³.

Table 1.2: Chromosomal abnormalities presumptive of MDS diagnosis

-7/del(7q)
-5/del(5q)
del(13q)
del(11q)
del(12q) or t(12p)
del(9q)
idic(X)q13
t(17p) (unbalanced translocations) or i(17q) (i.e, loss of 17p)
t(11;16)(q23;p13.3)
t(3;21)(q26.2;q22.1)
t(1;3)(p36.3;q21)
t(2;11)(p21;q23)
inv(3)(q21q26.2)
t(6;9)(p23;q34)

Adapted from Jon C Aster RMS. Clinical manifestations and diagnosis of the myelodysplastic syndromes. In: Richard A Larson AGR, ed. *UpToDate*. Online2016.
<https://www.uptodate.com/contents/clinical-manifestations-and-diagnosis-of-the-myelodysplastic-syndromes>

MDS is one of the most challenging myeloid neoplasms to diagnose¹⁰.

Heterogeneity in the subtypes of MDS adds a layer of complexity to the diagnostic process. The World Health Organization (WHO) classification system classifies MDS into 7 subtypes (Table 1.3)¹⁰. This classification system is based on a combination of morphology, immunophenotype and genetic features of peripheral blood and bone marrow, and clinical features¹⁰.

Table 1.3: Peripheral blood and bone marrow findings in MDS

Disease	Peripheral blood findings	Bone Marrow findings
Refractory cytopenia with unilineage dysplasia (RCUD): (refractory anemia[RA]; refractory neutropenia [RN]; refractory thrombocytopenia [RT])	Unicytopenia or bicytopenia* No or rare blasts (< 1%)†	Unilineage dysplasia: ≥ 10% of the cells in one myeloid lineage < 5% blasts < 15% of erythroid precursors are ring sideroblasts
Refractory anemia with ring sideroblasts (RARS)	Anemia No blasts	≥ 15% of erythroid precursors are ring sideroblasts Erythroid dysplasia only < 5% blasts
Refractory cytopenia with multilineage dysplasia (RCMD)	Cytopenia(s) No or rare blasts (< 1%)† No Auer rods < 1 x 10 ⁹ /L monocytes	Dysplasia in ≥ 10% of the cells in ≥ 2 myeloid lineages (neutrophil and/or erythroid precursors and/or megakaryocytes) < 5% blasts in marrow No Auer rods ± 15% ring sideroblasts
Refractory anemia with excess blasts-1 (RAEB-1)	Cytopenia(s) < 5% blasts† No Auer rods < 1 x 10 ⁹ /L monocytes	Unilineage or multilineage dysplasia 5% - 9% blasts† No Auer rods
Refractory anemia with excess blasts-2 (RAEB-2)	Cytopenia(s) 5% - 19% blasts‡ No Auer rods ± ‡ < 1 x 10 ⁹ /L monocytes	Unilineage or multilineage dysplasia 10% - 19% blasts‡ No Auer rods ± ‡
Myelodysplastic syndrome-unclassified (MDS-U)	Cytopenias <1% blasts†	Unequivocal dysplasia in < 10% of cells in one or more myeloid lineages when accompanied by a cytogenetic abnormality considered as presumptive evidence for a diagnosis of MDS (Table 1.2) < 5% blasts
MDS associated with isolated del(5q)	Anemia Usually normal or increased platelet count No or rare blasts (< 1%)	Normal to increased megakaryocytes with hypoblasted nuclei < 5% blasts Isolated del(5q) cytogenetic abnormality No Auer rods

*Bicytopenia may occasionally be observed. Cases with pancytopenia should be classified as MDS-U.

†If the marrow myeloblast percentage is 5% but there are 2% to 4% myeloblasts in the blood, the diagnostic classification is RAEB-1. Cases of RCUD and RCMD with 1% myeloblasts in the blood should be classified as MDS-U.

‡Cases with Auer rods and 5% myeloblasts in the blood and less than 10% in the marrow should be classified as RAEB-2. Although the finding of 5% to 19% blasts in the blood is, in itself, diagnostic of RAEB-2, cases of RAEB-2 may have 5% blasts in the blood if they have Auer rods or 10% to 19% blasts in the marrow or both. Similarly, cases of RAEB-2 may have 10% blasts in the marrow but may be diagnosed by the other 2 findings, Auer rod and/or 5% to 19% blasts in the blood.

Adapted from Vardiman JW, Thiele J, Arber DA, et al. The 2008 revision of the World Health Organization (WHO) classification of myeloid neoplasms and acute leukemia: rationale and important changes. *Blood*. 2009;114(5):937-951.

In addition to the heterogeneity of MDS, differential diagnosis involves exclusion of other conditions that may present with cytopenia and/or dysplasia such as AML³. AML is of particular interest in the differential diagnosis of MDS because it can occur as a continuum of disease with progression of MDS as the distinction between the two diseases is largely based on blast percentage¹⁰. The WHO

recommends 20% blast cells as a cut off between MDS and AML¹⁰. MDS diagnosis is based on the evaluation of peripheral blood and bone marrow smears³. Chromosomal abnormalities play a crucial role in diagnosis as they distinguish between MDS and AML and aid in the classification of MDS subtypes¹⁰. Three main features (Table 1.4) which present in most cases of MDS are used as guideline for diagnosis³.

Table 1.4: Three most common features of MDS

1	Otherwise unexplained quantitative changes in one or more of the blood and bone marrow elements (i.e, red cells, granulocytes, platelets). The values used to define cytopenia are: hemoglobin <10 g/dL (100g/L); absolute neutrophil count <1.8 x 10 ⁹ /L (<1800/μL); platelets <100 x 10 ⁹ /L (<100,000/μL). However, failure to meet the threshold for cytopenia does not exclude the diagnosis of MDS if there is definite morphologic evidence of dysplasia.
2	Morphologic evidence of significant dysplasia (ie, ≥10% of erythroid precursors, granulocytes, or megakaryocytes) upon visual inspection of the peripheral blood smear, bone marrow aspirate, and bone marrow biopsy in the absence of other causes of dysplasia (Table 1.1). In the absence of morphologic evidence of dysplasia, a presumptive diagnosis of MDS can be made in patients with otherwise unexplained refractory cytopenia in the presence of certain genetic abnormalities (Table 1.2).
3	Blast forms account for less than 20% of the total cells of the bone marrow aspirate and peripheral blood. Cases with higher blast percentages are considered to have acute myeloid leukemia (AML). In addition, the presence of myeloid sarcoma or certain genetic abnormalities, such as those with t(8;21), inv(16), or t(15;17), are considered diagnostic of AML, irrespective of the blast cell count.

Adapted from Jon C Aster RMS. Clinical manifestations and diagnosis of the myelodysplastic syndromes. In: Richard A Larson AGR, ed. *UpToDate*. Online2016.

EPIDEMIOLOGY, INCIDENCE AND PROGNOSIS OF MDS

MDS can occur *de novo* (classified as primary MDS) or after exposure to potentially mutagenic therapy (classified as secondary therapy-related MDS)¹¹. Therapy-related myelodysplastic syndrome (t-MDS) is thought to be a late complication that can occur after cytotoxic therapy (chemotherapy, radiotherapy, or both) for both malignant and non-malignant disease¹²⁻¹⁴. Although the

mechanism by which exposure to cytotoxic agents causes t-MDS remains unknown, t-MDS is a well-recognized clinical syndrome that is included in the classification of myeloid neoplasms by the World Health Organization (WHO)^{10,12,14,15}. Generally, 10-20% of diagnosed MDS cases are t-MDS¹⁶. Median latency from the time of initial cytotoxic therapy to t-MDS diagnosis can vary from 3 – 7 years^{13,14,17}. MDS is thought to be a disease of the elderly as the risk of MDS increases with age¹⁸. Reported median age of diagnosis varies by study cohort from 65 – 76 years and incidence is slightly significantly higher in males^{3,18-20}. Therapy-related MDS on the other hand can occur at any age as onset depends on the age of exposure to cytotoxic therapy^{14,21}. Although rare, pediatric MDS cases have also been reported^{22,23}.

The incidence of MDS in the United States is not known but conservative estimates suggest at least 30, 000 new cases occur annually^{18,24}. Several studies have demonstrated the actual incidence of MDS is likely higher than is predicted from cancer registries²⁴⁻²⁶. This is in part because MDS only became a reportable malignancy in 2001, long after the creation of the National Cancer Institute (NCI) cancer surveillance program in 1973^{24,27,28}. Moreover, because BM evaluation is required for definitive diagnosis, some cases go undiagnosed especially in older individuals who usually have other comorbidities^{24,25}. Survival of MDS patients is generally very poor. The response rate of current FDA approved therapies, azacitidine, decitabine and lenalidomide, is low and often not durable. Just about 50% of MDS patients respond to these drug therapies and a majority of responders relapse within 2-3 years^{27,29}. A follow up study of 5q MDS

patients found that achieving erythroid and cytogenetic responses on lenalidomide does not prevent progression to AML³⁰.

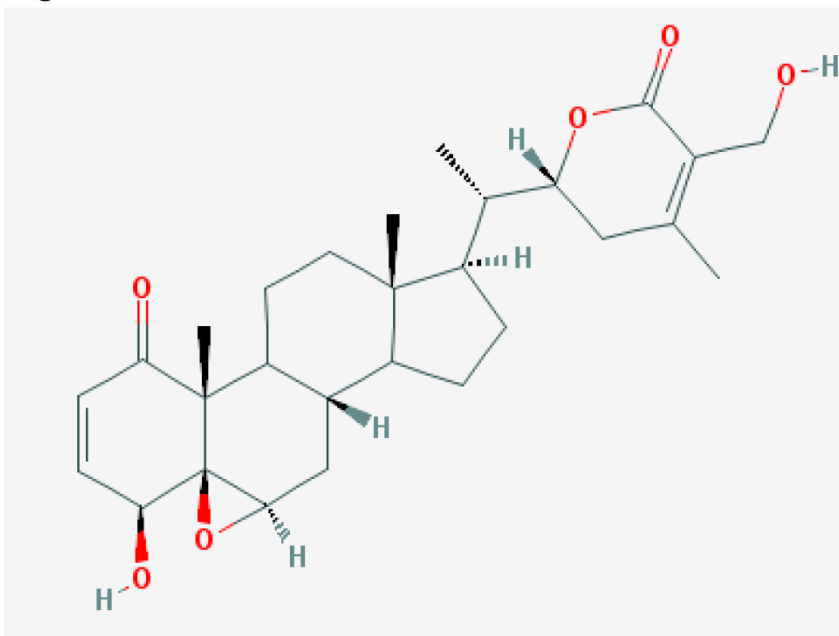
The prognosis of patients who do not respond to azacitidine or decitabine is even more abysmal with an overall survival of < 6 months³¹. Several cytogenetic abnormalities are observed in MDS but deletions or complete loss of chromosomes 5 and/ or 7 are the most commonly observed^{11,16}. The prognosis of patients with complete loss of chromosomes 5 and/ or 7 is significantly unfavorable compared to other karyotypes¹¹. It has been recognized for a long time that hematopoietic stem cell transplant (HSCT) is the only available potentially curative treatment for MDS but the use of HSCT for MDS remains low to date, < 10% of MDS patients are referred for HSCT^{20,31,32}. A study of 27 t-MDS cases found that all treatments but HSCT, were not effective for MDS resulting in 100% fatality in patients < 55 years¹⁷. Although potentially curative, HSCT treatment for MDS can fail in certain instances^{33,34}. Several factors, such as age and intensive preconditioning regimens could adversely impact the success of HSCT for MDS treatment³³. One study assessed the impact of age on the outcome of HSCT in cancer patients in general. They found a 2.24 fold increased risk of treatment related mortality in patients aged ≥ 50 years³⁵. This is particularly true for the older patients in whom age and comorbidities limit tolerability to intensive preconditioning HSCT treatments³¹. Given that current MDS treatments are mostly ineffective and the high risk of disease-related complications especially from anemia, there is an unquestionable need to investigate potential alternative therapeutic options for MDS.

WITHAFERIN A (WFA)

Although great advancements have been made in the treatment of cancer, toxicity is a major problem with most of the established chemotherapy drugs routinely used for cancer treatment³⁶. It is strongly believed that the use of plant derived compounds for cancer treatment could reduce adverse side effects because they are natural³⁶⁻³⁸. Withaferin A (WFA) is a plant-derived compound that has been shown to have potential in anticancer treatment³⁹. It is one of the most bioactive steroidal lactones (Figure 1.2) isolated from the winter cherry plant, *Withania somnifera*⁴⁰. *Withania somnifera*, also known as “Indian Ginseng” or “Indian Winter cherry” has been used in herbal formulations for centuries in Ayurvedic medicine for a wide range of ailments such as chronic fatigue, dehydration and rheumatism^{41,42}. Ayurvedic medicine is a traditional healthcare system which originated from India more than 3, 000 years ago that uses a variety of herbal compounds, special diets, exercise and lifestyle recommendations⁴³. WFA exhibits anticancer effects by targeting several processes known to promote cancer. Studies have demonstrated that WFA can inhibit cell proliferation, angiogenesis, metastasis, inflammation, and induce apoptosis in cancer model systems^{41,44}. The therapeutic potential of WFA in cancer is illustrated by the fact that it has been shown to have anticancer effects in several cancers including prostate, breast, cervical and pancreatic cancers, as well as melanoma and lymphoma^{44,45}. Although anticancer activities of WFA have been studied in several systems, the molecular mechanisms underlying these activities are not completely understood. In silico analysis identified

vimentin, IKK γ and Cdc37 as possible direct molecular targets of WFA⁴¹. Direct interactions of vimentin and IKK β with WFA have been demonstrated^{46,47}. There is also strong evidence suggesting WFA directly binds to heat shock protein 90 (Hsp90), a molecular chaperone which mediates the folding, assembly and maturation of client proteins such as the pro-survival protein AKT⁴⁸. WFA regulates the activity of several transcription factors and kinases but it is not known if this regulation is by direct or indirect mechanisms^{41,44}. WFA has also been shown to inhibit complex III activity in mitochondria but it was not investigated if a direct interaction occurred between the two molecules⁴⁹. It is now clear that WFA can target multiple pathways and the pathways targeted could be cell type specific^{44,50}. Therefore, the critical pathway for each system would need to be determined systematically. Some commonly reported mechanisms by which WFA inhibits proliferation and/ or induces apoptosis of cancer cells include induction of cell cycle arrest^{45,51-57}, inhibition of NF- κ B^{45,58-63}, and increased production of reactive oxygen species (ROS)^{49,62-66}.

Figure 1.2: Structure of Withaferin A



PubChem CID: 16760705

REACTIVE OXYGEN SPECIES (ROS)

ROS are a heterogeneous group of oxygen-containing species with highly reactive chemical properties^{67,68}. ROS exist in two flavors; radicals which contain one or more unpaired electron(s), and non-radical species which are equally reactive but lack unpaired electron (s) and can be converted to radical species⁶⁸. Examples of radical and non-radical ROS commonly seen in biological systems are listed in Table 1.5⁶⁹. There are both exogenous and endogenous sources of ROS. Some exogenous sources of ROS include γ -irradiation, UV irradiation, ultrasound, food, drugs, pollutants (e.g. car exhaust, cigarette smoke and industrial contaminants), xenobiotics, and toxins⁶⁹. There are multiple mechanisms by which cells produce ROS endogenously. Electron leakage from the mitochondrial respiratory chain is a major source of endogenous ROS

production^{68,70}. ROS can also be produced as a by-product of certain enzymatic reactions such as, catabolism of purines, fatty acid peroxidation, prostaglandin synthesis and detoxification reactions by cytochrome P450^{68,70}. Some enzymes are direct producers of ROS such as nitric oxide synthase which produces nitric oxide (NO·)⁶⁹. Phagocytic cells activated by recognition of an antigen undergo a series of reactions called the respiratory burst that is catalyzed by nicotinamide adenine dinucleotide phosphate-oxidase (NADPH-oxidase), which is another source of endogenous ROS production⁷¹.

Table 1.5: Radical and non-radical oxygen metabolites produced at high concentrations in a living cell

Name	Symbol
Oxygen radicals	
Oxygen (bi-radical)	\ddot{O}_2
Superoxide ion	O_2^-
Hydroxyl	$\cdot OH$
Peroxyl	$ROO\cdot$
Alkoxy	$RO\cdot$
Nitric oxide	$NO\cdot$
Non-radical oxygen species	
Hydrogen peroxide	H_2O_2
Organic peroxide	$ROOH$
Hypochlorous acid	$HOCl$
Ozone	O_3
Singlet oxygen	1O_2
Peroxynitrite	$ONOOH$

Adapted from Kohen R, Nyska A. Oxidation of biological systems: oxidative stress phenomena, antioxidants, redox reactions, and methods for their quantification. *Toxicologic pathology*. 2002;30(6):620-650.

EFFECTS OF ROS

Given that ROS are chemically reactive, they can react with cellular components such as lipids, proteins, carbohydrates and nucleic acids to cause tissue damage^{69,70}. The antioxidant defense system has evolved to counteract the damaging effects of ROS in body tissues⁷². Antioxidants act by direct and

indirect mechanisms to terminate oxidative chain reactions by deactivating already formed ROS and by preventing ROS generation⁷³. The antioxidant defense system consists of both enzymatic and non-enzymatic molecules⁷². Enzymatic antioxidants include superoxide dismutase (SOD), catalase (CAT), and glutathione peroxidase (GPx)^{70,72}. Ascorbic acid (Vitamin C), α -tocopherol (Vitamin E), carotenoids, flavonoids, uric acid, coenzyme Q, lipoic acid, and glutathione (GSH) are some non-enzymatic antioxidants known to play key roles in antioxidant defense mechanisms^{70,72}. GSH, a tripeptide of glutamine, cysteine and glycine, is ubiquitously expressed in all mammalian tissues and is thought to be the principal non-enzymatic antioxidant involved in antioxidant cellular defense⁷⁴. The importance of glutathione in redox metabolism is owed to its ability to perform multiple roles including: GSH directly scavenges free radicals and acts as a substrate for GPx during the detoxification of hydrogen peroxide and lipid peroxides; GSH is a co-factor of several enzymatic antioxidants; GSH is able to regenerate the active forms of non-enzymatic antioxidants, Vitamins C and E^{70,75}. Reduced glutathione (GSH) is converted to glutathione disulfide (GSSG-oxidized glutathione) in oxidative stress⁷⁴. Since glutathione is the major redox buffer of the cell, the relative amount of the reduced and oxidized forms (GSH/GSSG) is a good measure of oxidative stress or the redox state of an organism^{74,76}.

Paradoxically, physiological redox homeostasis favors mild oxidative stress because ROS have some useful roles⁷⁷. This means that the antioxidant defense must minimize ROS damage while allowing the useful effects of

ROS^{72,78}. ROS have a critical role in the immune response against pathogens; directly causing oxidative damage to phagocytosed pathogens or indirectly by activating a variety of innate and adaptive mechanisms for pathogen elimination⁷⁹. Studies have shown that ROS are also important anti-inflammatory and immunoregulatory molecules⁸⁰. ROS can regulate signal transduction pathways by activating kinases⁸¹ and transcription factors^{68,82}, and by modulation of intracellular calcium levels⁸³. Redox signaling is integrated into a variety of cellular processes such as: DNA damage response; antioxidant and anti-inflammatory responses; regulation of iron homeostasis; cell differentiation, metabolism and migration; cell proliferation; and apoptosis^{68,81,84}.

ROS AND CELL CYCLE PROGRESSION

There is overwhelming evidence suggesting that cell cycle progression and therefore cell proliferation is subject to redox control^{85,86}. It is now appreciated that the effect of ROS on cell cycle progression is influenced by multiple factors. The type, amount and location of ROS production, duration of ROS exposure, and the presence or absence of other proteins like cell division cycle 25 (Cdc25), are examples of factors that affect redox signaling on cell cycle^{85,87}. Cyclin dependent kinases (Cdk), cyclins and Cdk inhibitors cooperate to ensure a precise and orderly progression through the cell cycle⁸⁸. Hence, ROS impacts cell cycle progression by regulating the activity and expression of these cell cycle regulators via phosphorylation, ubiquitination and other protein modification events^{85,87,89}. ROS mediated regulation of cell cycle progression is very complex but induction of the Cdk inhibitor p21, seems to have a crucial

role⁸⁵. Increased p21 expression causes cell cycle arrest⁹⁰. ROS can induce p53-independent expression of p21 through redox sensitive transcription factors like activator protein-1 (AP-1) and specificity protein 1 (Sp1)⁸⁵. Alternatively, ROS-induced DNA damage can lead to increased p53 activity which in turn induces p21 expression^{85,90}. Expression of p21 plays a unique role in redox-regulated cell proliferation because temporal expression allows for DNA damage repair by cell cycle arrest and resumption of proliferation once redox homeostasis is achieved and p21 levels are normalized. However, prolonged ROS production sustains p21 expression and cells eventually undergo apoptosis⁸⁵. In fact, p21 has been shown to be involved in the transcriptional repression of several cell cycle genes including cyclins and Cdks⁹¹.

ROS AND JNK-MEDIATED APOPTOTIC SIGNALING

c-Jun N-terminal Kinases (JNKs) are a subfamily of the mitogen-activated protein kinase (MAPK) superfamily comprised of three well-characterized members: extracellular signal-regulated kinases (ERKs), p38 MAPKs, and JNKs⁹². MAPKs regulate cellular responses to external stimuli and cellular processes including cell proliferation, differentiation, and apoptosis^{92,93}. MAPKs mediate most of the signal transduction in eukaryotic cells by modulating the activity, degradation, subcellular localization, and protein interactions of their target proteins via phosphorylation⁹⁴. MAPKs are activated via a three-tier signaling cascade module in which a MAPK kinase kinase (MAP3K) activates a MAPK kinase (MAP2K) that in turn activates a MAPK⁹². JNKs are at the last tier of this signaling module.

JNKs are encoded by three distinct genes, two of which are ubiquitously expressed (JNK1 and JNK2) and JNK3, whose expression is restricted to the heart, brain and testes^{95,96}. All three genes are alternatively spliced into ten variants from which both 46kDa and 54kDa isoforms are derived⁹⁶. MKK4 and MKK7 are two MAP2Ks known to directly phosphorylate JNKs^{93,95,97}. Unlike MKK4 which can activate JNK and p38 MAPK, MKK7 is highly specific to JNK activation⁹⁸. At least twelve MAP3Ks have been observed to be involved in MKK4 and MKK7 activation, including the ROS sensitive MAP3K, apoptosis signal-regulating kinase 1 (ASK1)^{81,99}. The first target of active JNKs identified was c-Jun, hence their naming¹⁰⁰. c-Jun is a subunit of the AP-1 family of transcription factors that consists of homodimers and heterodimers of Jun (c-Jun, JunB, JunD), Fos (c-Fos, FosB, Fra-1, Fra-2) or activating transcription factor 2 (ATF2) proteins¹⁰¹. Active JNKs activate c-Jun by phosphorylating serines 63 and/or 73 in the amino terminal A1 transactivation domain^{102,103}. It is now recognized that JNKs can modulate the activity of a myriad of proteins (both nuclear proteins, most of which are transcription factors, and non-nuclear proteins) positively or negatively by phosphorylation¹⁰⁰. c-Jun, ATF2, Elk-1, c-Myc, p53, FOXO4, STAT3 and PAX2 are examples of nuclear proteins positively regulated by JNKs while HSF1, PPAR γ 1, Nur77, TIF1A, NFATc3 and Androgen R are some of the nuclear proteins inhibited by JNKs¹⁰⁰. Some non-nuclear proteins activated by JNKs are Bim, Bax, MK1, Bcl-2 and Itch, while Bcl-XL, IRS-1, Bcl2, Tau and kinesin - are examples of non-nuclear proteins that have been shown to be inhibited by JNKs¹⁰⁰. Several cellular responses; morphogenesis, metabolism,

motility, DNA repair cell differentiation, cell proliferation, cell survival, and cell death, are controlled by these JNK substrates^{104,105}. Hence not surprisingly, JNKs are implicated in a number of diseases including cancer^{104,105}. Since the cellular response to JNK activation is cell type and context dependent^{93,106}, it can either promote or inhibit disease states^{105,107}.

It is well known that ROS-induced activation of JNKs via the redox sensitive MAP3K, ASK1, leads to cellular apoptosis^{93,108}. The thioredoxin (Trx)/ASK1 complex functions as the redox switch of ROS-induced ASK1/JNK apoptosis signaling¹⁰⁸. Homophilic interaction of ASK1 mediated by the N-terminal coiled coil (NCC) domain is required for activation of the ASK1¹⁰⁹. The reduced form of Trx but never the oxidized form is found in complex with ASK1¹¹⁰. Binding of Trx to the N-terminal Trx-binding region of ASK1 inhibits its NCC domain-mediated homophilic interactions and therefore its activation^{109,110}. Increase in ROS levels results in oxidation of Trx which dissociates from the Trx/ASK1 complex, enabling ASK1 activation^{109,110} (Figure 1.3). Active ASK1 phosphorylates and activates JNKs which regulate apoptosis by nuclear and mitochondrial signaling events⁹³. Activated nuclear JNK promotes AP-1 mediated expression of pro-apoptotic proteins like BIM^{111,112} and Fas-ligand (Fas-L)¹¹³. Active JNK on the other hand can translocate to mitochondria where it directly activates the mitochondrial apoptosis machinery in the absence of new protein synthesis¹¹⁴. Phosphorylation of mitochondrial proteins such as Bcl2 and Bcl-x_L and decreased mitochondrial membrane permeability by active JNK have been reported to induce mitochondrial apoptosis^{114,115}.

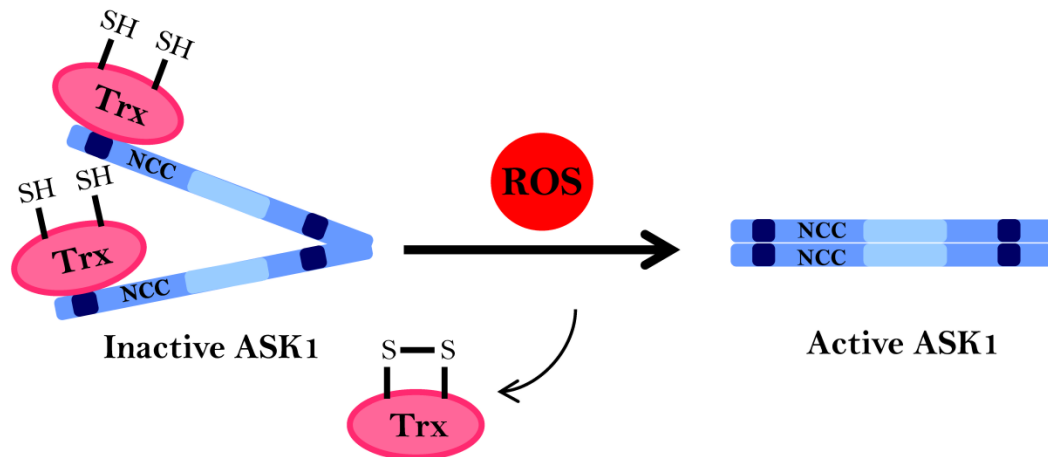


Figure 1.3: Redox regulation of ASK1 activation

Adapted from Soga M, Matsuzawa A, Ichijo H. Oxidative stress-induced diseases via the ASK1 signaling pathway. *Int J Cell Biol.* 2012;2012:439587.

ROS IN CANCER

Evidence suggests the malignant cells in most cancers including MDS, have increased levels of ROS compared to their normal counterparts¹¹⁶⁻¹¹⁹. A delicate balance of ROS levels is essential for normal cell growth and survival since a moderate increase ROS can promote cell proliferation while excessively high concentrations of ROS lead to cell death⁸⁵. Since cancer cells are already in a state of increased oxidative stress, they could be more susceptible to agents that further increase ROS generation^{67,116}. Hence, manipulation of ROS levels could be a means to selectively target cancer cells while sparing normal cells^{68,116}. Indeed there have been several reports demonstrating the selective therapeutic potential of some agents by increased ROS production¹¹⁹⁻¹²³.

Modulation of ROS homeostasis has been extensively exploited for AML therapy

in the past decade¹²⁴ but this therapeutic strategy has not been exploited for the closely related disease, MDS. The implication of increased oxidative stress in the development and prognosis of MDS¹¹⁸ suggests ROS producing agents such as WFA could have therapeutic value in MDS.

STUDY MODEL AND OBJECTIVES

There is no widely accepted animal model that completely recapitulates clinical features of MDS. Engraftment of primary MDS cells into immunocompromised mice is poor and highly inefficient^{125,126}. We therefore used the human MDS-L cell line, a subline of MDS92¹²⁷ for this study. The MDS92 cell line was derived from the bone marrow of an MDS patient¹²⁸ and was described by an independent group of investigators as the “chosen one” of the 31 cell lines investigated¹²⁹. MDS-L cells have deletions in chromosomes 5 and 7¹²⁷, the most common cytogenetic abnormalities observed in MDS which have also been associated with significantly worse prognosis^{12,14,16,17}. Moreover, MDS-L cells successfully engraft and induce reproducible disease in NOD/SCID-IL2R_γ (NSG) and NSG-hSCF/hGM-CSF/hIL3 (NSGS) mice¹³⁰.

As discussed above, the prognosis of MDS patients is generally very poor but the treatment options for these patients are very limited. The anticancer potential of the plant derived-compound, WFA has been demonstrated in several cancer models including prostate, breast, cervical and pancreatic cancers, as well as melanoma and lymphoma^{44,45}. In this study, we utilized the MDS-L model

of MDS to investigate the anticancer potential of WFA in MDS by addressing the following specific aims:

1. Determine the *in vitro* and *in vivo* effects of WFA on MDS-L cells and primary bone marrow cells from MDS and AML patients.
2. Elucidate the mechanisms of action of WFA in this MDS model.

CHAPTER 2

MATERIALS & METHODS

2a) Cell Culture

MDS-L cells (a generous gift from Dr. Kaoru Tohyama, Department of Laboratory Medicine, Kawasaki Medical School, Japan) were maintained in IMDM/F-12 (50:50) medium supplemented with 12% fetal bovine serum (Atlanta Biologicals), 0.005mg/ml apotransferrin, 50 μ M 2-mercaptoethanol (2-ME) and 20 ng/ml of human IL-3 (PeproTech). KG-1 cells (kindly provided by Dr. Ying Liang, Department of Toxicology and Cancer Biology, University of Kentucky, USA) were cultured in IMDM medium supplemented with 10% fetal bovine serum. KG1 is a human AML cell line. IRB protocol # 88-00241 permitted acquisition of human primary cells. Normal human primary bone marrow cells were courtesy of Dr. Ahmed Abdel-Latif at the University of Kentucky. Bone marrow mononuclear cells were isolated by Ficoll-paqueTM plus (GE Healthcare) and maintained in RPMI medium supplemented with 50 μ M 2-mercaptoethanol, 1 μ M sodium pyruvate and 10% fetal bovine serum (FBS). MDS/AML samples were obtained from Leukemia Tissue Bank of the Ohio State University Comprehensive Cancer Center (OSU CCC). MDS/AML cells were thawed and maintained in RPMI medium supplemented with 10% fetal bovine serum and 10 ng/ml hIL-3, GM-CSF and stem cell factor (R&D Systems). All media were purchased from Gibco-Life Technologies.

2b) Reagents

WFA was isolated from *Withania somnifera* extract (Sabinsa Corp) using a series of solvent extractions and silica gel-based vacuum liquid column chromatography at the University of Louisville and at the laboratory of Dr. I. P. Singh, National Institute of Pharmaceutical Education Research (NIPER), India. The purity was found to be >94% by UPLC. WFA was reconstituted in dimethyl sulfoxide (DMSO). Biotin conjugated rat anti-CD45R/B220 (553086), anti-CD11b (553309), anti-Gr-1 (553125), anti-CD8a (5532029), anti-Ter-119 (553672), anti-CD5 (553019); streptavidin APC CY7 (554063) and anti c-KIT-APC (553356) were purchased from BD Pharmingen (San Diego, CA). Anti-Sca-1-PB (122520) was purchased from BioLegend (San Diego, CA). Cremophor (C5135), Carbonyl cyanide 4-(trifluoromethoxy)phenylhydrazone (FCCP) (C2920), hydrogen peroxide (H₂O₂) (H1009), Phorbol 12-myristate 13-acetate (PMA) (P1585), N-acetyl-cysteine (NAC) (A8199), SP600125 (S5567), JNK-IN-8 (SML-1246), JC-1 (T4069), RNase A (R6513), HEPES solution (H0887), ethylenediaminetetraacetic acid (EDTA) solution (E7889), dimethyl sulfoxide (D2438) and monoclonal anti-β-actin (A5441) were purchased from MilliporeSigma-Aldrich (St. Louis, MO). Antibodies to P-p38 (9211S), total p38 (9212), cleaved caspase-3 (9661S), total caspase-3 (9665S), P-MKK7 (4171S), P-c-Jun (9261S), total c-Jun (9162), CDK2 (2546P), cyclin A (4656P), CDK1 (9116), cyclin B (4135) and GAPDH (2118S) were obtained from Cell Signaling Technology (Danvers, Massachusetts). Anti-total MKK7 was purchased from Zymed (32-7000). Antibodies to RGS2 (100761), Hdac1 (7872), P-JNK (6254) and total JNK (571) were obtained from

Santa Cruz Biotechnology (Santa Cruz, CA). Peroxidase coupled goat anti-rabbit (SC-2004) and anti-mouse (SC-2005) Ig secondary antibodies were also acquired from Santa Cruz Biotechnology (Santa Cruz, CA). 1X phosphate buffered saline (16750-078) was obtained from VWR (Radnor, PA).

2c) MTT and Trypan Blue Dye Exclusion Cell Viability Assays

MDS-L cells were treated with increasing concentrations of WFA (0 – 20 μ M) in 96 well flat-bottom microtiter plates for 48 h in 0.2 ml of media. Cells were cultured in quadruplicates. Treated cells were incubated with 0.5 mg/ml MTT (3-(4,5-Dimethylthiazol-2-yl)-2,5-diphenyltetrazolium bromide) dye (Sigma Aldrich) for 4 h followed by solubilization of formazan salt with acidic isopropanol and spectrophotometric measurements at 560 nm and 690 nm. Optical density variation was corrected by subtracting OD 690 from OD 560 nm values. Media background was subtracted from all treatment groups and a DMSO control group was included in each experiment. For trypan blue exclusion, MDS-L cells were treated with increasing concentrations of WFA (0 – 20 μ M) in 0.5 ml of media per well of 24 well flat-bottom plates for 48 h and cell viability was assessed by counting live cells by trypan blue exclusion.

2d) Effect of WFA on MDS-L Engraftment in vivo

Animal studies were conducted under an approved protocol by the Institutional Animal Care and Use Committee (IACUC) at the University of Kentucky (Protocol # 2011-0904). NOD/SCID-IL2R γ -hSCF/hGM-CSF/hIL3 (NSGS) breeding pairs were obtained from The Jackson Laboratories (Bar

Harbor, ME) and bred at the University of Kentucky's Division of Laboratory Animal Resources (DLAR) AAALAC certified animal facility. Animals had free access to food and water, and were housed at constant temperature with a 12 hour light–dark cycle. 6 -7 month old male and female littermates were exposed to 2.5Gy irradiation (IR) in a Mark I-68 ¹³⁷Cesium γ -irradiator (J.L Shepherd and Associates) on a rotating platform, as a pre-conditioning regimen for bone marrow engraftment. Four hours after irradiation, mice were engrafted by intravenous tail vein injection with MDS-L cells (1×10^6 cells in 100 μ l/mouse).

Mice were treated from day 14 with 8 mg/kg of WFA IP 5X a week for 6 weeks. Control mice received vehicle (10% DMSO, 20% Cremophor-Ethanol (1:3), 70% phosphate buffered saline (PBS)). MDS-L engraftment was assessed by the percentage of human CD45⁺/CD33⁺ double positive cells in the bone marrow compartment since MDS-L cells are positive for these markers. Tibiae and femora were harvested from mice and the bones were flushed with a 26G syringe in HBSS containing 2% fetal bovine serum to obtain bone marrow cells. The cells were washed and suspended in fluorescence activated cell sorter (FACS) buffer (1X phosphate buffered saline without calcium or magnesium, supplemented with 25mM Hepes, 5mM EDTA and 1% FBS). 2×10^6 cells were stained with anti-mouse CD45-APC, anti-human CD45-PE and anti-human CD33-PE for 1 h at 4°C in the dark. Positively stained cells were detected by the BD LSRII flow cytometer and the data was analyzed by the FlowJo (Ashland, OR) single cell analysis software. Anti-human CD45-PE (12-9459-42) and CD33-

FITC (11-0339-42) were purchased from eBioscience (San Diego, CA). Anti-mouse CD45-APC was obtained from BioLegend (San Diego, CA).

2e) Staining and identification of bone marrow stem cells

Bone marrow cells were incubated with normal rat IgG ($10 \mu\text{g}/1 \times 10^6$ cells) at 4°C for 15 min to block Fc γ receptors and then labeled with biotin coupled rat anti-mouse lineage specific antibodies to CD11b (Mac-1), B220, Gr-1, CD8 α , Ter-119 and CD5. The cells were stained with c-KIT-APC, Sca-1-PB and streptavidin APC CY7 antibodies for 30 min at 4°C in the dark and washed with 1X FACS buffer. Positively stained cells were detected on the BD LSRII flow cytometer and data was analyzed by the BD CellQuest™ Pro software. Lineage negative cells which were double positive for both Sca-1 (stem cell antigen-1) and c-KIT (LSK) were identified as stem cells.

2f) Annexin-V Apoptosis Assay

The annexin-V apoptosis detection kit (A432) from Leinco Technologies (St. Louis, MO) was used for annexin-V assays. Thawed human primary MDS/AML cells were maintained in culture for 24 h and then treated with increasing concentration of WFA for 24 h. Treated cells were stained with annexin-V-FITC and PI following the manufacturer's protocol. Data was acquired with the Becton-Dickinson FACSCalibur flow cytometer and analyzed by the BD CellQuest™ Pro software (San Jose, CA). For MDS-L cells, 7.5×10^5 cells/ml were treated with increasing WFA concentrations for 48 h before staining. In the case of JNK or ROS inhibition studies, 7.5×10^5 MDS-L cells/ml after a 4 h JNK-

IN-8 (10 μ M) or NAC (25 mM) pretreatment, or no pretreatment were treated with WFA (10 μ M) for 24 h and stained with annexin-V/PI. Stained MDS-L cells were detected by the BD LSRII flow cytometer and BD CellQuest™ Pro software was used for data analyses.

2g) NF- κ B Nuclear Translocation by Immunocytofluorescence

MDS-L cells (5×10^6) were incubated with WFA (10 μ M) or DMSO for 4 h. The cells were fixed with 70% ethanol for 1 h, blocked for 1 h in 10% normal goat serum and stained with 1:200 dilution of NF- κ B p65 primary antibody (Santa Cruz-372) overnight at 4 °C. Cells were washed and stained with 1:200 DyLight 488 conjugated AffiniPure F(ab')₂ goat anti-rabbit secondary antibody (Jackson ImmunoResearch #111–486–046) for 1 h in the dark. After 1X wash with FACS buffer, the cells were again stained 1:4000 DAPI (Life Technologies, #D1306) for 15 min at room temperature. Prolong^R Gold Anti-Fade Reagent (Life Technologies, #P36930) was used to mount the cells after washing following DAPI staining. Slides were viewed and pictures taken on a FV1000 v1.5 confocal microscope (Olympus, Shinjuku, Tokyo, Japan).

2h) Immunoblotting

MDS-L cells (7.5×10^5 cells/ml) were cultured with 10 μ M WFA or DMSO for different time points. Cells were lysed in Cell Signaling lysis buffer (#9803) containing 1mM PMSF (Sigma P7626), 2mM NaF (Sigma S-1504), 2mM Na₃VO₄ (Sigma S-6508) and 1x protease inhibitor cocktail (Roche 5892953001). To obtain nuclear and cytoplasmic lysates, the cell pellets were lysed following

the Thermo Scientific Nuclear and Cytoplasmic Extraction kit (#78833) manual. Protein concentration in cell lysates was estimated by the Bicinchoninic Acid (BCA) assay kit (Thermo Scientific #23227). Protein lysates were diluted in 4x sodium dodecyl sulfate (SDS) sample buffer (100mM Tris-HCl, pH 6.8, 30% glycerol, 4% SDS, 5% 2-ME and 0.01% W/V bromophenol blue) to a 1x final concentration and boiled for 10 min. 35 µg total protein/sample of total lysate was subjected to SDS polyacrylamide gel electrophoresis. 10 µl of Precision Plus Protein™ dual color ladder (BIO-RAD #1610394) with a size range spanning 10-250 kDa was used as a size standard for every gel. The BIO-RAD Mini PROTEAN Tetra System was used for both gel electrophoresis and transfer. 12, 10 or 9% polyacrylamide gels were run with running buffer (25 mM Tris, 192 mM glycine, 0.1% SDS, pH 8.3) at 90 V and 3 A for 10 min to stack the proteins, and later at 140 V and 3 A for 1 h to separate the proteins. Separated proteins were transferred to polyvinylidene difluoride membranes (EMD Millipore IPVH00010) with transfer buffer (25 mM Tris, 192 mM glycine, 20% methanol, pH 8.3). Transfer was performed at 90 V and 300 mA for 1.5 h at 4°C. Membranes were blocked at room temperature for 1 h with 5% milk or bovine serum albumin (when probing for phosphorylated proteins) in 1x TBST that was diluted from 10x TBST (0.5 M Tris, 1.5 M NaCl and 1% Tween-20). The membranes were then probed with appropriate primary antibodies at 4°C overnight, followed by horseradish peroxidase-conjugated secondary antibodies at room temperature for 1 h. Membranes were washed 7X with 1x TBST after primary or secondary antibody incubations. The blots were developed with HyGLO chemiluminescence reagent

(Denville Scientific #E2400) and exposed to HyBlot CL autoradiography film (Denville Scientific #E3012), which were scanned with a flat-bed scanner (UMAX Technologies, Hsinchu, Taiwan). When comparing two blots, both gels were run side by side and the blots were developed on the same film. Band densitometry analysis was performed using the NIH ImageJ program. Protein expression was normalized to GAPDH, β -actin or total target protein expression as appropriate.

2i) Affymetrix Microarray Analysis

Gene expression profile of MDS-L cells was examined in triplicate samples. 10×10^6 MDS-L cells were treated with WFA (10 μ M) or DMSO for 6 h or 12 h at 37⁰C in a CO₂ incubator. Total RNA was extracted using the Direct-zolTM RNA miniprep kit (Zymo Research #R2051) according to the manufacturer's instructions. The Agilent RNA 6000 Nano assay kit (#5067-1511) was used to assess RNA purity on the Agilent 2100 Bioanalyzer (Agilent Technologies, Santa Clara, CA). RNA integrity number (RIN) was ≥ 9 for all samples. WT Plus Reagent kit (Affymetrix, Santa Clara, CA), was used to generate amplified and biotinylated sense-strand DNA (ss-cDNA) from 100 ng total RNA per sample. 30 μ g of fragmented biotin-labelled ss-cDNA was hybridized to Affymetrix human gene 2.0 ST arrays at 45 ⁰C and 60 rpm for 16 h. The arrays were washed and stained using Affymetrix fluidics station FS 450 and scanned using the Affymetrix 7G GeneChip Scanner. Data was collected using the Affymetrix Command Software. The raw microarray data files were processed through Oligo [Doi:10.1093/bioinformatics/btq431] for data extraction and normalization. Differential expression analyses comparing WFA-treated

groups and the control group were performed by limma [DOI:10.1093/nar/gkv007]. Significantly up/downregulated genes were determined as fold change > 3 and q-value < 0.05, where q-value is a p-value corrected for multiple testing. The functional analyses were performed through QIAGEN's Ingenuity Pathway Analysis (IPA®, QIAGEN Redwood City, www.qiagen.com/ingenuity). The heat map was used to demonstrate the expression of differentially expressed genes, where genes belonging to the top 15 enriched diseases and function categories from IPA were highlighted. The gene set enrichment analysis was performed using GSEA software and the Hallmark gene sets in the Molecular Signature Database (MSigDB)¹³¹ [<http://www.broad.mit.edu/gsea/>].

2j) Quantitative Real-Time PCR (qRT-PCR)

Total RNA was extracted from BM-MNCs using TRIzol^R reagent (LifeTechnologies #15596-018) according to the manufacturer's instructions. cDNA was synthesized from 500 ng of total RNA with qScript reverse transcriptase (Quanta Biosciences #95048-100) using random and oligo(dT) primers as per manufacturer's protocol. The CFX96TM Real-Time C1000 Touch thermal cycler system (BIO-RAD, Hercules, California) was used with the iTaqTM universal SYBR^R green fluorescent supermix (Biorad #172-5121) to quantify mRNA expression. RNA polymerase II was used as an internal control. BIO-RAD CFX Manager software was used to perform relative quantification of target genes using the comparative C_T ($\Delta\Delta C_T$) method. Specificity of PCR reactions was confirmed by melting curves. The primer sequences used are described in

Table 2.1. Primers were designed on NCBI/Primer-Blast using the default parameters with the following modifications; primer must span exon-exon junction, primer must have at least 6 total mismatches to unintended targets and ignore targets that have one or more mismatches to the primer. Primers were obtained from Integrated DNA Technologies (IDT, Coralville, Iowa).

Table 2.1: List of qRT-PCR Primers

Gene	Primers	
<i>BAG3</i>	Forward	5'-GGAGATCAAGATCGACCCGC-3'
	Reverse	5'-CAGAGGATGGAGTCTCCTTGG-3'
<i>RGS2</i>	Forward	5'-TTCAACACGACTGCAGACCC-3'
	Reverse	5'-CTTCCTCAGGAGAAGGCTTGAT-3'
<i>JUN</i>	Forward	5'-GCCAACTCATGCTAACGCAG-3'
	Reverse	5'-GGCAGGCCAGAAAGAGTTCA-3'
<i>FOSB</i>	Forward	5'-GCGTACTTTGAGGACTCGCT-3'
	Reverse	5'-TTCCTCTGGGGTGAGCGTCT-3'
<i>BCL2L11 (BIM)</i>	Forward	5'-ACCAGATCCCCGCTTTTCAT-3'
	Reverse	5'-GAAGAGGCATCCTCCTTGCATA-3'
<i>CDKN1A (P21)</i>	Forward	5'-AGTACCCTCTCAGCTCCAGG-3'
	Reverse	5'-TGTCTGACTCCTTGTTCCGC-3'
<i>CCNA2 (CYCLIN A2)</i>	Forward	5'-TCGCGGGATACTTGAAGTGC-3'
	Reverse	5'-GTGCAACCCGTCTCGTCTT-3'
<i>CDK2</i>	Forward	5'-GGATGCCTCTGCTCTCACTG-3'
	Reverse	5'-ACAGGGTCACCACCTCATGG-3'
<i>CCNB1 (CYCLIN B1)</i>	Forward	5'-GCCTGAGCCTATTTTGGTTGA-3'
	Reverse	5'-AGTGACTTCCCGACCCAGTA-3'
<i>CDK1</i>	Forward	5'-AAGCCGGGATCTACCATAACC-3'
	Reverse	5'-GCTCTGGCAAGGCCAAAATC-3'
<i>RPOL2</i>	Forward	5'-GCACCACGTCCAATGACAT-3'
	Reverse	5'-GTGCGGCTGCTTCCATAA-3'

2k) Mitochondrial Membrane Potential by JC-1

MDS-L cells (7.5×10^5 cells/ml) were exposed to WFA (10 μ M) or DMSO for 8 h. Cells treated with 50 μ M of the proton translocator, FCCP for 2 h were used as a positive control. JC-1 was added at a 1 μ M final concentration to cells for the last 30 min of treatment at 37 $^{\circ}$ C. The cells were washed, suspended in PBS and fluorescence was measured using the iCyt Synergy sorter system (Sony Biotechnology Inc., San Jose, CA). We used the 488 and 561 nm lasers because the 561 nm laser efficiently excites J-aggregates but does not excite JC-1 monomers¹³². This ensured optimal discrimination of the JC-1 monomers from the aggregates. The WinList 3d 8.0 software (Verity Software House Inc., Topsham, Maine) was used for data analyses.

2l) ROS Measurement

Cell permeant 6-Carboxy-2',7'-Dichlorodihydrofluorescein Diacetate (Carboxy-H₂DCFDA) (ThermoFisher Scientific #C400), was used as an indicator for intracellular ROS measurement. MDS-L cells were treated with DMSO, WFA (10 μ M) or H₂O₂ (1mM) for 30 min at 37 $^{\circ}$ C. Alternatively, cells were treated with N-acetyl-cysteine (NAC) (25 or 50 mM) for 4 h followed by DMSO, WFA (10 μ M) or H₂O₂ (1mM) for additional 30 min at 37 $^{\circ}$ C. Treated cells were washed with warm 1X PBS and suspended in warm H₂DCFDA solution (1.25 μ g/ml in PBS). The cells were incubated in the dark at 37 $^{\circ}$ C for 20 min. Fluorescence was detected on the BD LSR II flow cytometer and the BD CellQuest™ Pro software was used for data analyses. The oxidized form of DCFDA, 5-(and-6)-Carboxy-

2',7'-Dichlorofluorescein Diacetate (Carboxy-DCFDA (ThermoFisher Scientific #C369), was used as a control for uptake, cellular esterase activity and decay.

2m) AP-1 Luciferase Assay

AP-1 pGL3 promoter luciferase and empty vectors were kindly provided by Dr. Sanjit Dhar, Department of Toxicology and Cancer Biology, University of Kentucky, USA. The Tk-renilla luciferase vector was a generous gift from the laboratory of Dr. Martha Peterson, Department of Microbiology, Immunology and Molecular Genetics, University of Kentucky, USA. MDS-L cells were transfected by electroporation. 2.5×10^6 cells were co-transfected with 20 μg of Tk Renilla luciferase vector and 40 μg of firefly luciferase vector (AP-1 or empty vector) at 250 mV, 960 μF and 200 Ω in 200 μl of MDS-L culture medium with a Gene Pulser electroporator (BIO-RAD, Hercules, CA). Transfected cells were cultured in MDS-L culture medium for 24 h at 8.5×10^5 cells per well in 6 well flat bottom plates (Corning #353224). 24 h after transfection, 1×10^5 cells per well were treated with 10 μM WFA or 30 ng/ml phorbol 12-myristate-13-acetate (PMA) for 12 h in white 96 well flat bottom polystyrene plates (Corning #3917, Corning Incorporated Inc, Durham, NC). Alternatively, cells were pretreated with NAC (25mM) for 4 h before WFA treatment for an additional 12 h. Promoter activity was assessed by the Dual-Glo® Luciferase assay system (Promega #E2920, Promega Corporation, Madison, WI). Luminescence was measured using the GloMax® Explorer luminometer (Promega). Media background luminescence was subtracted and the ratio of firefly to renilla luminescence was calculated.

2n) Cell Cycle Analyses

MDS-L cells (7.5×10^5 cells/ml) were exposed to increasing concentration of WFA (0 – 5 μ M) for 48 h. Treated cells were fixed with cold 70% ethanol for 1 h at 4 °C. The cells were washed 3X with PBS and incubated in a Propidium Iodide (PI) and RNase A cocktail (20 μ g/ml and 250 μ g/ml respectively, in 0.1% Triton X-100 in PBS) at 37 °C for 30 min. PI fluorescence was detected on the BD FACSCalibur flow cytometer and analyses were performed using the ModFit Software (Verity Software House Inc., Topsham, Maine).

2o) Statistical Analysis

GraphPad Prism 6.05 was used for statistical analyses (GraphPad Software, Inc., La Jolla, CA). Statistical significance of differences between groups was evaluated by Student's t test, linear regression analysis or Tukey's multiple comparisons test as appropriate and p values < 0.05 were considered significant.

CHAPTER 3

WFA has a potent but selective anti-proliferative effect on MDS-L cells *in vitro* and *in vivo*

The complex and heterogeneous nature of MDS has made it challenging to generate a widely accepted mouse model that recapitulates a complete disease phenotype¹³³. Efforts to develop a xenotransplantation model of primary MDS cells into immunocompromised mice have been thwarted by poor and highly inefficient bone marrow engraftment of these cells^{125,126}. Development of cell line models for MDS has not been met with much success either. Several human MDS cell lines have been described in the literature but only the MDS-L cell line has been validated to be a legitimate cell line that is representative of MDS¹²⁹. MDS-L is a subline of the MDS92 cell line that was derived from the bone marrow of an MDS patient^{127,128}. Importantly, MDS-L cells successfully engraft the bone marrow of immunocompromised mice to induce an MDS-like disease that recapitulates some key features of human MDS¹³⁰. Like human MDS, the MDS-like disease induced by MDS-L engraftment is clonal^{1,130}. In addition, mice develop anemia and thrombocytopenia as the disease progresses, two commonly observed cytopenias in human MDS^{3,130}. The MDS-L model is therefore considered an appropriate model for preclinical MDS studies and was our model of choice to investigate the therapeutic potential of WFA in MDS.

3a) WFA effectively decreased viability of MDS-L cells *in vitro*

Initial studies were performed to determine the effect of WFA on MDS-L cells *in vitro*. WFA caused a dose dependent decrease in cell viability of MDS-L cells by MTT assay (Figure 3.1A). Observed IC₅₀ varied depending on the seeding cell density. 2 – 3 μM when 0.75×10^5 cells were seeded per well, 3 – 5 μM for 1×10^5 cells and 5 - 7 μM for 1.5×10^5 cells (Fig 3.1A). The decrease in viability of MDS-L cells by WFA was also demonstrated by trypan blue exclusion assay. Similar to the MTT assay, WFA caused a dose dependent decrease in viability of MDS-L cells by trypan blue exclusion (Figure 3.1B). Lenalidomide (LENA) is the US Food and Drug Administration (FDA) approved treatment of MDS with a deletion in chromosome 5q (del (5q))¹³⁴. Since MDS-L cells have a deletion in chromosome 5¹²⁷, we evaluated how WFA compared to LENA in inducing growth inhibition of MDS-L cells. To our surprise, WFA was substantially more effective than LENA in inhibiting the proliferation of MDS-L cells *in vitro* (Figure 3.2A). This observation was not dependent on the seeding cell density as similar results were obtained even with a lower seeding cell density (Figure 3.2B). The markedly low or more of a complete lack of cytotoxicity by LENA on MDS-L cells (Figure 3.2A, B) led us to consider the possibility that our drug might be inactive since published reports have shown the cytotoxic effects of LENA on MDS-L cells¹²⁷ and human primary MDS cells with a 5q chromosomal deletion¹³⁵. To address this possibility, we replicated a published experiment in which the effect of LENA on the proliferation of MDS-L cells was assessed by adding 10 μM of drug every 24 h and counting the number of viable cells over time¹²⁷. The

marked difference we observed between WFA and LENA was not due to drug inactivation because addition of LENA every 24 h to MDS-L cells inhibited their proliferation (Figure 3.3A) and our results were very similar to the published results (Figure 3.3B). This requirement of replenishing LENA every 24 h in order to observe its cytotoxicity might be due to its reported half-life of about 8 h *in vitro*¹³⁶. However, a single dose of LENA inhibited the proliferation of human multiple myeloma cell lines¹³⁶. After establishing that we had to replenish LENA every 24 h to observe its cytotoxic effects on MDS-L cells, we investigated whether the cytotoxic effects of WFA and LENA could be combinatorial. Combining a single dose of WFA to everyday addition of LENA on MDS-L cells was not superior to either drug alone (Figure 3.4). In fact, WFA was distinctly superior to LENA in inhibiting the proliferation of MDS-L cells under these conditions. Since transformation to AML occurs in approximately 30 – 40% of MDS cases¹³⁵, we also investigated if WFA is cytotoxic to the human AML KG1 cell line. WFA caused a dose dependent decrease in viability of KG1 cells (Figure 3.5).

3b) WFA inhibited bone marrow engraftment of MDS-L cells in NSGS mice

In vivo efficacy was evaluated using the MDS-L NSGS xenograft model, where mice exposed to 2.5Gy irradiation are injected with 1×10^6 MDS-L cells 4 h later¹³⁰. We chose to use NSGS mice for these studies because although MDS-L was reported to successfully engraft the bone marrow of both NSG and NSGS mice, we found engraftment to be less efficient in NSG mice (< 1%). Irradiation serves as a preconditioning regimen to enhance bone marrow

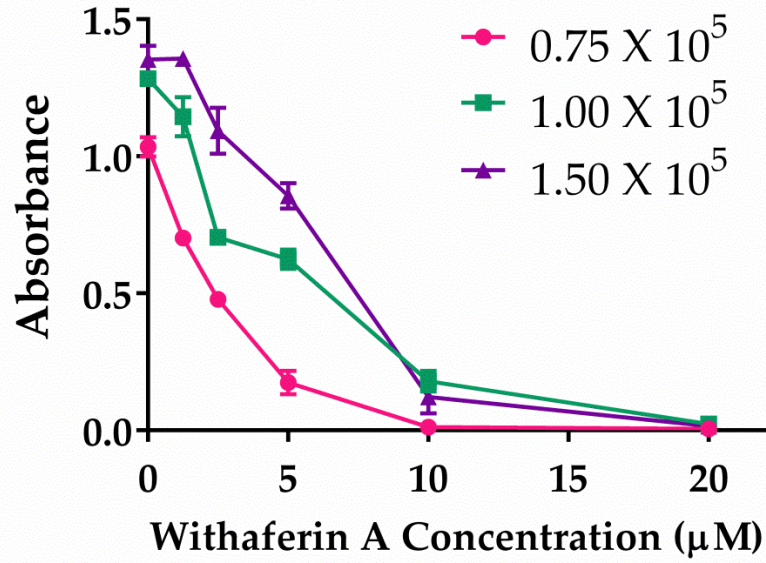
engraftment. We had found from our previous studies that the combination of radiation and WFA was toxic to BALB/c mice. It was therefore essential to determine the best tolerated dosing schedule for the radiation and WFA combination especially since *scid* mice are hypersensitive to radiation¹³⁷. We found that NSGS mice had not completely recovered from radiation-induced weight loss even at 14 days post exposure to 2.5Gy irradiation (Figure 3.6). However, WFA treatment from day 14 post irradiation did not adversely impact complete recovery by day 21 (Figure 3.6). We therefore decided to begin WFA treatment on day 14 post irradiation and engraftment as illustrated in Figure 3.7A. A combination of mouse and human cell surface markers was used to positively identify engrafted MDS-L cells (Figure 3.7B). 8 mg/kg WFA treatment significantly reduced engraftment of MDS-L cells in the bone marrow of NSGS mice (Figure 3.7C, D). The 8 mg/kg dose was well tolerated as minimal weight loss was observed in WFA treated mice compared to vehicle controls (Figure 3.7E). Remarkably, WFA treatment did not cause any apparent bone marrow suppression of endogenous mouse stem cells at the dose used (Figure 3.8). This is of particular importance because nearly all chemotherapy drugs cause bone marrow suppression which leads to treatment delays and significant dose reductions¹³⁸. In fact, it is estimated that about 56% of patients on chemotherapy receive less than 85% of the minimum optimal dose for treatment¹³⁸. We also found that WFA treatment expanded the stem cell population of non-engrafted mice over control mice (Figure 3.8, $p = 0.07$). However, additional studies with a larger sample size are needed to confirm this observation. While the prospect of

stem cell expansion by WFA has potential therapeutic benefits, serial transplantation studies are required to determine the functionality of these expanded stem cells.

3c) Cytotoxicity of WFA is selective to malignant cells

The clinical relevance of the results obtained with the MDS-L and KG1 cell lines were validated by testing the effect of WFA on the viability of human primary bone marrow cells from MDS and AML patients. WFA induced a dose-dependent increase in apoptotic cell death of primary MDS and AML bone marrow patient cells (Figure 3.8A, B). The cytotoxic effects of WFA are selective to malignant cells because it had no significant impact on the viability of normal human primary bone marrow cells even at the highest dose tested (Figure 3.9).

3.1A



3.1B

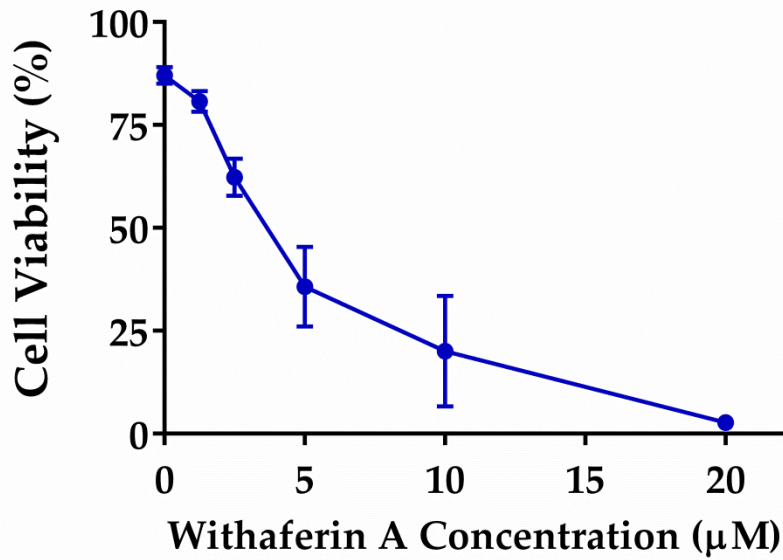
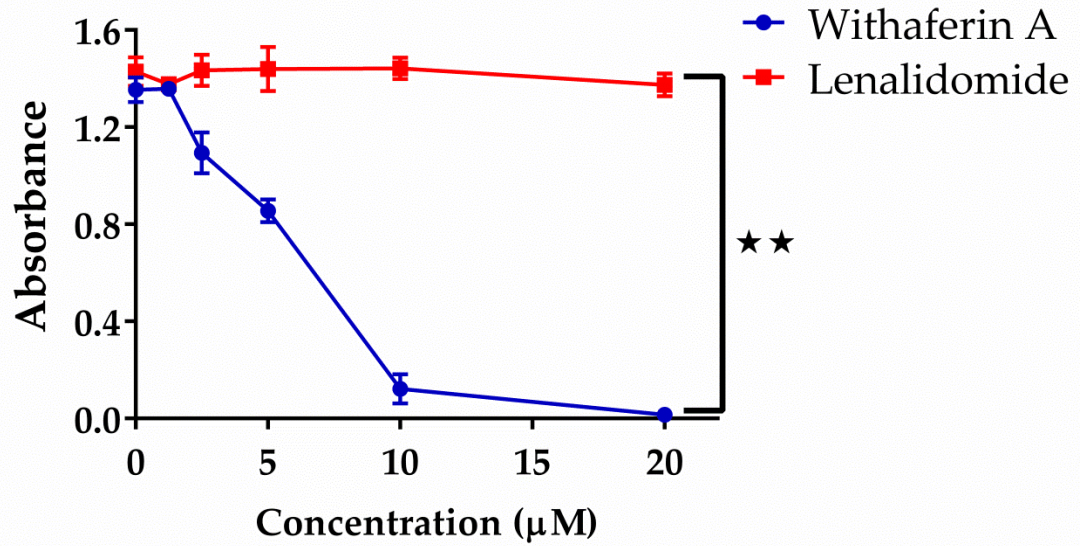


Figure 3.1: WFA significantly decreased the viability of MDS-L cells *in vitro*

(A) MDS-L cells were treated with WFA at different cell densities (0.75×10^5 , 1×10^5 or 1.5×10^5 cells per well in 200 μ l of media of a 96 well plate) for 48 h and cell viability was measured by MTT assay. Data are presented as mean \pm SD of triplicate cultures. Results are representative of more than 3 experiments. (B) MDS-L cells (7.5×10^5 cells/ml) were treated with increasing concentrations of WFA for 48 h and cell viability was determined by trypan blue dye exclusion. Data are presented as mean \pm SD of triplicate cultures and results from one of 2 similar experiments are shown.

3.2A



3.2B

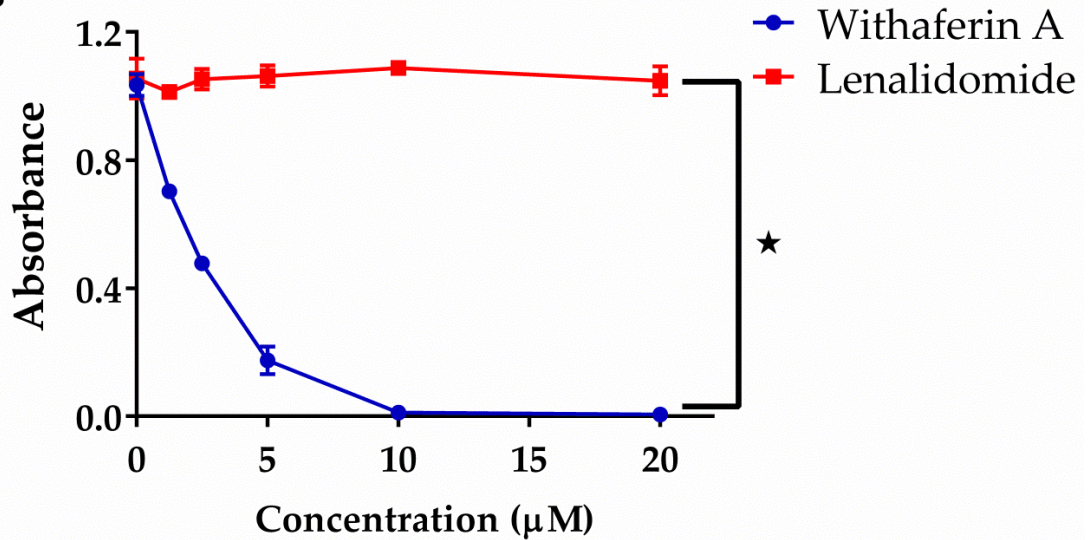
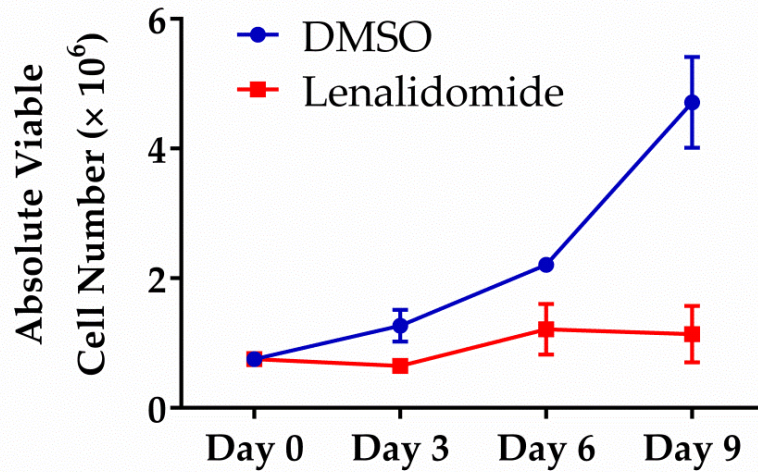


Figure 3.2: WFA is substantially more cytotoxic to MDS-L cells compared to lenalidomide

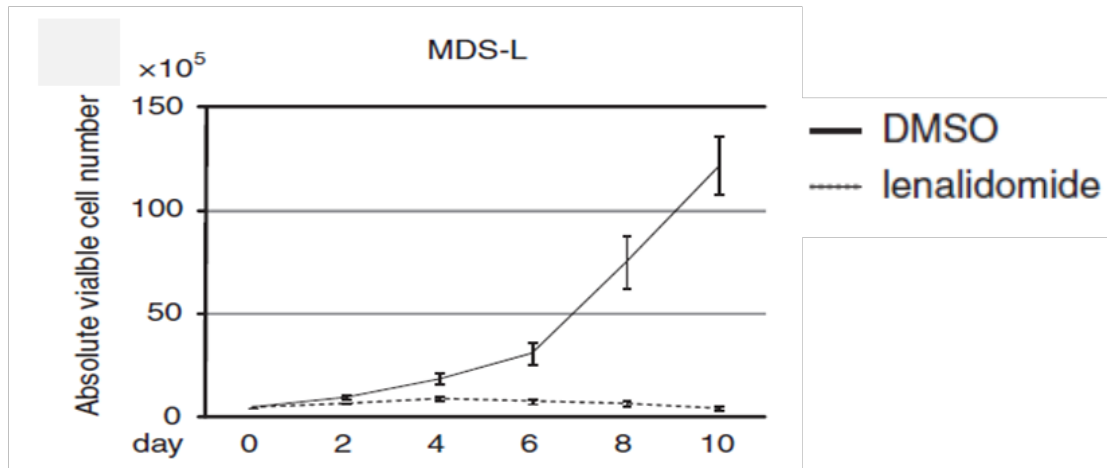
MDS-L cells were treated with WFA or LENA at 1.5×10^5 cells (A) or 0.75×10^5 cells (B) per well of a 96 well plate), for 48 h and cell viability was measured by

MTT assay. Data are presented as mean \pm SD of triplicate cultures. Data are representative of three independent experiments. * = $p < 0.05$, ** = $p < 0.005$.

3.3A



3.3B



Matsuoka et al., Leukemia. 2010; 24:748-755

Figure 3.3: Drug replenishment every 24 h is required to observe lenalidomide-induced cytotoxicity of MDS-L cells

(A) MDS-L cells were cultured in the presence of DMSO or lenalidomide (10 μ M) which were added daily. The number of viable cells was counted by trypan blue exclusion on the indicated days. Data are presented as mean \pm SD of triplicate

cultures. (B) Published data of a similar experiment using MDS-L cells and the same concentration of lenalidomide. Reproduced with permission from Nature Publishing Group; license number 3991040149727.

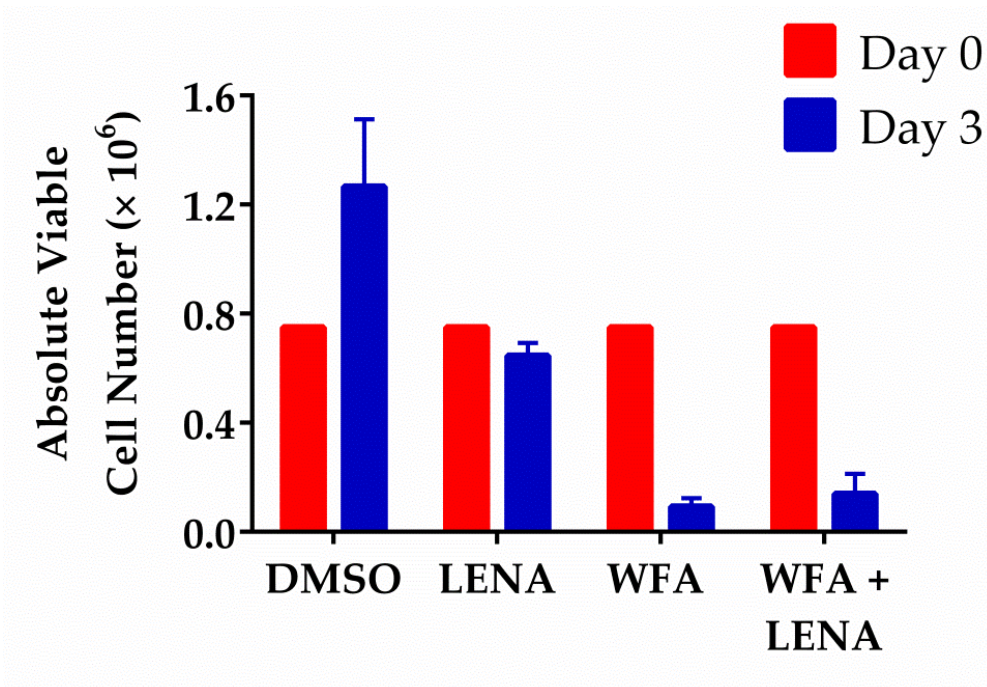


Figure 3.4: The combined cytotoxic effects of WFA and lenalidomide are neither additive nor synergistic

MDS-L cells were cultured with DMSO, lenalidomide (10 μ M), WFA (5 μ M) or WFA (5 μ M) and lenalidomide (10 μ M). WFA was added on day one of the experiment while lenalidomide was added daily during the course of the experiment. The number of viable cells was determined by trypan blue exclusion. Data are presented as mean \pm SD of triplicate cultures. Representative data of two independent experiments are presented.

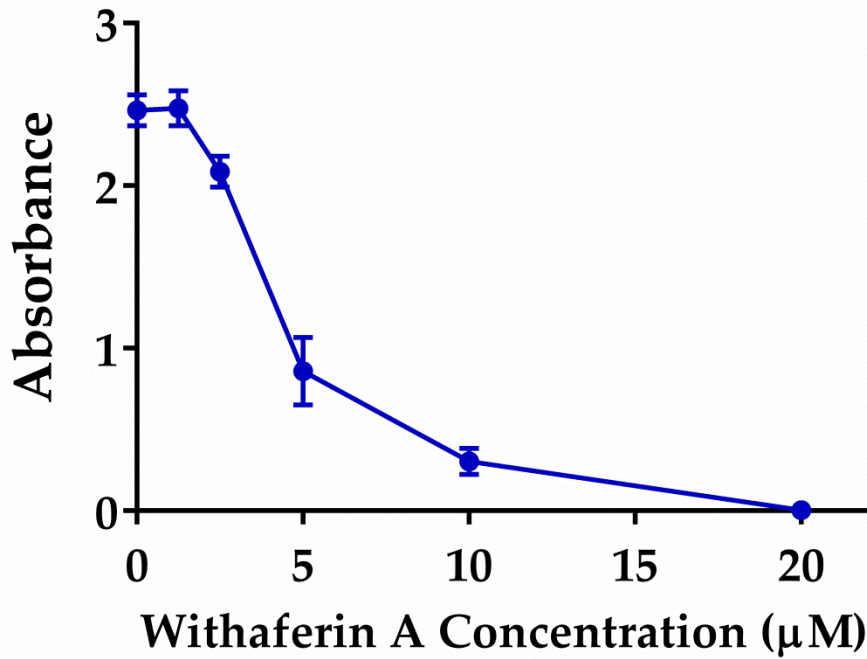


Figure 3.5: WFA significantly decreased the viability of KG1 cells *in vitro*

KG1 cells were treated with DMSO or WFA at 1.5×10^5 cells per well of a 96 well plate for 48 h and cell viability was measured by MTT assay. Data are presented as mean \pm SD of triplicate cultures. Results are representative of two experiments.

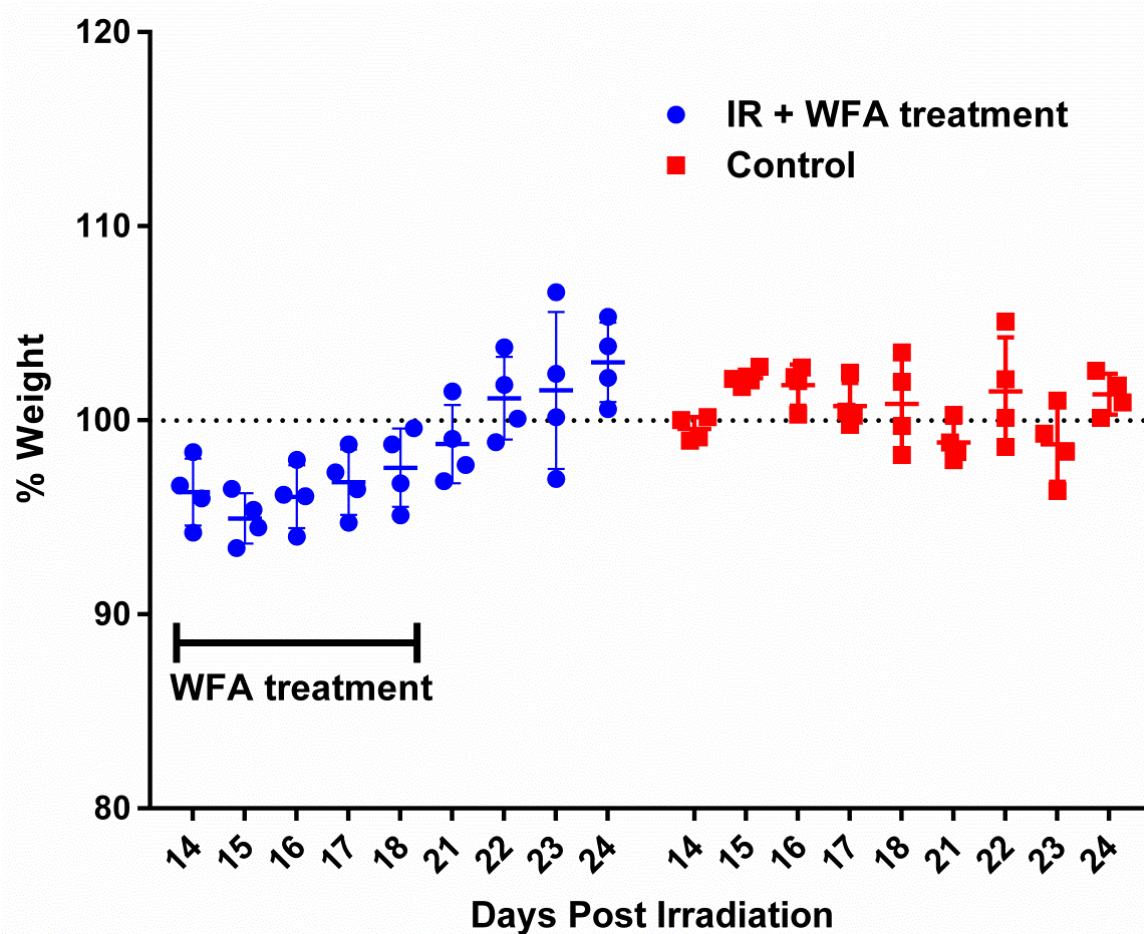
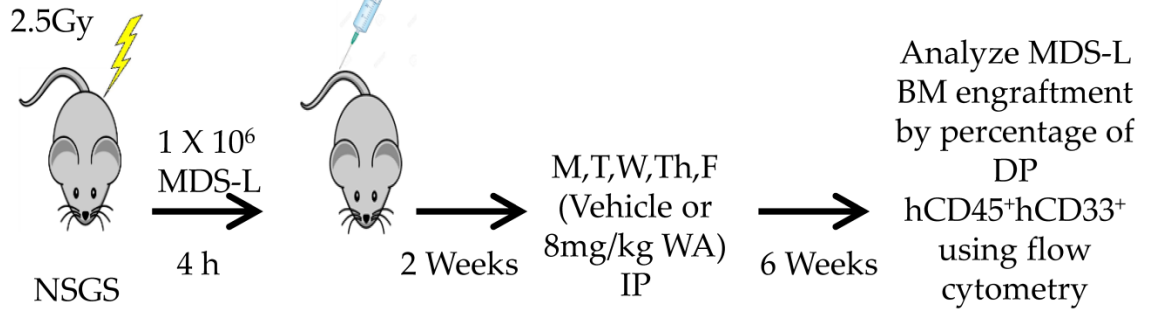


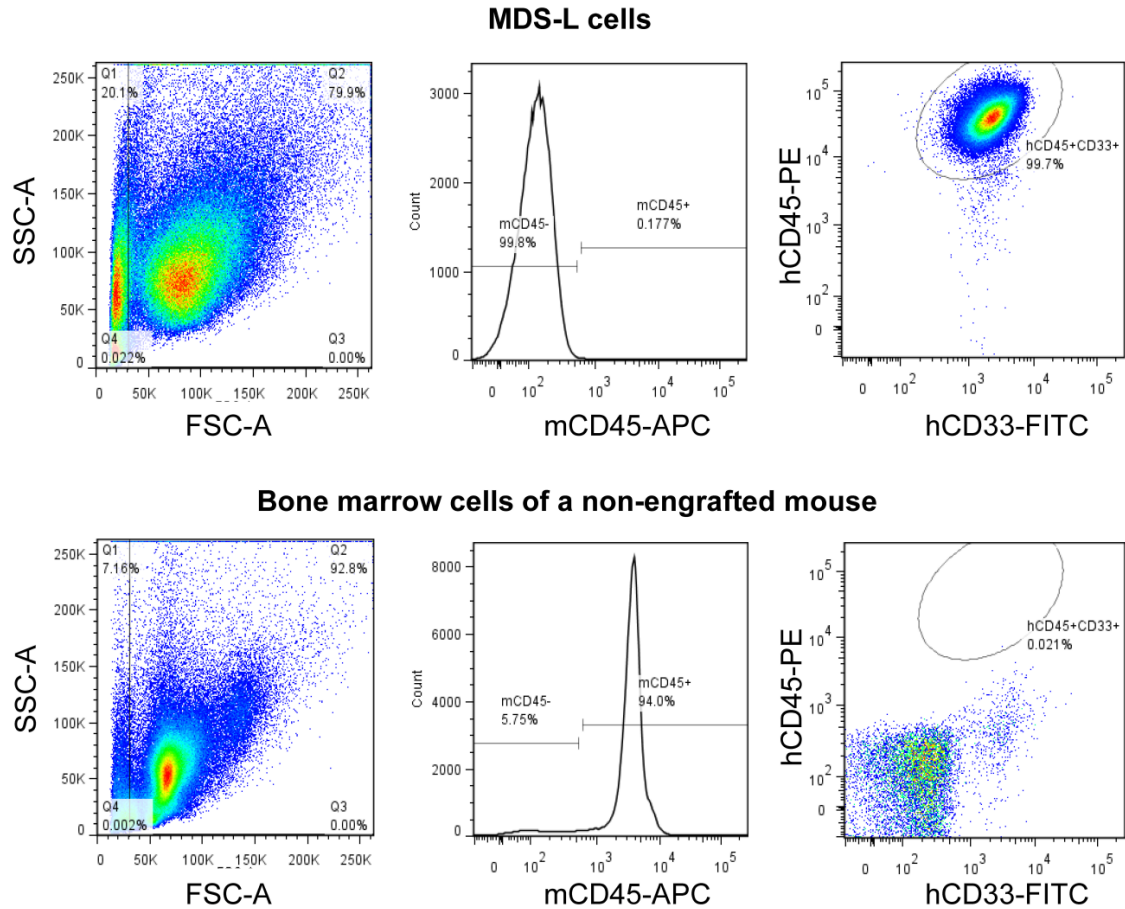
Figure 3.6: Toxicity from combining radiation and WFA treatment is prevented by delaying WFA treatment

Mice were weighed on day 0 to determine baseline weights and exposed to 2.5Gy total body irradiation. On day 14 post irradiation, irradiated mice were treated with WFA (8 mg/kg) for 5 consecutive days. Weights were monitored during and after WFA treatment. Littermate mice neither exposed to radiation nor treated with WFA were used as controls.

3.7A

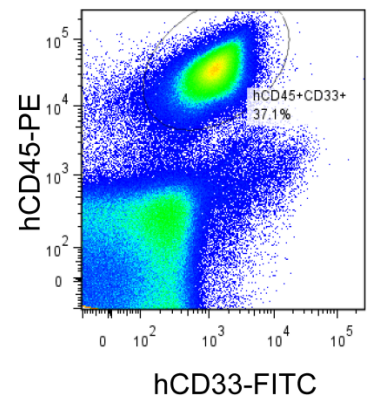
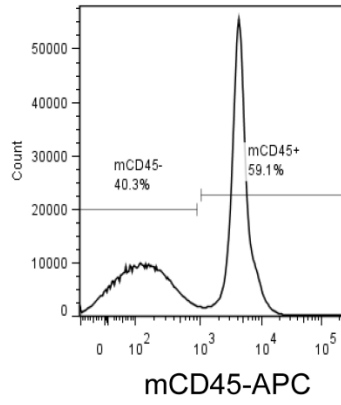
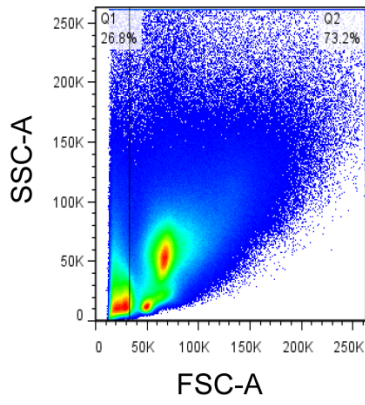


3.7B

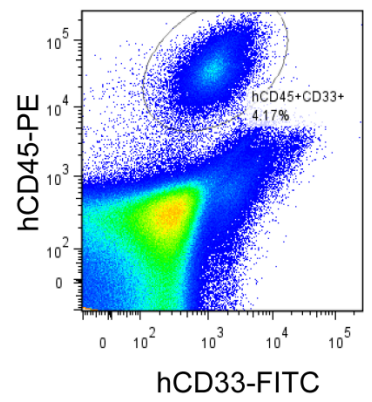
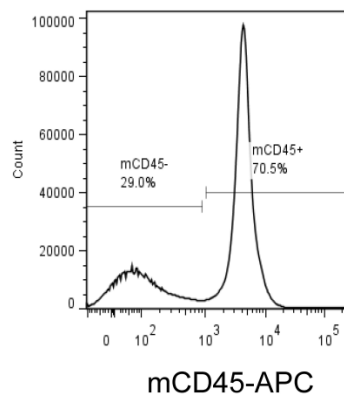
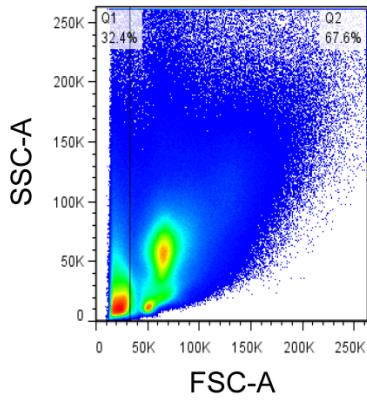


3.7C

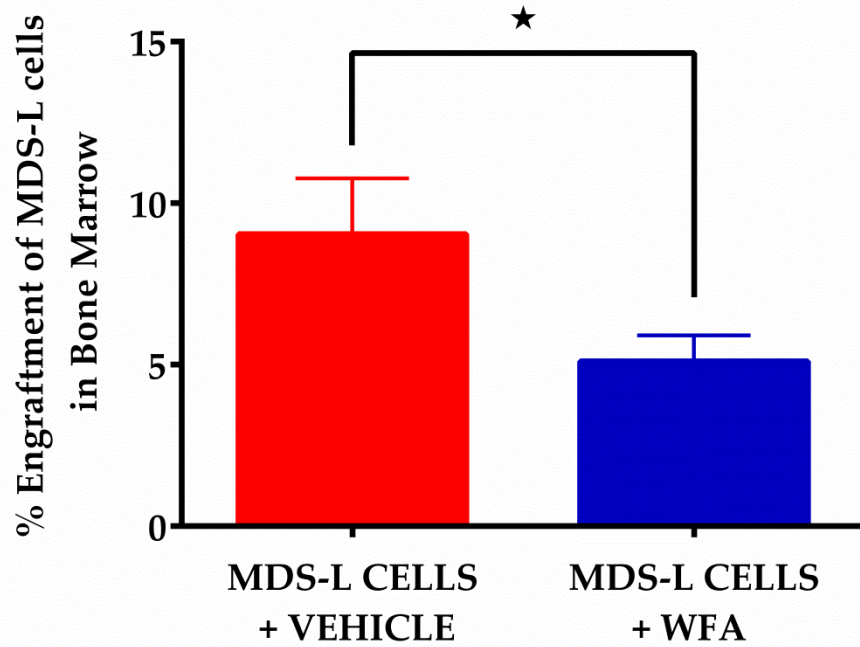
Vehicle control



8 mg/kg WFA



3.7D



3.7E

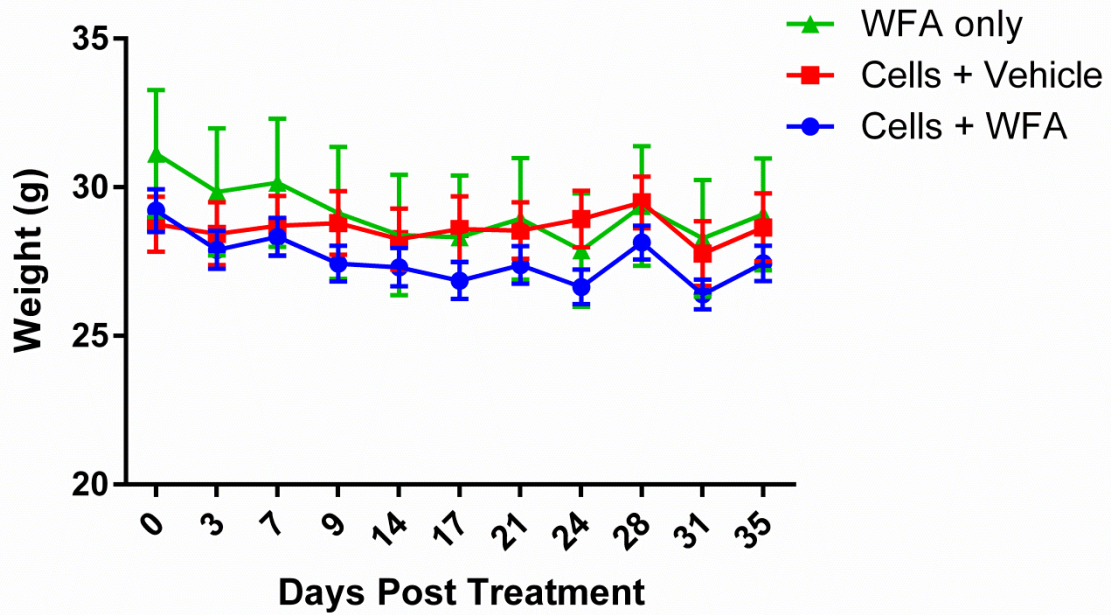


Figure 3.7: WFA significantly reduced engraftment of MDS-L cells in the bone marrow of NSGS mice

(A) Schematic representation of the experiment conducted to test the *in vivo* effect of WFA in the MDS-L NSGS mice xenograft model. (B) Flow cytometry gating scheme used for positive and specific identification of engrafted human MDS-L cells. Bone marrow cells were stained with mouse anti-mouse CD45-APC, and anti-human antibodies (CD45-PE and CD33-FITC) to identify mouse and MDS-L cells respectively. The human markers were applied to the mouse CD45 negative gate to ensure accuracy and specificity as false positive cells were not detected in non-engrafted mice. (C) Representative flow cytometry profiles of vehicle or WFA treated mice using the gating scheme illustrated in (B). (D) Engraftment of MDS-L cells was calculated as a percentage of total bone marrow cells. Average engraftment of 20 mice in the vehicle control group and 27 mice in the WFA group \pm SD is shown. (E) Average weight variation of mice during the course of the study. * = $p < 0.05$.

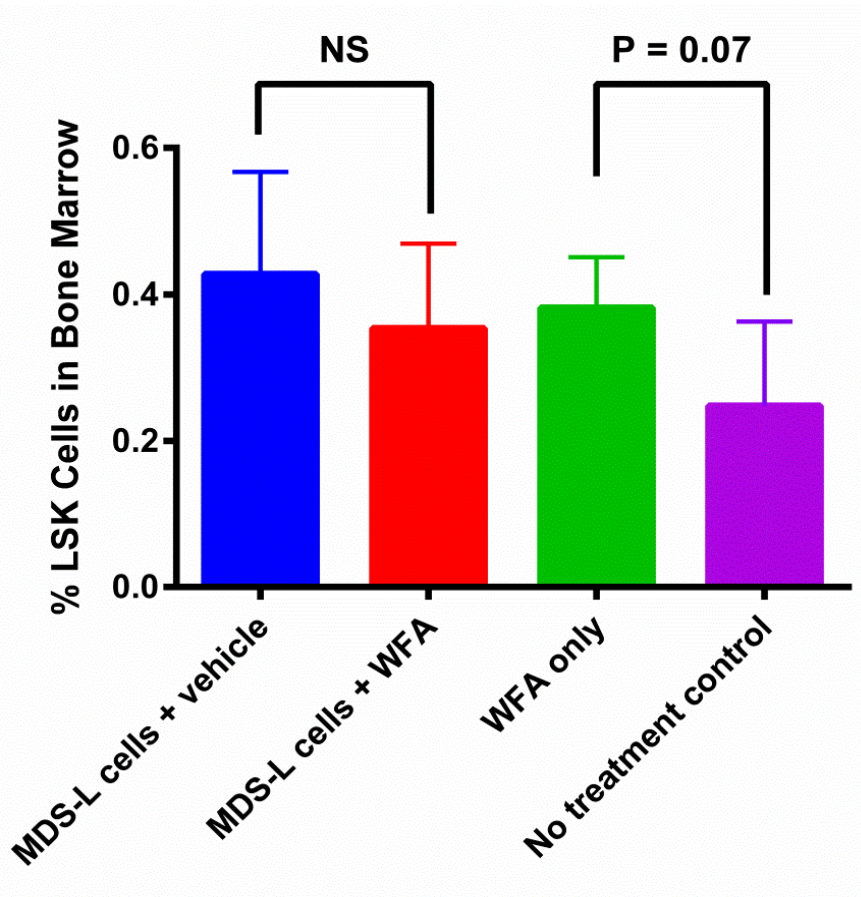
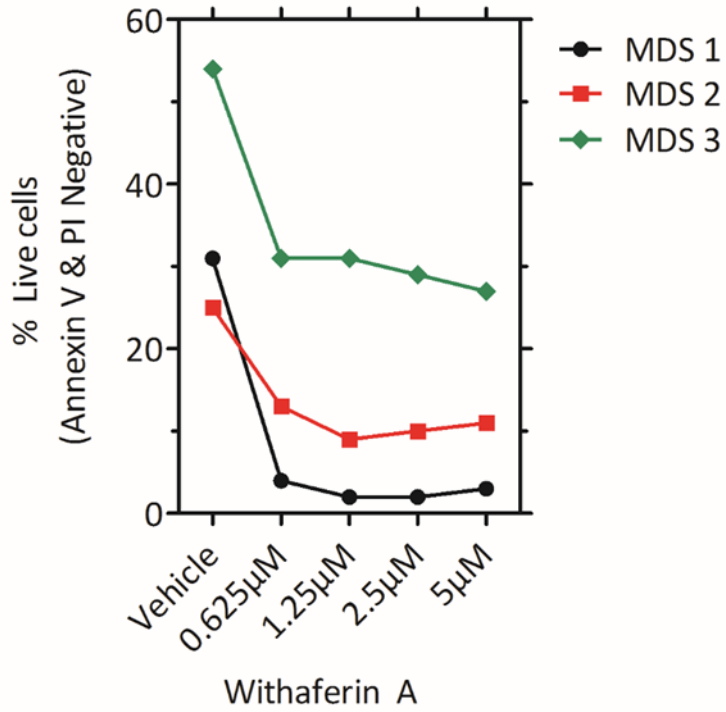


Figure 3.8: WFA treatment does not cause mouse bone marrow suppression

Bone marrow cells from MDS-L engrafted and non-engrafted mice treated with WFA or vehicle; or control mice were labeled with biotin-coupled rat anti-mouse lineage specific antibodies to CD11b (Mac-1), B220, Gr-1, CD8 α , Ter-119 and CD5. Lineage negative, Sca-1 positive and c-KIT positive (LSK) stem cells were identified by flow cytometry analyses of lineage labelled cells stained with streptavidin APC CY7, Sca-1-PB and c-KIT-APC. Mean % of LSK cells for a minimum of 5 mice per group \pm SD is shown. ** = $p < 0.005$

3.9A



3.9B

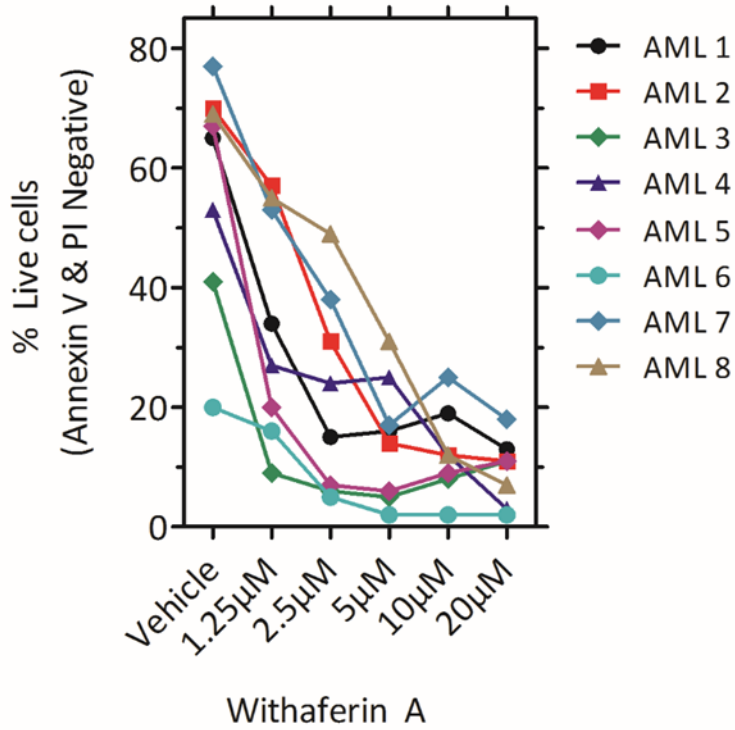


Figure 3.9: WFA induced apoptosis of human primary MDS and AML bone marrow cells

Human primary MDS (A) or AML (B) samples were treated with various concentrations of WFA and stained with annexin-V and PI after 24 h of culture. Cell viability was assayed by flow cytometry and the percentage of live or non-apoptotic cells defined as annexin-V and PI negative are shown.

Experiment performed in collaboration with Rajeswaren Mani DVM, PhD.

3.10

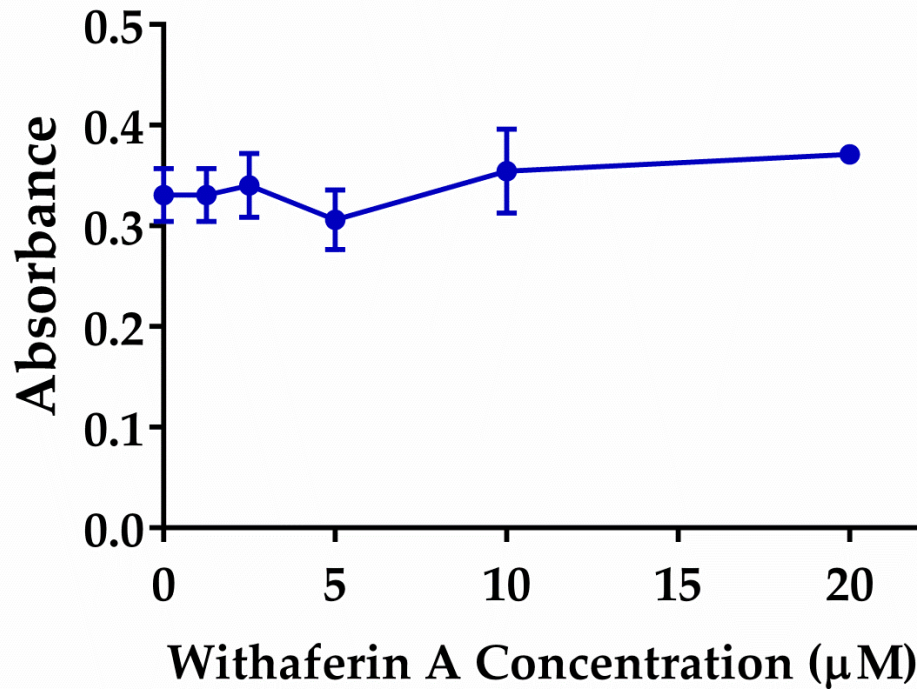


Figure 3.10: WFA had no significant effect on the viability of normal human primary bone marrow cells

Normal human primary bone marrow cells were treated with DMSO or WFA at 1×10^6 cells per well of a 96 well plate for 48 h and cell viability was measured by MTT assay. Data are presented as mean \pm SD of triplicate cultures.

Representative results of two independent experiments are shown.

Summary

WFA induced a dose dependent decrease in viability of MDS-L cells *in vitro*. The IC50 varied by cell density per well. Dose response variability with cell density suggests that a minimum threshold of drug might be required to induce WFA cytotoxicity in cells, i.e, insufficient drug is available to meet that threshold in all cells when high cell density is used. WFA was markedly more effective than lenalidomide, the current FDA approved drug for the treatment of 5q MDS, in inhibiting the viability of MDS-L cells *in vitro*. Consistent with the *in vitro* data, WFA significantly inhibited engraftment of MDS-L cells in NSGS mice without bone marrow suppression which is an important dose-limiting side effect of most chemotherapy drugs. WFA was also cytotoxic to human primary MDS cells but had no significant effect on the viability of normal human primary bone marrow cells. We also found WFA to be cytotoxic to the AML cell line KG1 as well as several human primary AML cells. These data suggest that WFA could be a novel therapeutic agent for the treatment of MDS/AML with minimal side effects.

CHAPTER FOUR

Signaling pathways involved in WFA-induced apoptosis in MDS-L cells

To investigate possible mechanisms mediating WFA-induced growth suppression of MDS-L cells, our initial efforts tested whether the mechanisms widely reported to mediate growth inhibitory effects of WFA in other cancer models were true for MDS as well. Inhibition of NF- κ B is amongst the mechanisms most commonly reported to mediate the anticancer effects of WFA^{41,44}. NF- κ B has been implicated in hematologic and solid tumors¹³⁹. The oncogenic potential of NF- κ B is demonstrated by its ability to stimulate cell proliferation, inhibit apoptosis and promote metastasis¹⁴⁰. In fact, NF- κ B has been suggested as a potential therapeutic target in MDS¹³⁹. Therefore, we tested if NF- κ B was involved in the inhibition of MDS-L cell survival by WFA. To our surprise, NF- κ B was unaffected by WFA treatment in MDS-L cells as shown by both immunofluorescence (4.1A, B) and immunoblotting (4.1C) analyses of the nuclear and cytoplasmic distribution of the p65 subunit. In fact, we found that NF- κ B was not constitutively active in MDS-L cells.

These results prompted us to perform mechanistic studies from a different angle. We used gene expression changes mediated by WFA to explore possible mechanisms mediating the cytotoxic effects of WFA in MDS-L cells. To this end, we performed microarray gene expression analysis using the Affymetrix human gene 2.0 ST array platform. The gene expression profile of MDS-L cells treated with 10 μ M WFA for 6 h or 12 h was compared to control. Three independent

samples were used per experimental group. We focused on early time points in an effort to identify primary gene alterations caused by WFA.

4a) WFA significantly altered expression of genes linked to cell death and survival, cell growth and proliferation, cell cycle regulation and cancer

Differentially expressed genes between control and WFA treatment groups determined as fold change > 3 and q-value < 0.05 were used as input for Bio Functional Analysis by the ingenuity pathway analysis (IPA) software. The top 15 enriched biological functions and /or diseases most in the data set are shown in Figure 4.2. Consistent with the results in chapter one, cell death and survival, cell growth and proliferation, cell cycle regulation and cancer were amongst the top significantly regulated biological processes at both 6 h (Figure 4.2A) and 12 h (Figure 4.2B). The top 10 elevated and repressed genes were arranged according to fold changes and we found that c-Jun (Jun) and FosB were among the top 3 up-regulated genes at 6 h and the top 2 up-regulated genes at 12 h (Figure 4.3). We also performed gene set enrichment analysis (GSEA) using the GSEA software to identify significantly enriched pathways. WFA resulted in a highly significant enrichment in expression of apoptosis related genes at both 6 h (Figure 4.4A, false discovery rate (FDR) q-value = 0.0001; family-wise error rate (FWER) p-value = 0.0001) and 12 h (Figure 4.4B, FDR q-value = 0.0001; FWER = 0.008). These results suggest the possibility that WFA inhibited MDS-L proliferation and viability (chapter one) by inducing apoptotic cell death.

4b) WFA induced apoptosis of MDS-L cells

Pathway enrichment analyses of the microarray data revealed WFA treatment significantly affected expression of apoptosis related genes (Figure 4.4). Therefore, we performed apoptosis assays to determine if changes in the expression of these genes had a functional consequence on MDS cells. A decrease in mitochondrial membrane potential (MMP) is a well-known indicator of apoptosis¹⁴¹. So we tested if WFA decreased the MMP of mitochondria in MDS-L cells. MMP measurement was performed by the widely used JC-1 assay. JC-1 is a lipophilic cationic dye with a unique property in that it reversibly changes color from orange-red to green as MMP decreases¹³². This property is due to the ability of JC-1 to form aggregates at high concentrations within the mitochondrial interior, which revert to monomers in the cytosol where concentration decreases¹³². The concentration of JC-1 within the mitochondria of viable cells is driven by the negative potential gradient between the mitochondrial interior and the cytosol¹³². The negative potential gradient between mitochondrial interior and the cytosol is lost as MMP decreases, causing a release of the dye into the cytosol where it is less concentrated¹³². Therefore, a decrease in the aggregate/monomer ratio is indicative of a decrease in MMP. Treatment of MDS-L cells with WFA resulted in a significant decrease in MMP (Figure 4.5A, B).

During apoptosis, a decline in MMP ultimately results in the activation of caspases^{141,142}. Caspases are a family of proteases that are crucial regulators of the apoptotic process and caspase-3 is the most frequently activated of the known human caspases¹⁴². Immunoblotting analysis revealed that WFA activated

caspase-3 in MDS-L cells as early as 6 h after WFA treatment which persisted at 12 h of WFA exposure (Figure 4.6). As expected, there was a concomitant decrease in total caspase-3 (Figure 4.6). To further establish the apoptosis induction by WFA, we performed an annexin-V apoptosis assay by flow cytometry on WFA-treated MDS-L cells. Consistent with the MMP and caspase-3 data, WFA caused a dose-dependent increase in apoptotic cells (Figure 4.7A, B).

4c) WFA activated JNK MAPK signaling in MDS-L cells

After having confirmed that growth suppression of MDS-L cells by WFA involved cell death by apoptosis, we next investigated possible signaling pathway (s) mediating apoptosis of MDS-L cells treated with WFA. Apoptosis pathways linked to up-regulated genes (Figure 4.3) were examined. Our process involved verifying the microarray data and scouring the literature for evidence suggesting the gene in question is involved in apoptosis induction. Bcl2-associated athanogene 3 (BAG3) and Regulator of G-protein signaling 2 (RGS2) highlighted in blue (Figure 4.3), are examples of genes which fell short, though they were highly up-regulated. Although we were able to verify induction of BAG3 by qRT-PCR (Figure 4.8), evidence from the literature suggest it plays more of an anti-apoptotic role¹⁴³. It is likely that BAG3 up-regulation was a secondary feedback effect from the induction of apoptosis rather than the mediator. This highlights the challenge of identifying primary gene expression changes from global gene expression data sets. For RGS2 on the other hand, although there is evidence from the literature suggesting RGS2 mediates apoptosis¹⁴⁴⁻¹⁴⁶, the microarray data could only be validated at the mRNA but not at the protein level (Figure 4.9).

In addition, the p38 MAPK pathway that is thought to be involved in RGS2 mediated apoptosis¹⁴⁴ is not activated by WFA in MDS-L cells (Figure 4.9B). The dramatic reduction in p38 MAPK activation at early time points may have some role in reduction of RGS2 but the decrease in these proteins suggests a pro-survival role for them in the context of MDS-L cells. However, this was not further investigated as we focused on genes that have positive effects on expression or activation of pro-apoptotic molecules.

c-Jun and FosB were also among the top 3 up-regulated genes at 6 h and the top 2 up-regulated genes at 12 h by WFA in MDS-L cells (Figure 4.3). c-Jun and FosB can heterodimerize to form an AP-1 transcription factor that is activated by phosphorylation of the c-Jun subunit by JNK^{93,101}. It has been demonstrated that apoptosis can be regulated by JNK/AP-1 signaling⁹³. Hence, we investigated if WFA activated JNK/AP-1 signaling in MDS-L cells. Even though JNK signaling can be triggered by cytokine receptor signaling, we chose to investigate an ROS mediated JNK activation pathway considering that ROS production has been shown to mediate WFA effects in other cancer systems^{44,93}. JNK cascade activation can be mediated by the ROS sensitive ASK1 which activates MKK7, the MAP2K known to specifically activate JNK^{98,108}. Taking all these facts together, we hypothesized that ROS mediated JNK activation will have a role in AP-1 expression in MDS-L cells treated with WFA as illustrated in Figure 4.10. To test this hypothesis, we first verified WFA-induced expression of c-Jun and FosB by qRT-PCR. As can be seen from figure 4.11, there was a robust increase in c-Jun (Figure 4.11A) and FosB mRNA (Figure 4.11B). Next,

we examined if WFA treatment caused any changes in ROS production in MDS-L cells since increase in ROS is the initiating event of the proposed signaling pathway activated by WFA (Figure 4.10). WFA increased ROS accumulation in MDS-L cells compared to DMSO control as measured by increased fluorescence of the ROS sensitive dye, carboxy-H₂DCFDA (4.12A, C). Pretreatment for 4 h with NAC, a ROS scavenger, before adding WFA led to complete inhibition of WFA generated ROS (Figure 4.12B, C). As illustrated in Figure 4.10, an increase in ROS can lead to ASK1 activation which is the MAP3K upstream of MKK7. Hence, we verified if the observed increase in ROS production by WFA activated ASK1 by examining the phosphorylation status of MKK7. Indeed, we found that WFA increased MKK7 phosphorylation or activation (Figure 4.13A). Given that MKK7 solely activates JNK⁹⁸, WFA treatment also led to increased JNK activation as expected (Figure 4.13B). Activated JNK is known to translocate to the nucleus where it phosphorylates c-JUN (Figure 4.10). Therefore, it was no surprise that c-Jun phosphorylation was increased by WFA treatment (Figure 4.13C). The fact that c-Jun phosphorylation was only detectable at 6 h compared to JNK phosphorylation which could be detected as early as 30 min, suggested a sequential activation of the signaling cascade (Figures 4.10 and 4.13). Total c-Jun protein levels increased at both 6 and 12 h (Figure 4.13C) which was in agreement with the qRT-PCR results (Figure 4.11A). These results suggest that increase in JNK activation and c-Jun expression could both contribute to the observed increase in c-Jun phosphorylation.

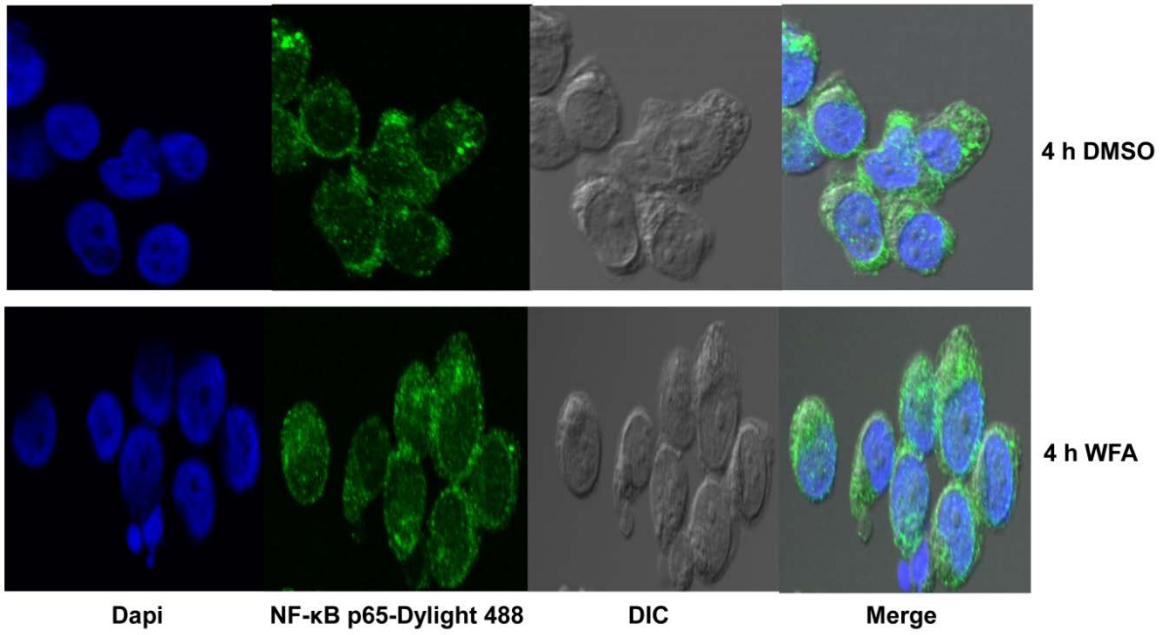
Phosphorylation of c-Jun is associated with transcriptional activation of AP-1¹⁰¹ (Figure 4.10). We therefore then performed an AP-1 luciferase assay to determine if WFA-induced increase in c-Jun and FosB in MDS-L cells had a functional consequence on the transcriptional activity of AP-1. MDS-L cells transfected with either the AP-1 reporter or empty vector expressing firefly luciferase were treated with WFA for 12 h and promoter activity was assessed by the dual Glo luciferase assay. The known activator of AP-1, PMA, was used as a positive control for luciferase assays¹⁴⁷. Cells were co-transfected with a control vector expression renilla luciferase under the control of a constitutively active thymidine kinase promoter. WFA potently induced AP-1 luciferase expression (Figure 4.14A). These data were expanded by demonstrating transcriptional activity of AP-1 even further by showing that WFA increased mRNA expression of BIM (BCL2L12) (Figure 4.14B) and p21 (Figure 4.14C), both of which are bona fide AP-1 targets^{85,111,112}.

4d) WFA arrested MDS-L cells at S and G2/M cell cycle phases

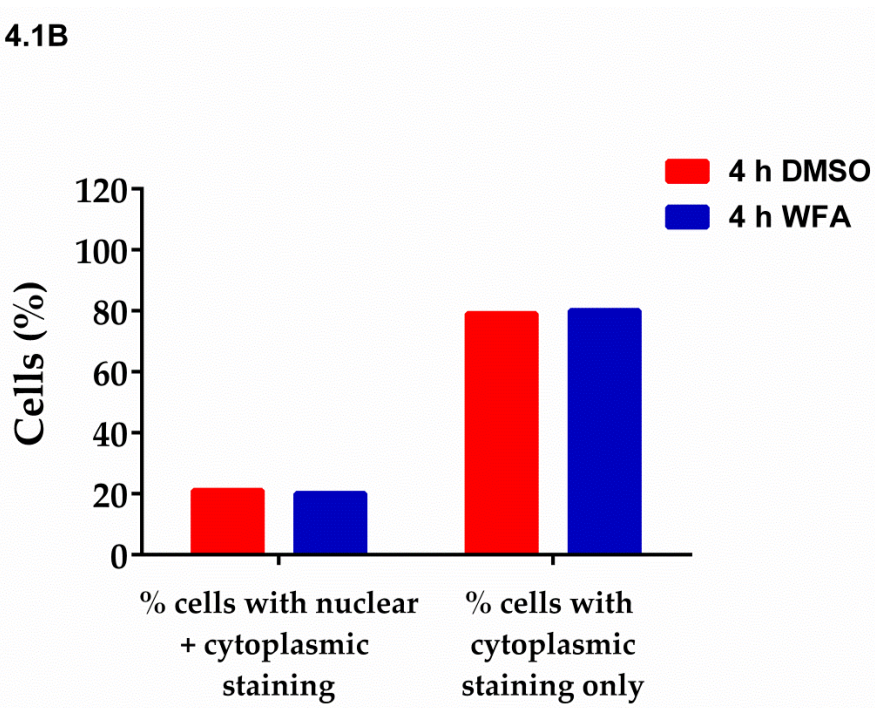
p21 is a well-known negative regulator of cell cycle progression¹⁰⁷. Therefore, the increase in p21 expression following WFA treatment (Figure 4.14C) suggested that WFA might cause cell cycle arrest of MDS-L cells. Moreover, WFA has been shown to induce cell cycle arrest of several other types of cancer cells^{44,45}. Hence, we asked if WFA treatment had an effect on the cycling of MDS-L cells. Cell cycle analysis by flow cytometry showed WFA indeed caused MDS-L cells to arrest at both S and G2/M phases (Figure 4.15). Consistent with cell cycle analysis data, treatment with WFA significantly

decreased mRNA and protein levels of the cyclins and CDKs required for completion of both S (cyclin A and CDK2) (Figure 4.16A-C) and G2/M (cyclin B and CDK1) (Figure 4.17A-C) phases of the cell cycle. The observed decreases in expression of these cyclins and Cdk's could likely be explained by increased expression of p21 (Figure 4.14C). Even though p21 inhibits cell cycle progression primarily by inhibiting the activities of CDK1 and CDK2, it has also been shown to be involved in transcriptional repression of several cell cycle genes including cyclins and Cdk's such as CDK1, CCNB1 and CCNA1^{91,148,149}. WFA-induced cell cycle arrest could also contribute to apoptotic death of MDS-L cells since prolonged arrest in S and G2/M phases eventually triggers apoptosis⁸⁵.

4.1A



4.1B



4.1C

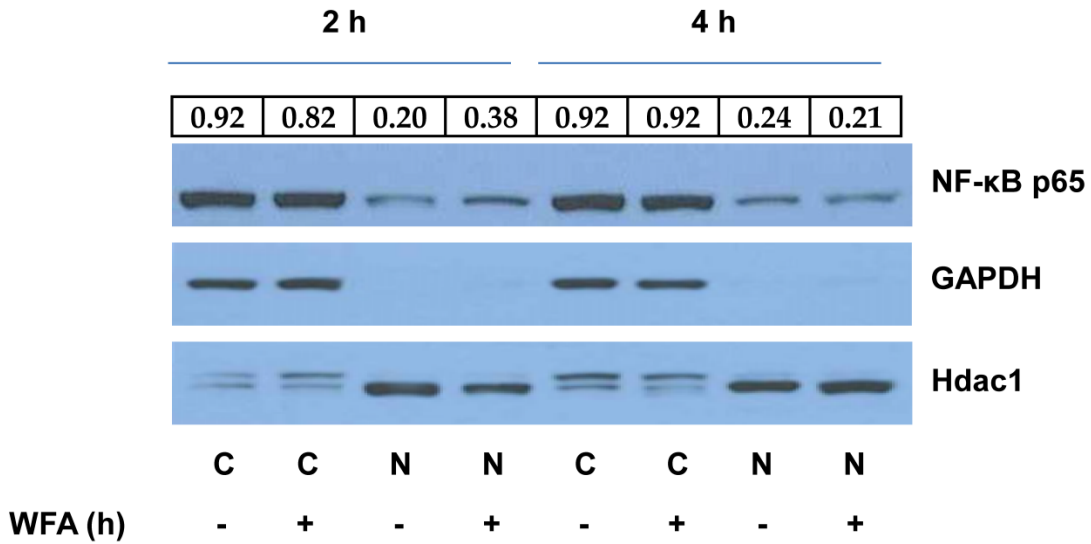
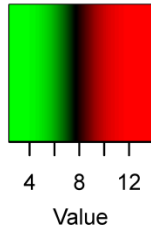


Figure 4.1: Cytotoxic effects of WFA in MDS-L cells are independent of NF- κ B activation

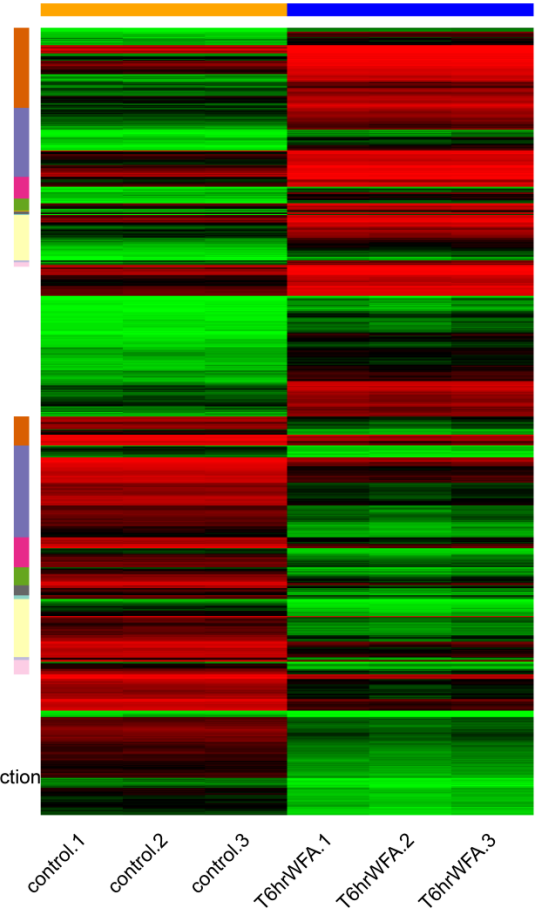
(A) MDS-L cells treated with 10 μ M WFA or DMSO for 4 h were stained for the p-65 subunit of NF- κ B and nuclear and cytoplasmic distribution of NF- κ B was determined by fluorescence microscopy. A representative field is shown. (B) Quantification of cells (> 200 cells) in several fields with nuclear and/ or cytoplasmic p-65 in MDS-L cells treated with 10 μ M WFA or DMSO for 4 h. (C) Nuclear and cytoplasmic protein fractions of cells treated with 10 μ M WFA or DMSO for 2 or 4 h were used for western blotting to examine the effect of WFA treatment on nuclear translocation of the p65 subunit of NF- κ B. Cytoplasmic (C) or nuclear (N) p65 NF- κ B was normalized to GAPDH or Hdac1 respectively and densitometric ratios are shown. Data are representative of two independent experiments.

4.2A

Color Key



- Neurological Disease
- Cell Death and Survival
- Cellular Development
- Cellular Growth and Proliferation
- Connective Tissue Development and Function
- Tissue Development
- DNA Replication, Recombination, and Repair
- Cell Cycle
- Cancer
- Organismal Injury and Abnormalities
- Tumor Morphology
- Cellular Movement
- Skeletal and Muscular System Development and Function
- Reproductive System Disease
- Gene Expression



4.2B

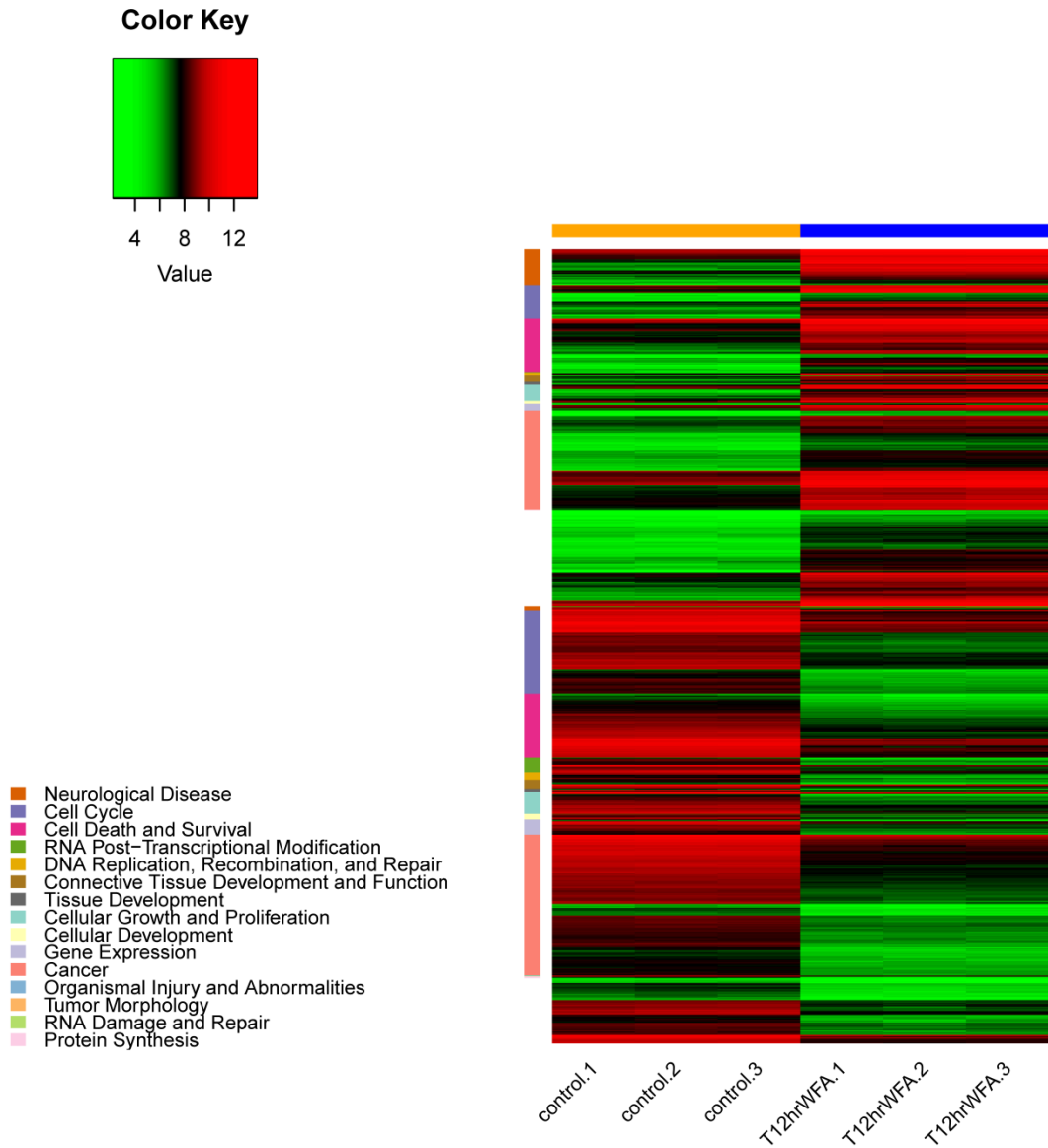


Figure 4.2: Biological functions and/ or diseases most significantly affected by WFA treatment in MDS-L cells

Heatmap of differentially expressed genes ($p < 0.05$) between control and 6 h WFA treated samples (A) or 12 h WFA treated samples (B). The top fifteen biological functions and /or diseases enriched in the data set identified by IPA are shown. Genes that belong to a specific IPA biological function are clustered and

represented by a colored square next to the heatmap. Color key legend represents \log_2 normalized expression values ranging from low expression (green) to high expression (red).

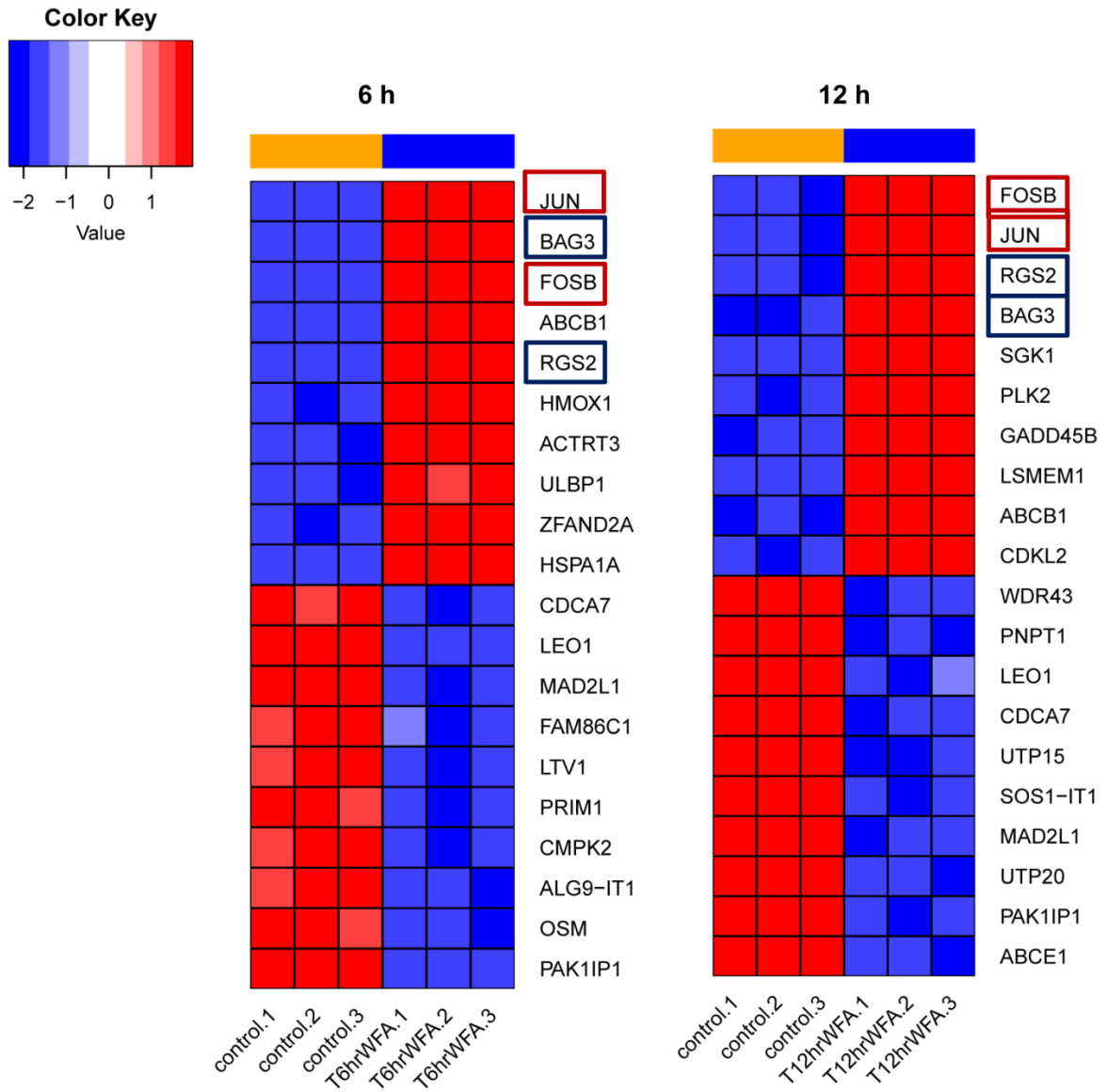
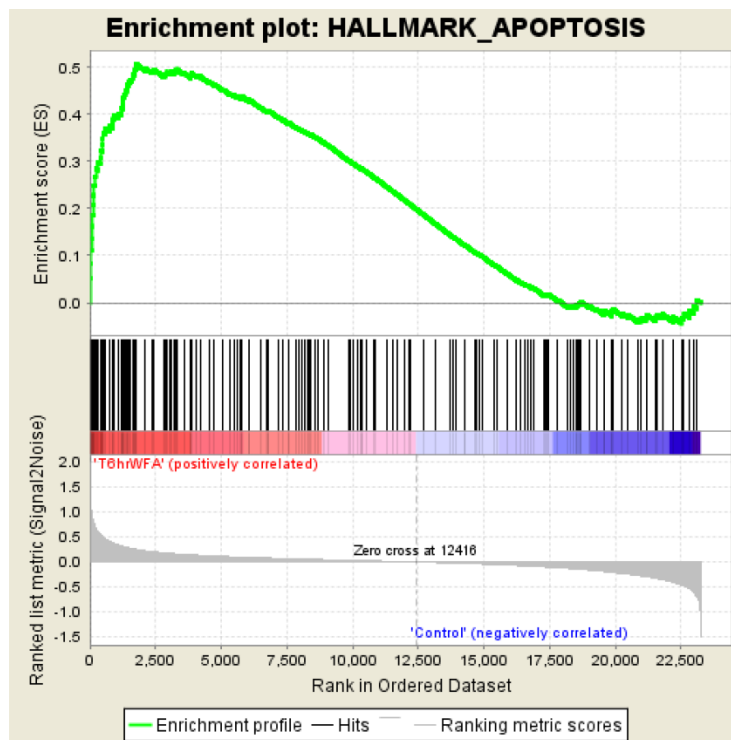


Figure 4.3: Heatmap of top 20 WFA regulated genes by fold change

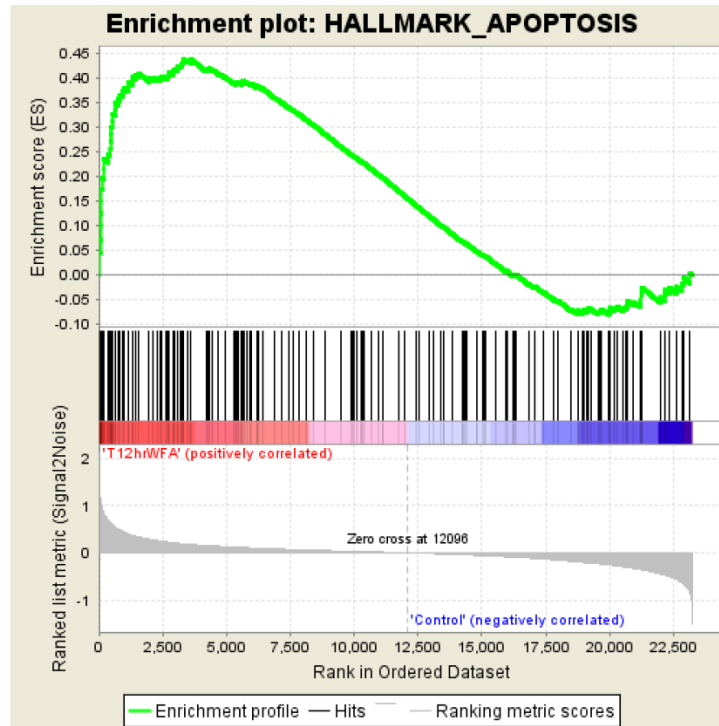
The top 10 elevated (top half) and repressed (bottom half) genes by WFA at 6 h and 12 h arranged by fold change are shown.

4.4A



Dataset	gsea.Control_vs_T6hrWFA.cls #T6hrWFA_versus_Control.Control_vs_T6hrWFA.cls #T6hrWFA_versus_Control_repos
Phenotype	Control_vs_T6hrWFA.cls#T6hrWFA_versus_Control_repos
Upregulated in class	T6hrWFA
GeneSet	HALLMARK_APOPTOSIS
Enrichment Score (ES)	0.50754654
Normalized Enrichment Score (NES)	2.0332267
Nominal p-value	0.0
FDR q-value	0.0
FWER p-Value	0.0

4.4B

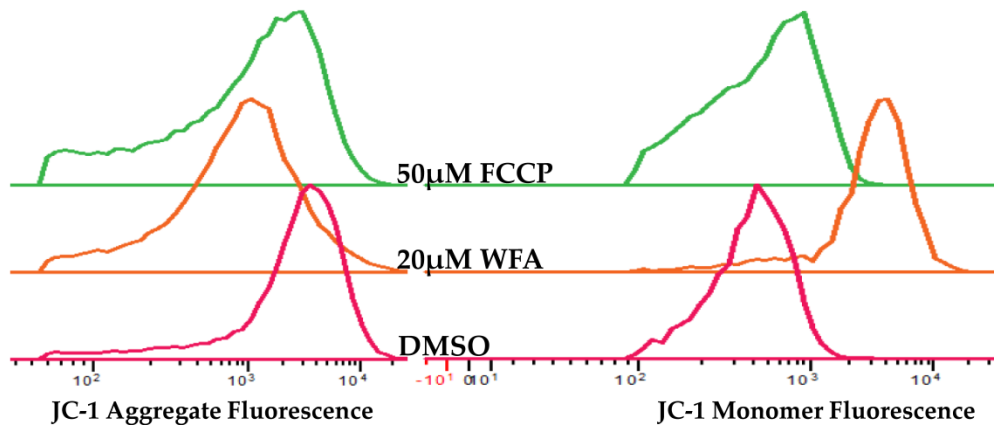
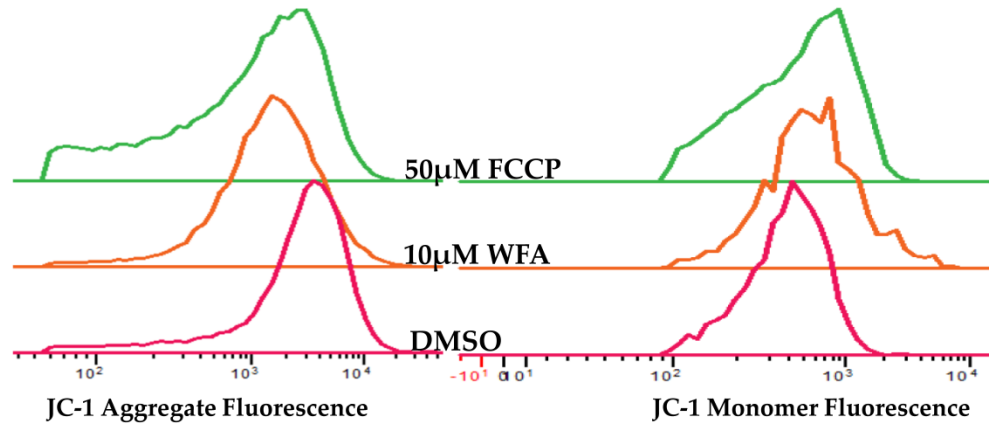


Dataset	gsea.Control_vs_T12hrWFA.cls #T12hrWFA_versus_Control.Control_vs_T12hrWFA.cls #T12hrWFA_versus_Control_repos
Phenotype	Control_vs_T12hrWFA.cls#T12hrWFA_versus_Control_repos
Upregulated in class	T12hrWFA
GeneSet	HALLMARK_APOPTOSIS
Enrichment Score (ES)	0.4382375
Normalized Enrichment Score (NES)	1.7445616
Nominal p-value	0.0
FDR q-value	0.0016486881
FWER p-Value	0.008

Figure 4.4: Genes differentially regulated by WFA are linked to apoptosis induction

Gene set enrichment analysis (GSEA) revealed enrichment of apoptosis related genes by WFA treatment at both 6 h (A) and 12 h (B) compared to control.

4.5A



4.5B

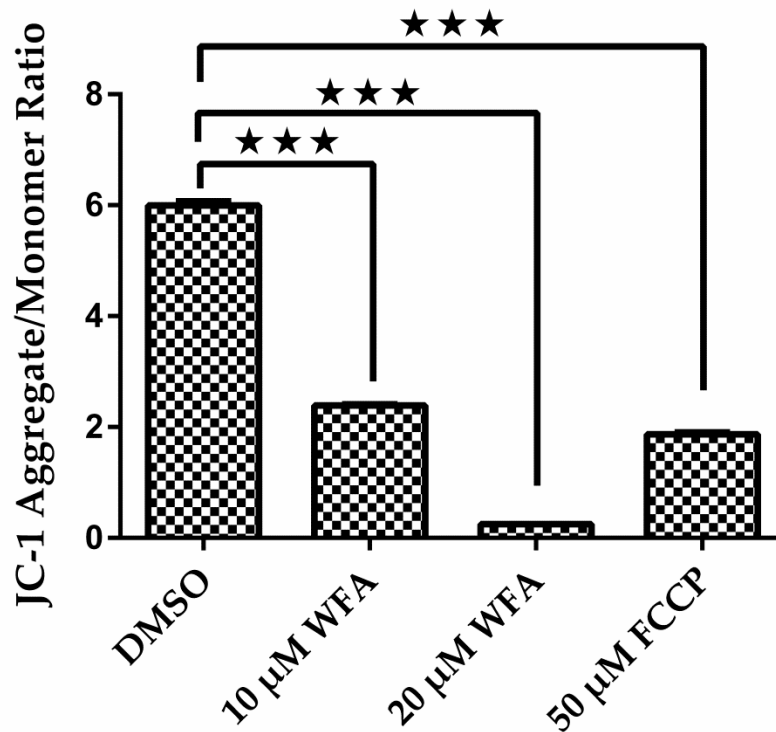


Figure 4.5: WFA decreased mitochondrial membrane potential in MDS-L cells

MDS-L cells were treated with WFA (10 μM or 20 μM) for 8 h or FCCP (50 μM) for 2 h. One μM JC-1 was added during the last 30 min of treatment and the distribution of JC-1 aggregates (red) and monomeric JC-1 (green) was analyzed by flow cytometry. (A) Representative overlays of JC-1 aggregates or monomers by mean fluorescent intensity. 10 μM WFA caused a decrease in fluorescence of JC-1 aggregates with a concomitant increase in JC-1 monomer fluorescence (upper panel) and the effect was even more dramatic with 20 μM WFA treatment (lower panel). (B) Results are shown as mean ratios \pm SD of JC-1

aggregates/monomers as a function of treatment (n = 3). *** = p<0.0005.

Representative data from one of several experiments with similar results are shown.

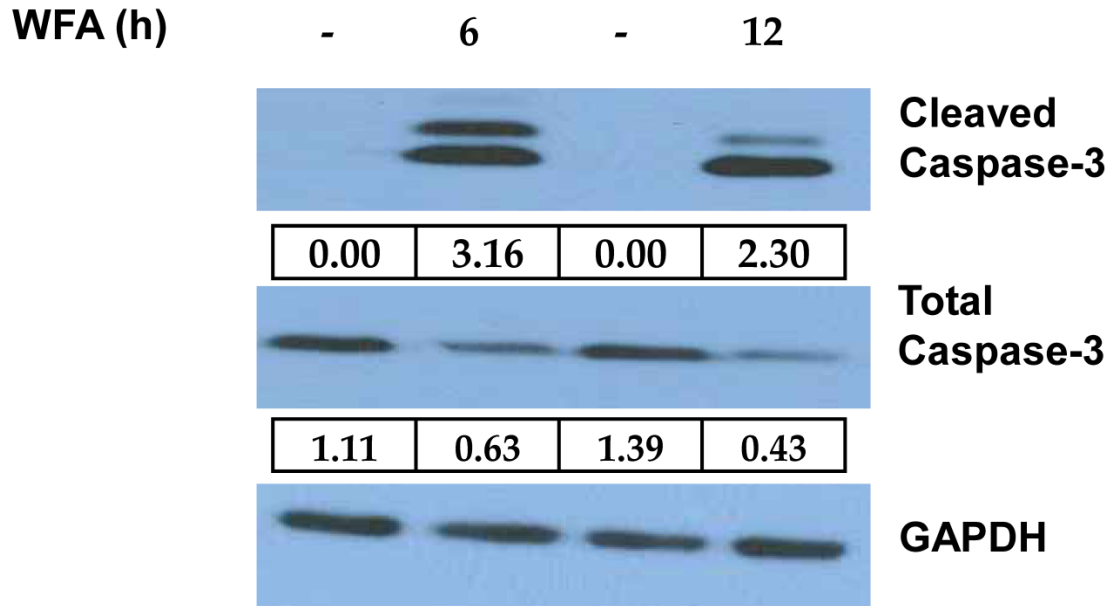
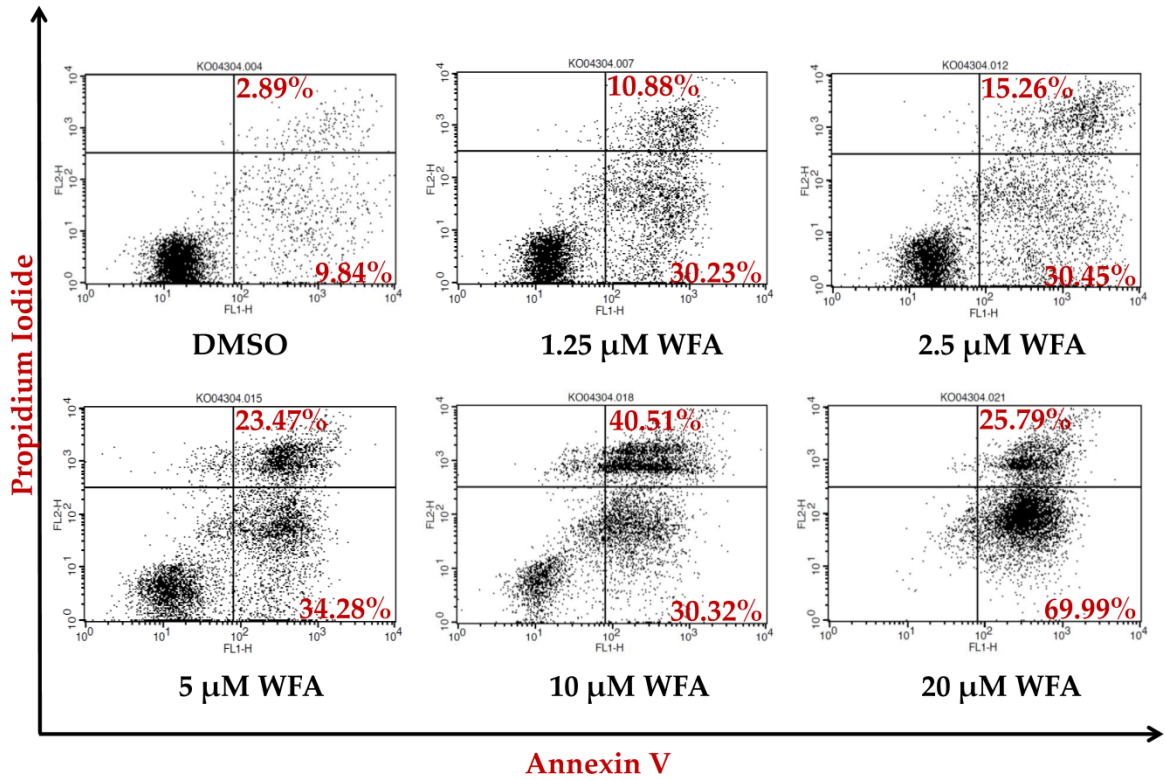


Figure 4.6: WFA stimulated activation of caspase-3

Whole cell lysates from control or WFA treated (6 h or 12 h) MDS-L cells were used for immunoblotting. Protein expression of activated (cleaved caspase-3) or total caspase-3 was normalized to GAPDH (loading control) expression and densitometric ratios are shown. Results are representative of several experiments.

4.7A



4.7B

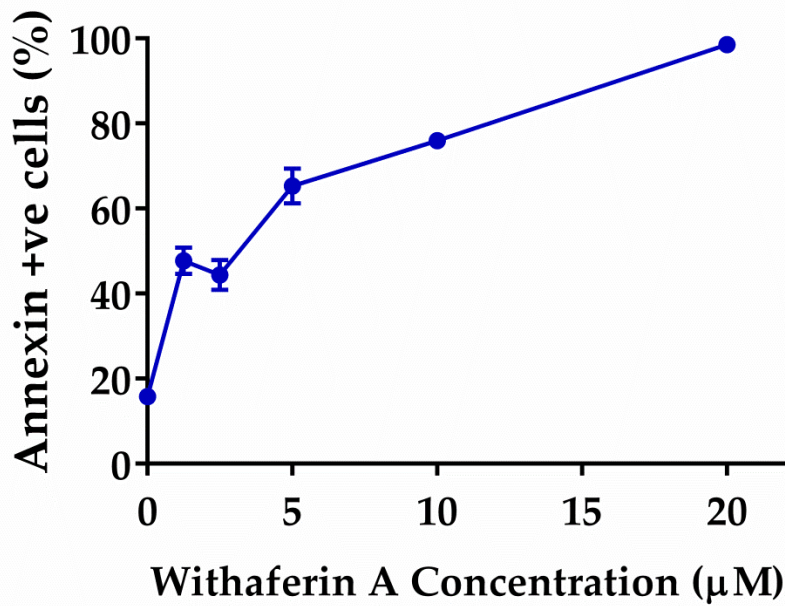


Figure 4.7: WFA induced apoptosis of MDS-L cells

Cells were treated with increasing concentration of WFA for 48 h and apoptosis was measured by annexin-V and PI staining. (A) Panels show representative flow cytometry profile for each WFA concentration used. (B) Graph shows percentage of annexin-V positive cells at different doses of WFA presented as mean \pm SD (n = 3). Data from one of three independent experiments with similar results are shown.

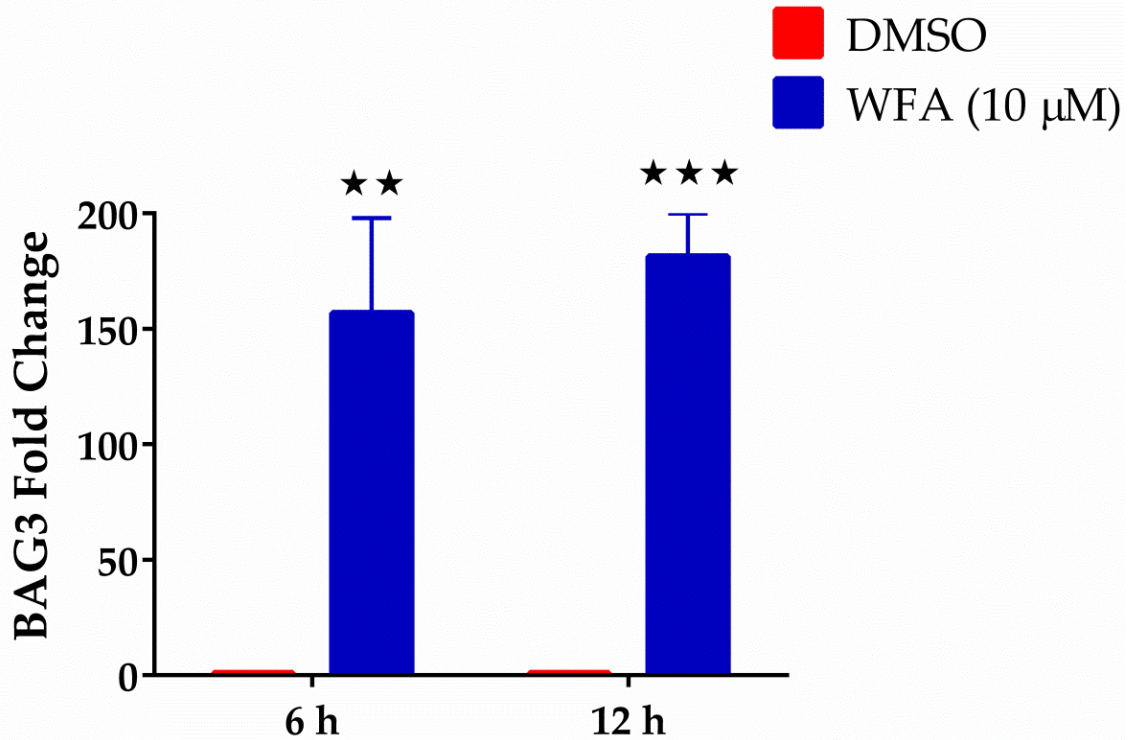
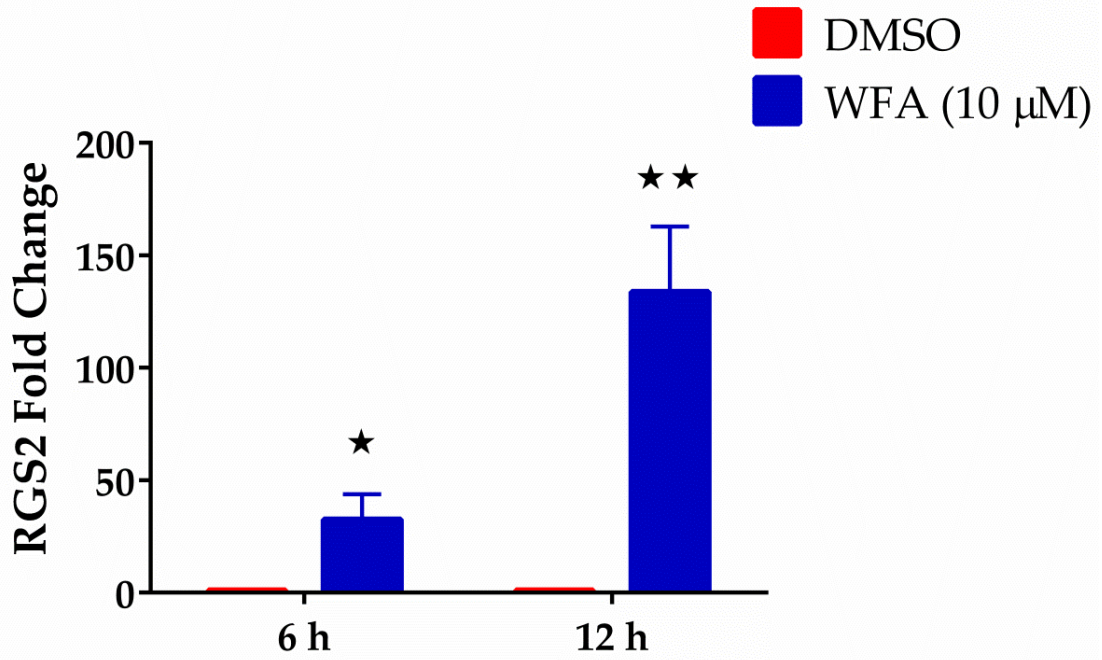


Figure 4.8: Up-regulated mRNA expression of BAG3 in MDS-L cells treated with WFA

qRT-PCR of BAG3 mRNA in cells treated with DMSO or WFA (6 h and 12 h). Gene amplification was normalized to *RPII* expression and relative amplification was determined by normalizing to DMSO control. ** = $p < 0.005$, *** = $p < 0.0005$.

4.9A



4.9B

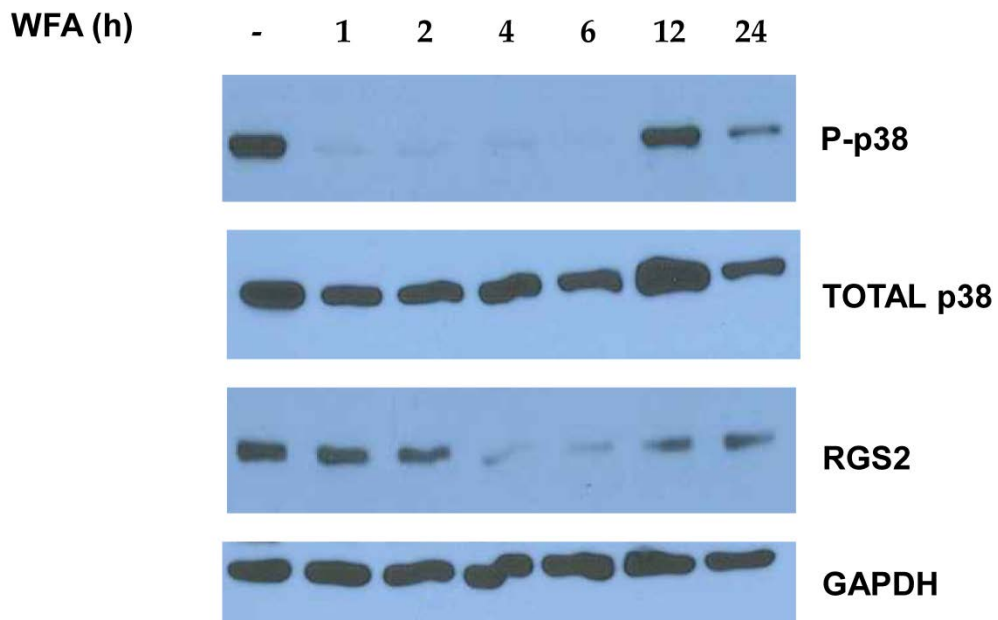


Figure 4.9: WFA increased mRNA but not protein expression of RGS2 or p38 MAPK activation in MDS-L cells

(A) Total RNA isolated from cells treated with DMSO or WFA (6 h and 12 h) was used to determine mRNA expression of RGS2 by qRT-PCR. Gene amplification was normalized to RPII expression and relative amplification was determined by normalizing to DMSO control. (B) Western blots showing the effect of WFA treatment on p38 MAPK activation and RGS2 protein expression. GAPDH was used as a loading control. Western blot analysis is representative of two independent experiments. * = $p < 0.05$, ** = $p < 0.005$.

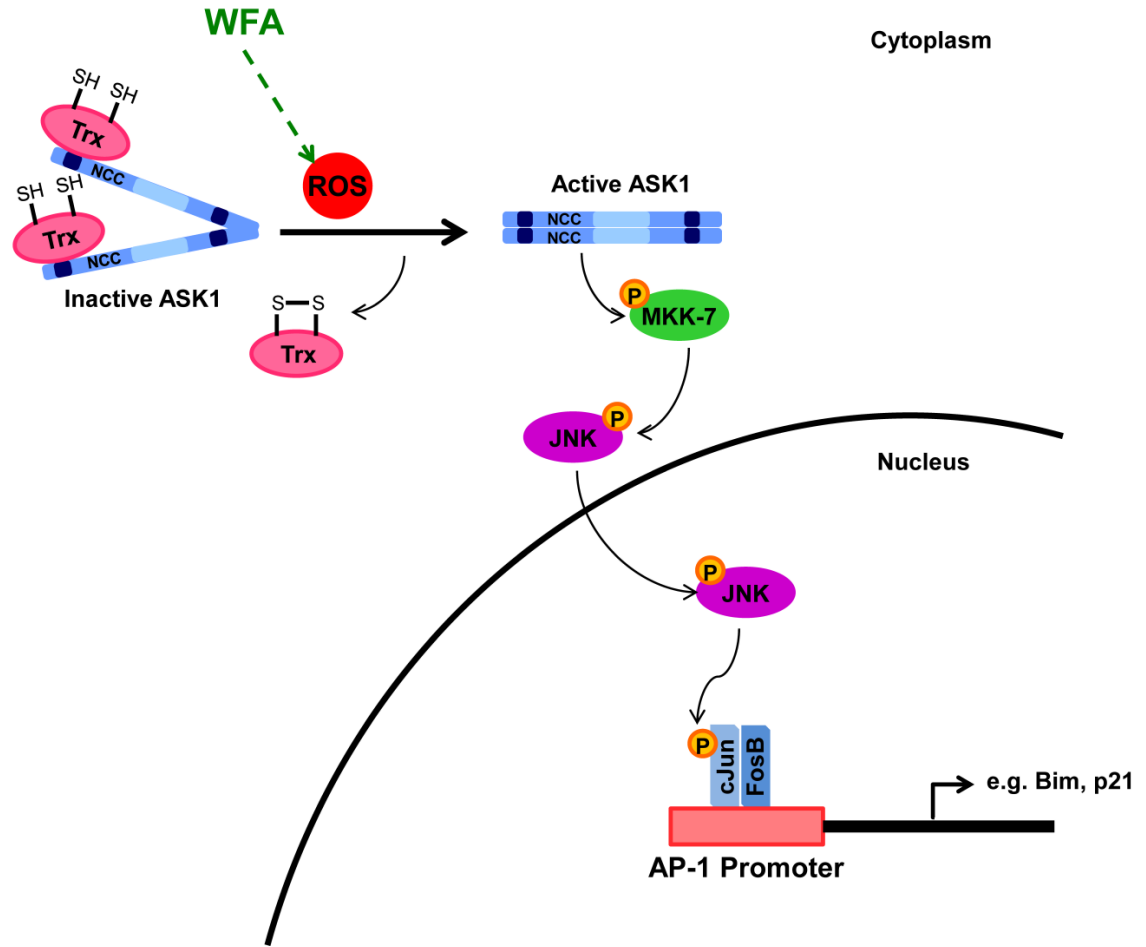
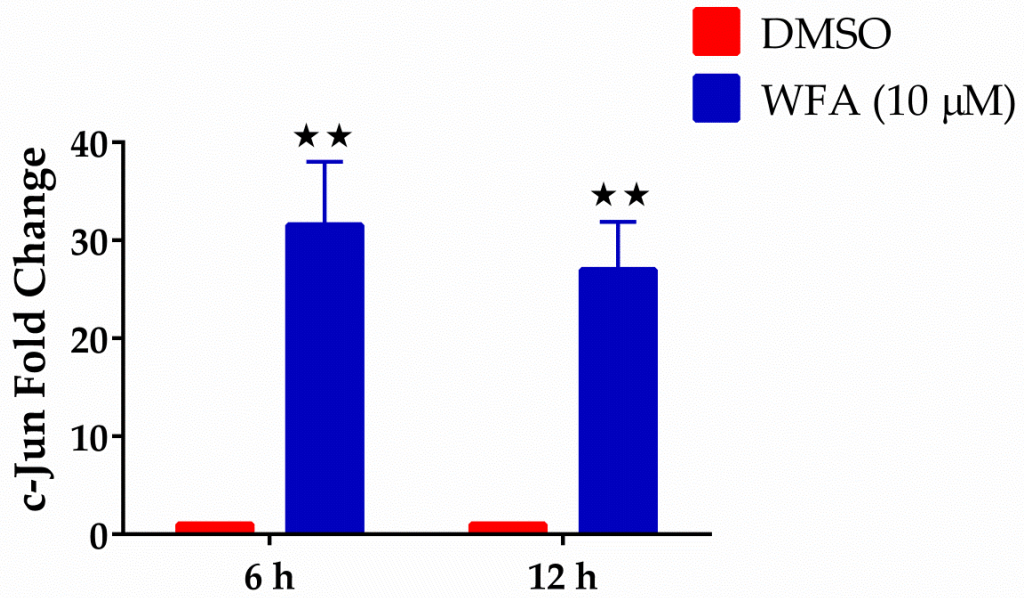


Figure 4.10: Schematic representation of ROS mediated JNK/AP-1 signaling

4.11A



4.11B

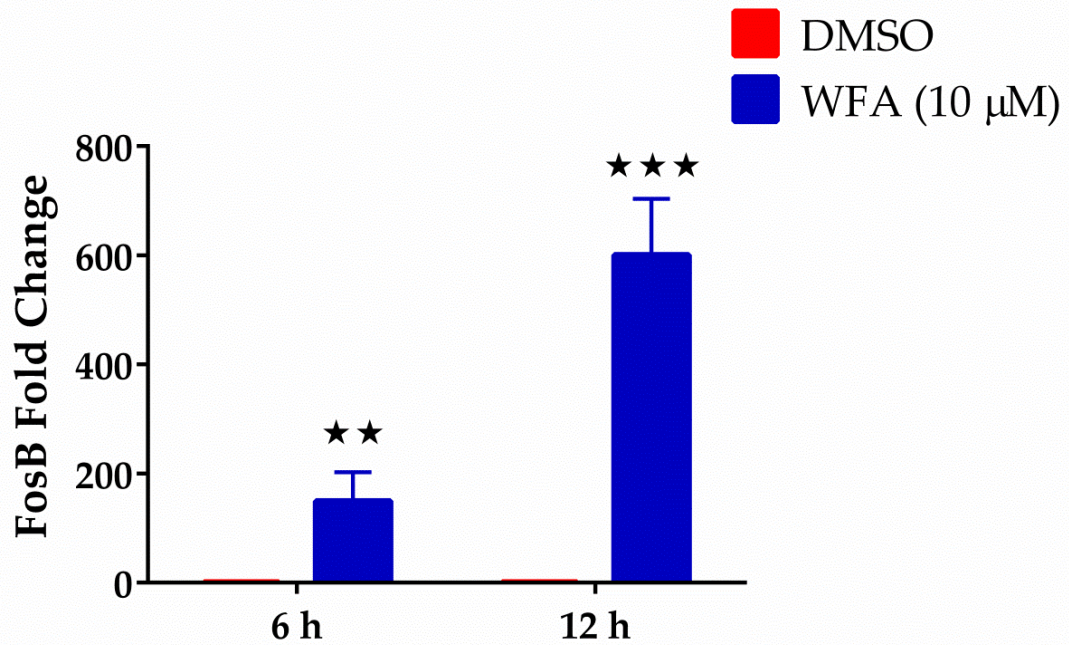
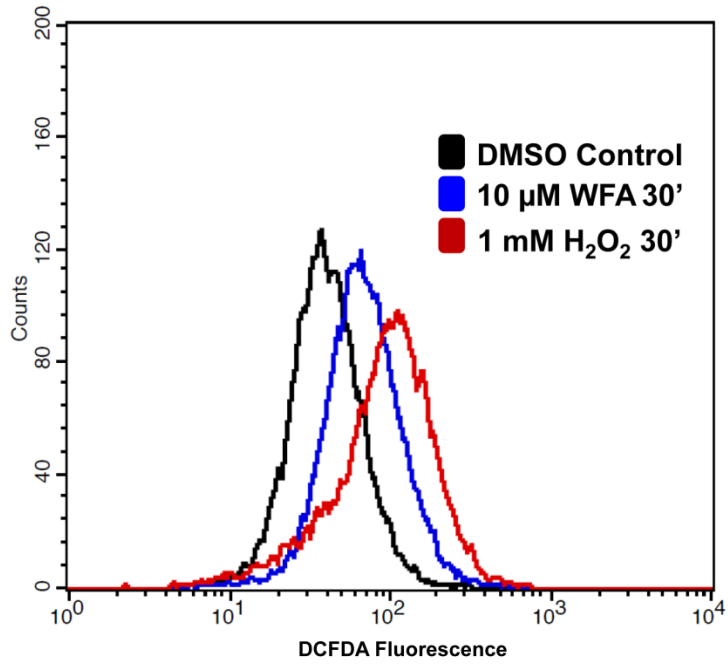


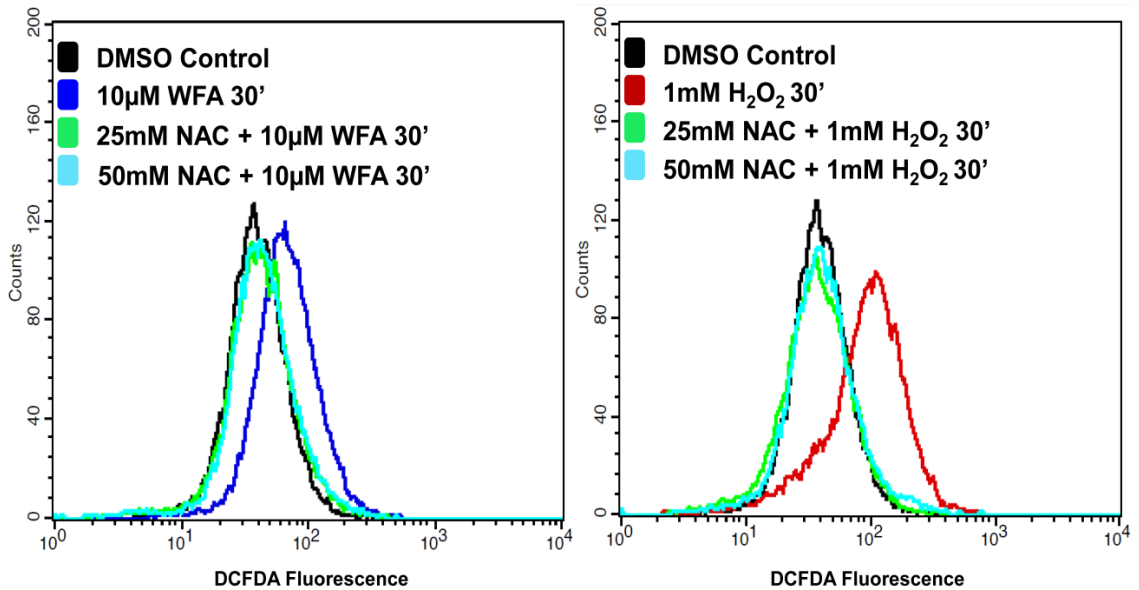
Figure 4.11: WFA enhanced mRNA expression of c-Jun and FosB

Total RNA was isolated from cells treated with DMSO or WFA (6 h and 12 h). The RNA samples were analyzed by qRT-PCR for c-Jun (A) and FosB mRNA levels(B) using human specific primers. Gene amplification was normalized to RPII expression and relative amplification was determined by normalizing to DMSO control. ** = $p < 0.005$, *** = $p < 0.0005$. Representative data of two independent experiments are shown.

4.12A



4.12B



4.12C

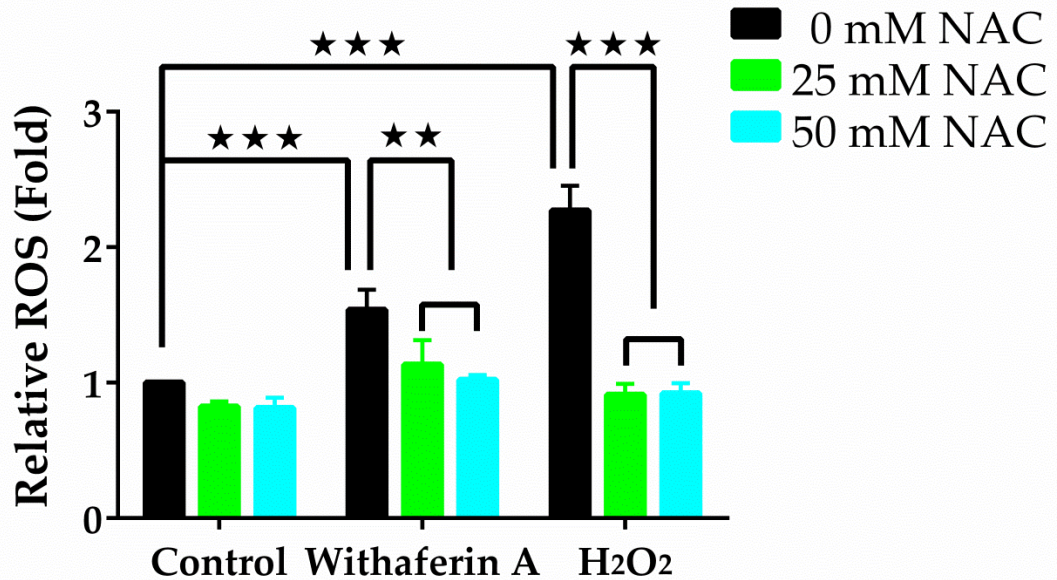
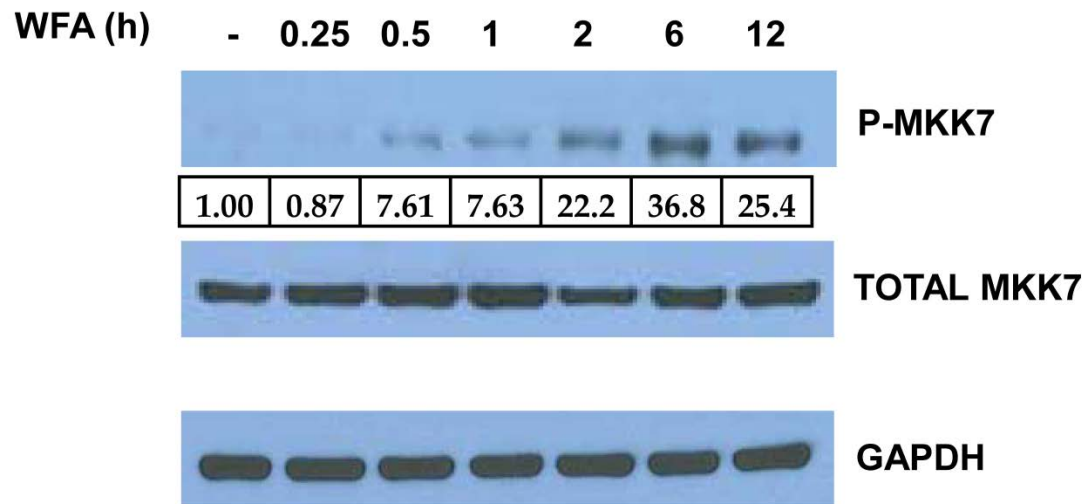


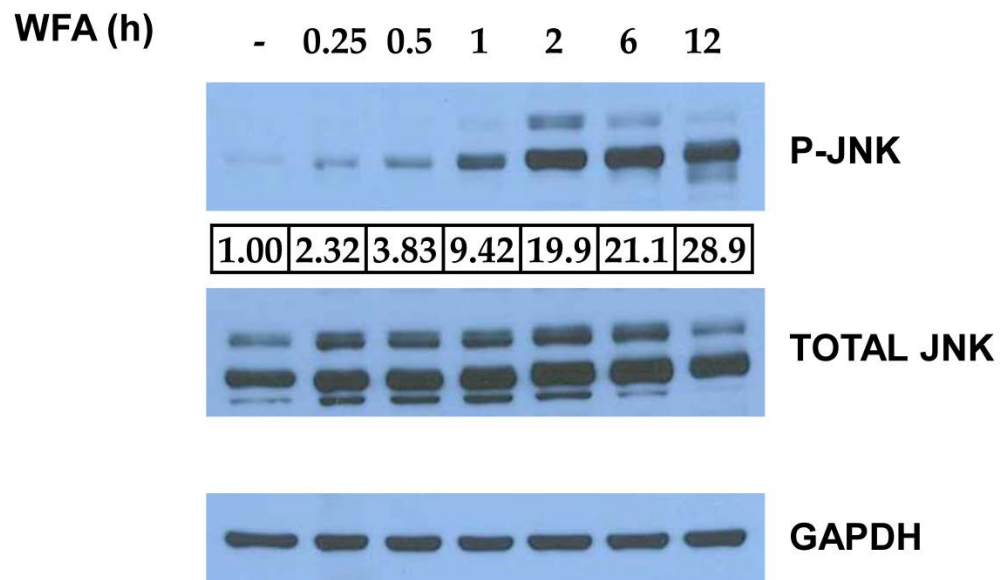
Figure 4.12: WFA treatment increased ROS production in MDS-L cells

Representative flow cytometry profiles of ROS production in MDS-L cells by DCF fluorescence (A, B). Increased ROS production in MDS-L cells exposed to 10 μ M WFA for 30 min (A). 4 h pretreatment with NAC before exposure to WFA inhibited ROS production (B). Amount of ROS produced normalized to DMSO control samples. Mean measurements \pm SD of three separate samples are shown (C). ** = $p < 0.005$, *** = $p < 0.0005$. Results are representative of several experiments.

4.13A



4.13B



4.13C

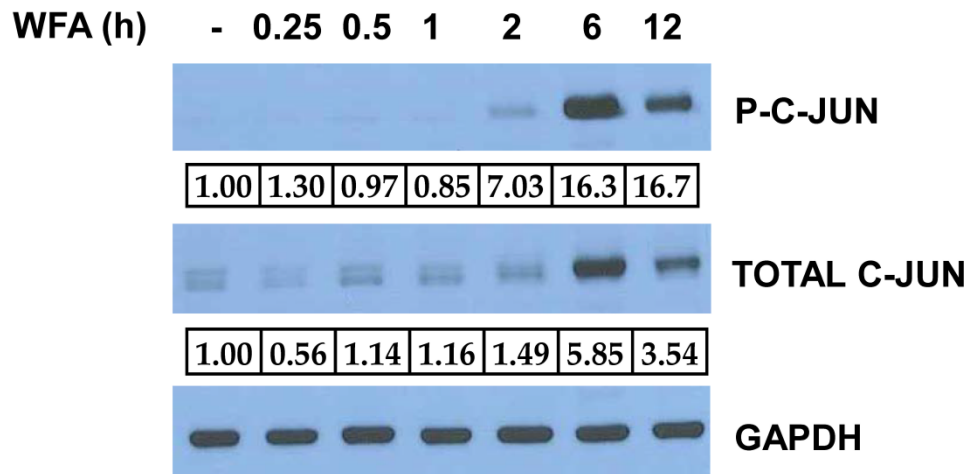
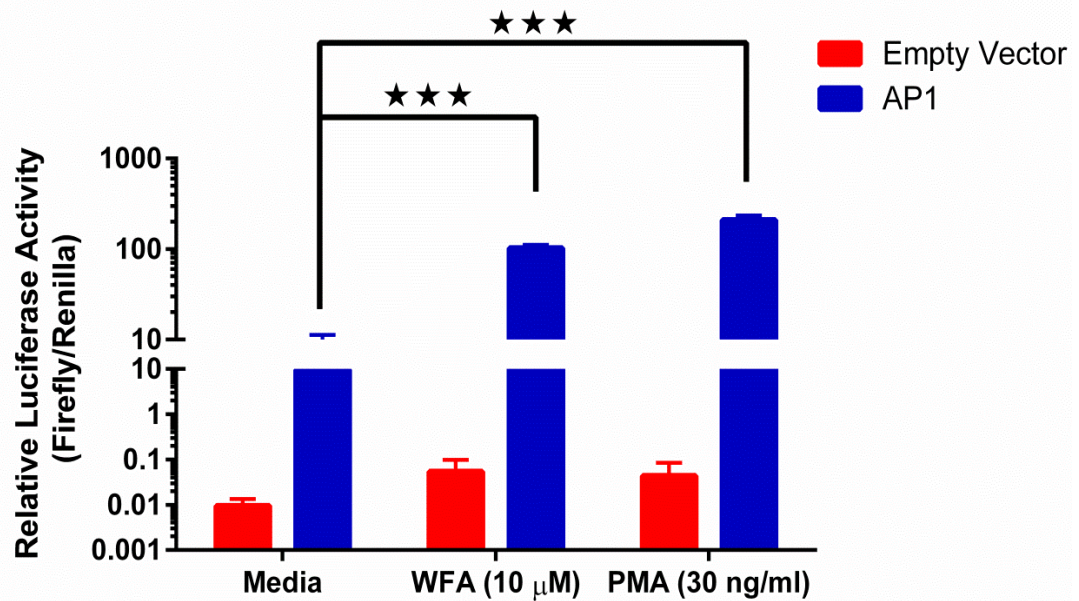


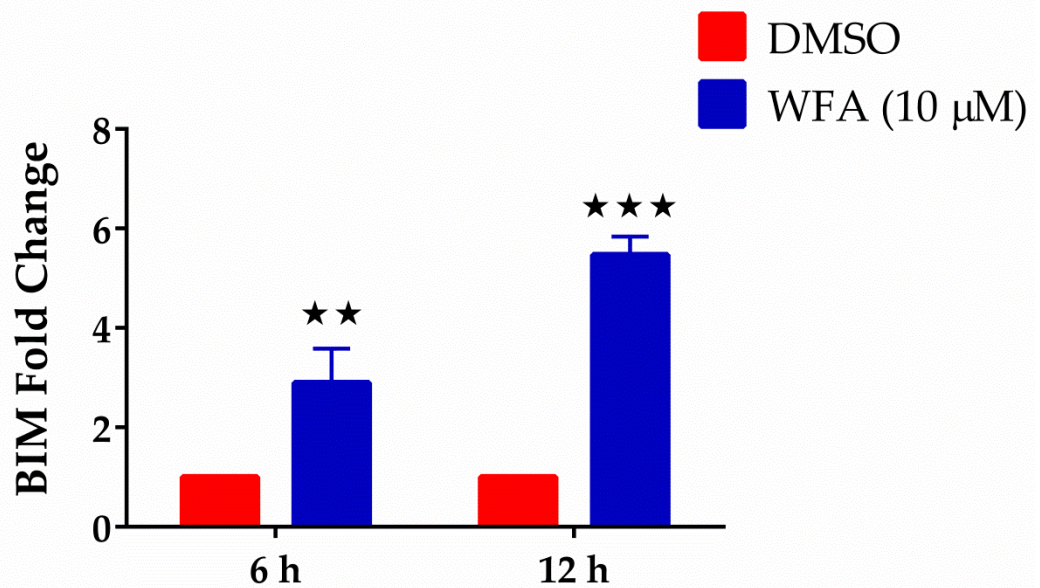
Figure 4.13: JNK MAPK signaling cascade is activated by WFA in MDS-L cells

Western blot analysis of P-MKK7 (A), P-JNK (B) and P-c-Jun (C) on cell lysates of MDS-L cells treated with or without WFA (10 μ M) for the indicated time-points. Activated or phosphorylated protein expression was normalized to the respective total protein expression. Total c-Jun expression was normalized to GAPDH which was also used as a loading control. Relative protein expression was analyzed by densitometry. The values shown are fold change protein expression with respect to DMSO controls. Data are representative of at least two independent experiments.

4.14A



4.14B



4.14C

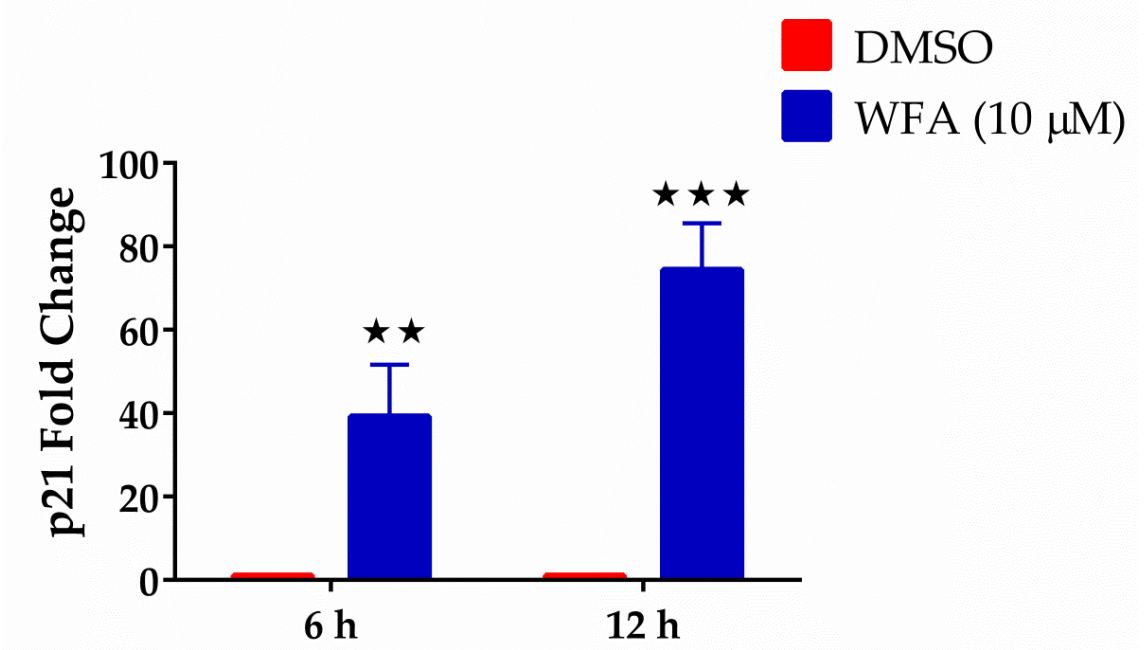


Figure 4.14: WFA triggered AP-1 transcriptional activity in MDS-L cells

(A) MDS-L cells were co-transfected with either an AP-1 or empty firefly luciferase expression vector and a renilla luciferase vector under the control of a constitutive promoter (2:1). Transfected cells were treated with WFA (10 μM) or PMA (30 ng/ml) for 12 h and promoter activity was assessed by the dual Glo luciferase assay. Firefly luciferase activity relative to renilla luciferase activity is shown. Data are presented as mean ± SD of triplicate cultures.

(B, C) Total RNA was isolated from cells treated with DMSO or WFA (6 h and 12 h). The RNA samples were analyzed by qRT-PCR for BIM (B) or p21 (C) expression using human specific primers. Gene amplification was normalized to RPII expression and relative amplification was determined by normalizing to

DMSO control. ** = $p < 0.005$, *** = $p < 0.0005$. Results from one of at least two similar experiments are shown.

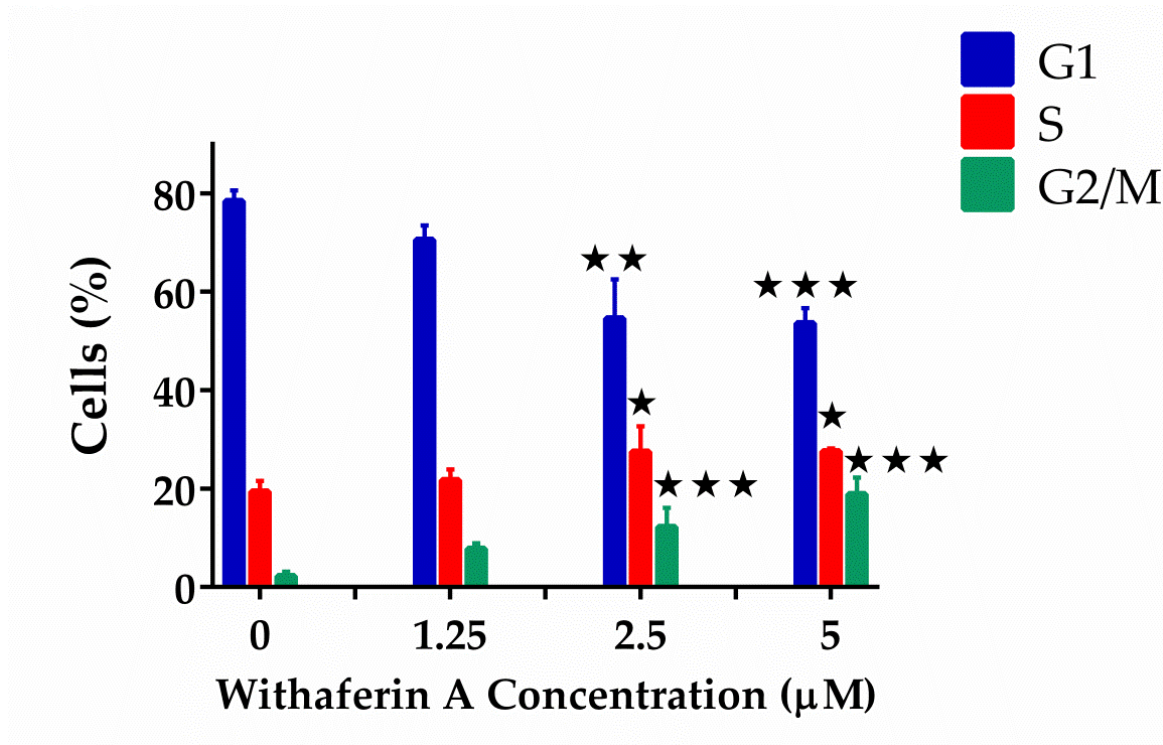
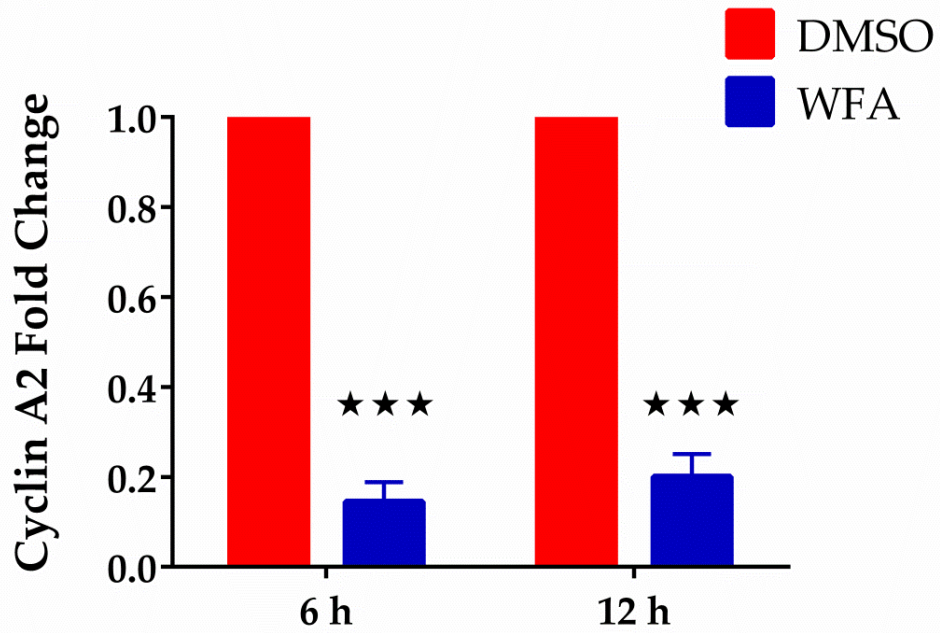


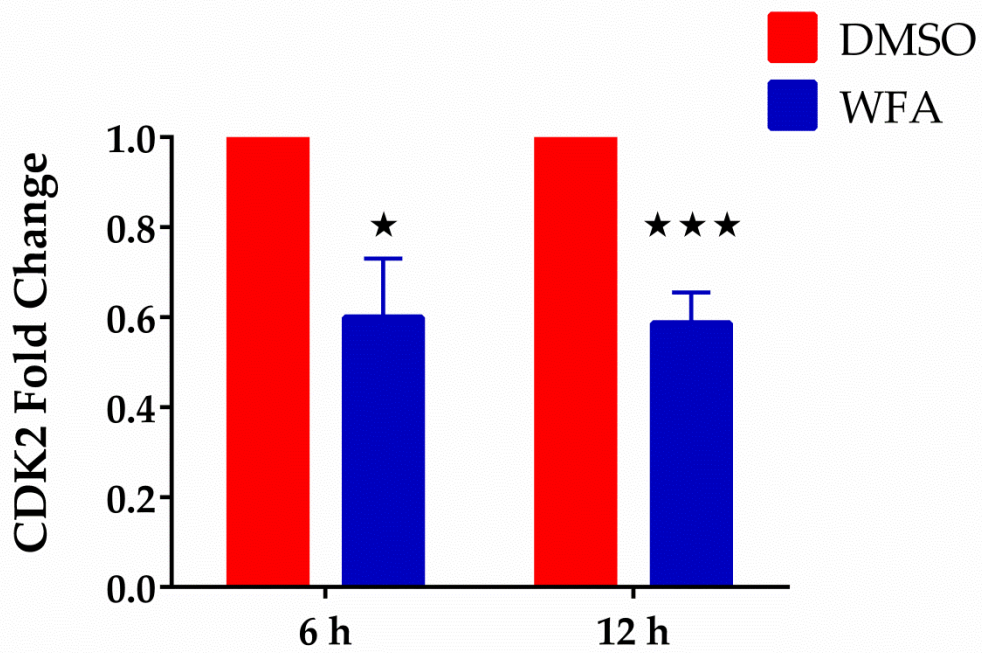
Figure 4.15: Induction of cell cycle arrest in WFA-treated MDS-L cells

Cells were treated with the indicated concentrations of WFA for 48 h and stained with PI. Intensity of PI staining which correlates with DNA content was analyzed by flow cytometry. The fraction of cells (%) at each phase is shown. Data are presented as mean \pm SD from triplicate cultures. * = $p < 0.05$, ** = $p < 0.005$, *** = $p < 0.0005$; denotes significant differences in G, S and G2/M fractions between cultures with and without WFA. Data shown are representative of three experiments.

4.16A



4.16B



4.16C

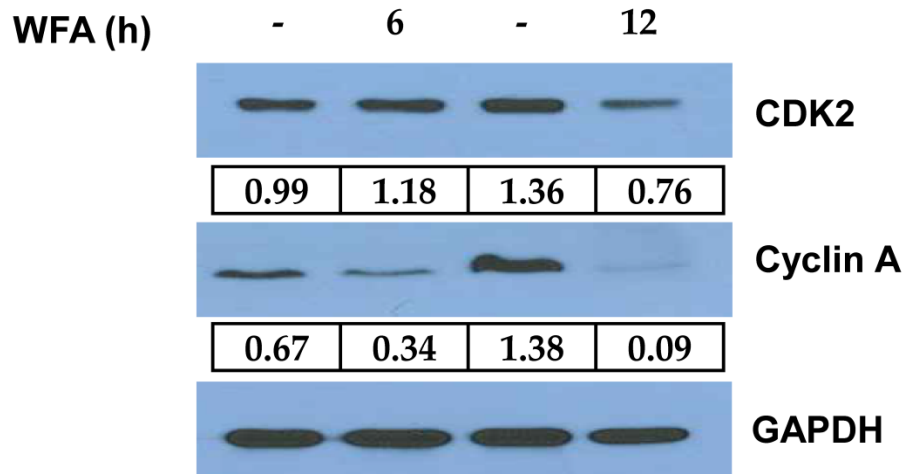
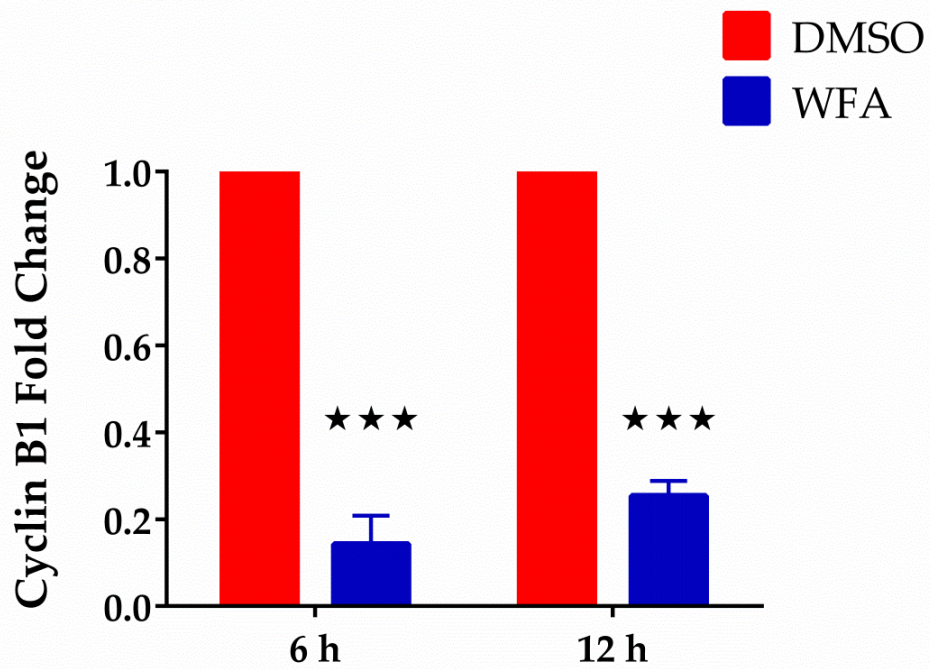


Figure 4.16: mRNA and protein expression of cyclin A and CDK2 decrease with WFA treatment

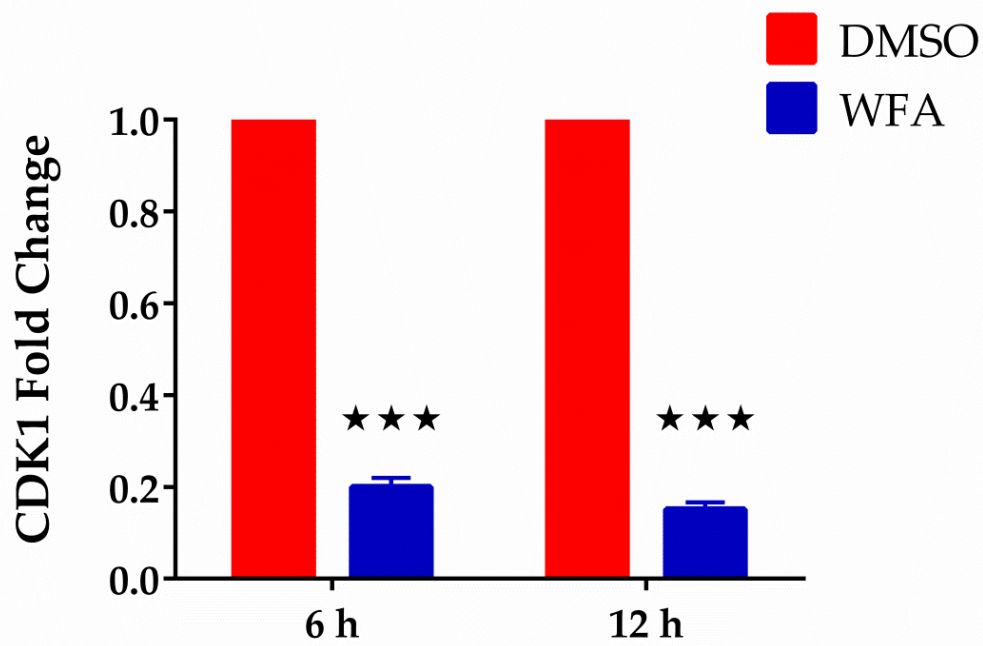
Total RNA samples isolated from cells treated with DMSO or WFA (6 h and 12 h) were analyzed by qRT-PCR for cyclin A (A) and CDK2 (B) expression using human specific primers. Gene amplification was normalized to RPII expression and relative amplification was determined by normalizing to DMSO control.

(C) Whole cell lysates from control or WFA treated (6 h or 12 h) MDS-L cells were analyzed by immunoblotting for cyclin A and CDK2 protein expression. Band intensities were normalized to GAPDH and are expressed as densitometric ratios. * = $p < 0.05$, *** = $p < 0.0005$. Results from one of two experiments with similar results are shown.

4.17A



4.17B



4.17C

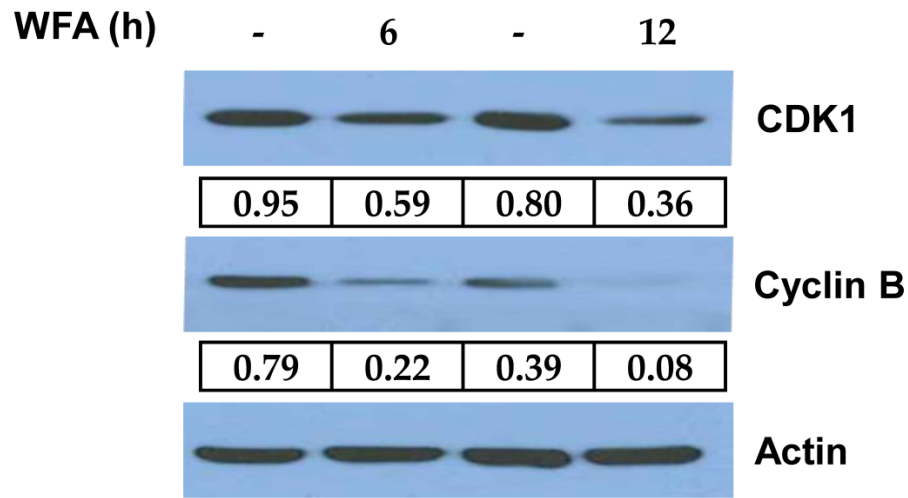


Figure 4.17: mRNA and protein expression of cyclin B and CDK1 decrease with WFA treatment

Total RNA samples isolated from cells treated with DMSO or WFA (6 h and 12 h) were analyzed by qRT-PCR for cyclin B (A) and CDK1 (B) expression using human specific primers. Gene amplification was normalized to RPII expression and relative amplification was determined by normalizing to DMSO control.

(C) Whole cell lysates from control or WFA treated (6 h or 12 h) MDS-L cells were analyzed by immunoblotting for cyclin B and CDK1 protein expression. Relative expression to β -actin is indicated by band intensity ratios. *** = $p < 0.0005$. Results from one of two similar experiments are shown.

Summary

We performed microarray gene expression analysis to identify the molecular mechanisms mediating WFA-induced cytotoxicity of MDS-L cells. Analysis of the differentially expressed genes revealed that WFA significantly regulated genes linked to apoptosis. The substantial increase in gene expression of AP-1 transcription factor subunits (c-Jun and FosB) suggested that WFA activated JNK/AP-1 signaling. We used a combination of biochemical techniques to validate the microarray data. Our results demonstrated that WFA caused apoptosis and activated JNK/AP-1 signaling in MDS-L cells. In depth investigation of AP-1 transcriptional activity induced by WFA treatment revealed increased transcription of p21, an AP-1 target and cell cycle inhibitor. This finding prompted us to test the effect of WFA on MDS-L cell cycle progression leading to the observation that WFA inhibited cycling of MDS-L cells by arresting them at S and G2/M cell cycle phases. This observation suggests that in addition to direct increase in pro-apoptotic factors such as BIM, cell cycle inhibition could potentially contribute to WFA-triggered MDS-L since prolonged arrest in S and G2/M phases eventually triggers apoptosis⁸⁵.

Copyright © Karine Zinkeng Oben 2017

CHAPTER FIVE

Selective WFA-induced cytotoxicity to MDS-L cells is primarily mediated by increased ROS production

After confirming that WFA treatment triggered apoptotic cell death and activated the JNK MAPK cascade in MDS-L cells, we sought to determine if the observed apoptotic cell death was by JNK signaling. We explored this possibility by determining the consequence of pharmacologically inhibiting JNK signaling in WFA-treated cells on apoptosis.

5a) JNK signaling plays a significant role in WFA apoptosis of MDS-L cells by WFA treatment

To determine if JNK signaling played a critical role in WFA-induced apoptosis of MDS-L cells, we investigated the effect of pretreating cells for 4 h with JNK-IN-8, a well characterized JNK inhibitor, on the level of caspase-3 activation by WFA. JNK-IN-8 is a potent and selective covalent JNK inhibitor directed to the ATP-site that was first described in 2012¹⁵⁰. Western blot analysis showed that pretreatment with JNK-IN-8 reduced phosphorylation of c-JUN induced by WFA, an excellent measure of JNK activation (Figure 5.1). JNK inhibition led to an expected decrease in AP-1 transcriptional activity, shown by a significant decrease in transcription of two well-known AP-1 targets, BIM (Figure 5.2A, B) and p21 (Figure 5.3A, B). Consistent with the crucial role of BIM in regulating apoptosis, inhibition of JNK signaling by JNK-IN-8 blocked caspase-3 activation by WFA (Figure 5.4A, B).

Off-target effects are always a concern with the use of small-molecule inhibitors in biological systems. We therefore employed a second widely used JNK inhibitor, SP600125, to verify our results demonstrating the critical role of JNK signaling in WFA-activated apoptosis. Similar results with a second inhibitor would further argue against the possibility that the phenotype observed with JNK-IN-8 was due to off-target effects, since SP600125, a reversible ATP-competitive JNK inhibitor¹⁵¹, is likely to have a different spectrum of off-targets. We verified inhibition of JNK by SP600125 by showing that it reduced WFA-induced phosphorylation of c-JUN (Figure 5.5A, B). Pretreatment of MDS-L cells with SP600125 also suppressed caspase-3 activation caused by WFA treatment (Figure 5.6A, B).

5b) WFA activated JNK signaling by increasing ROS production

We had demonstrated that WFA activated the ROS sensitive MAP3K (ASK1) of the JNK cascade by increased phosphorylation of its target kinase, MKK7 (Figure 4.13A). Hence, we hypothesized that WFA activated JNK/AP-1 signaling and apoptosis in MDS-L cells by increasing ROS production. We tested this hypothesis by investigating the effect of pretreatment with 25 mM NAC, a well-known antioxidant, on WFA-induced JNK/AP-1 activation and apoptosis. Pretreatment with NAC significantly inhibited WFA-mediated JNK activation compared to the no pretreatment control (Figure 5.7A, B). This inhibition traversed downstream of the JNK cascade as NAC pretreatment also substantially inhibited c-Jun phosphorylation (5.8A, B). In addition, NAC robustly inhibited WFA-induced AP-1 transcription demonstrated by both AP-1 driven

luciferase activity (Figure 5.9) and measurement of BIM (Figure 5.10A, B) and p21 (Figure 5.11A, B) transcripts. Inhibition of AP-1 transcription complimented the observed decrease in c-Jun phosphorylation with NAC pretreatment (Figure 5.8). Consistent with the concept of ROS-mediated JNK activation promoting apoptosis in MDS-L cells, NAC pretreatment remarkably abrogated activation of caspase-3 in these cells (5.12A). These results indicated that JNK/AP-1 activation and apoptosis in WFA treated cells was largely due to increased ROS production.

5c) Inhibition of ROS production completely protected MDS-L cells from cytotoxicity by WFA treatment

The significant role of ROS and JNK signaling activation in apoptotic cell death of MDS-L cells treated with WFA was further demonstrated using the annexin-V apoptosis assay. Inhibition of JNK signaling with JNK-IN-8 significantly reduced WFA-induced apoptosis of MDS-L cells (Figure 5.13A, B). On the other hand, NAC pretreatment completely protected MDS-L cells from apoptosis caused by WFA treatment (Figure 5.13A, B). These results demonstrated that not only was ROS upstream of JNK/AP-1 signaling activation (Figure 5.7-5.12), it was the predominant mediator by which WFA caused apoptosis in MDS-L cells. Of note, WFA failed to increase ROS in normal human primary bone marrow cells (Figure 5.14) which were shown previously (Figure 3.10) to be resistant to WFA-induced cell death. Hence, ROS production could explain why WFA was selectively cytotoxic to MDS-L cells but spared normal bone marrow cells *in vitro* and *in vivo* (Figures 3.6, 3.7, 3.8 and 3.10).

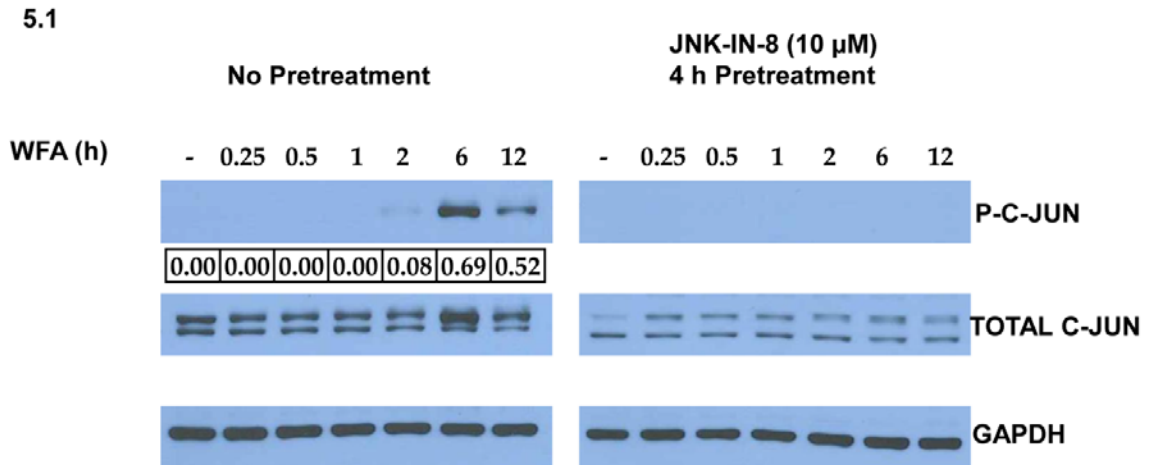
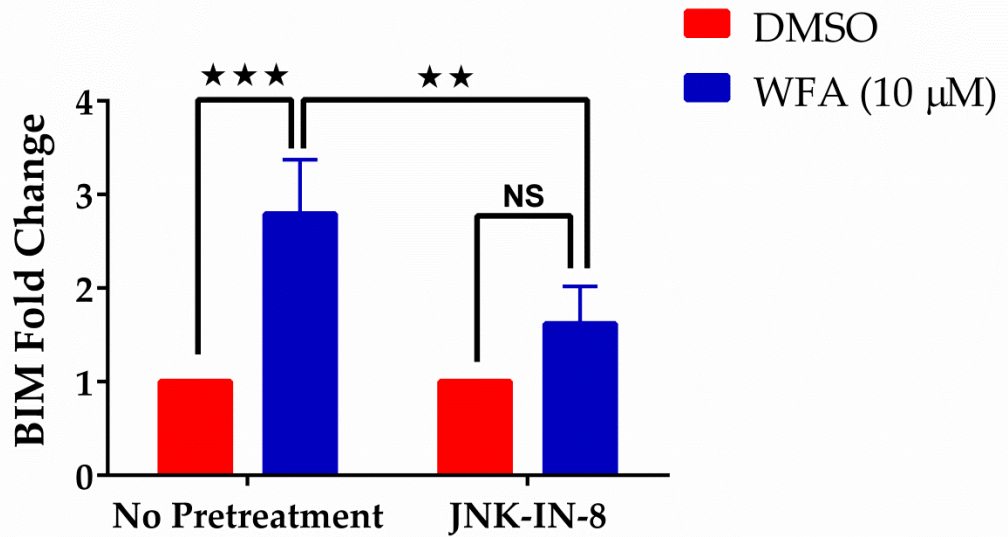


Figure 5.1: JNK-IN-8 effectively inhibits JNK activation by WFA

Immunoblot analysis of P-c-Jun, total c-Jun and GAPDH (loading control) in MDS-L cells treated with WFA for the indicated time-points after no pretreatment or pretreatment with JNK-IN-8 (10 μ M) for 4 h. P-c-Jun expression is presented relative to total c-Jun.

5.2A



5.2B

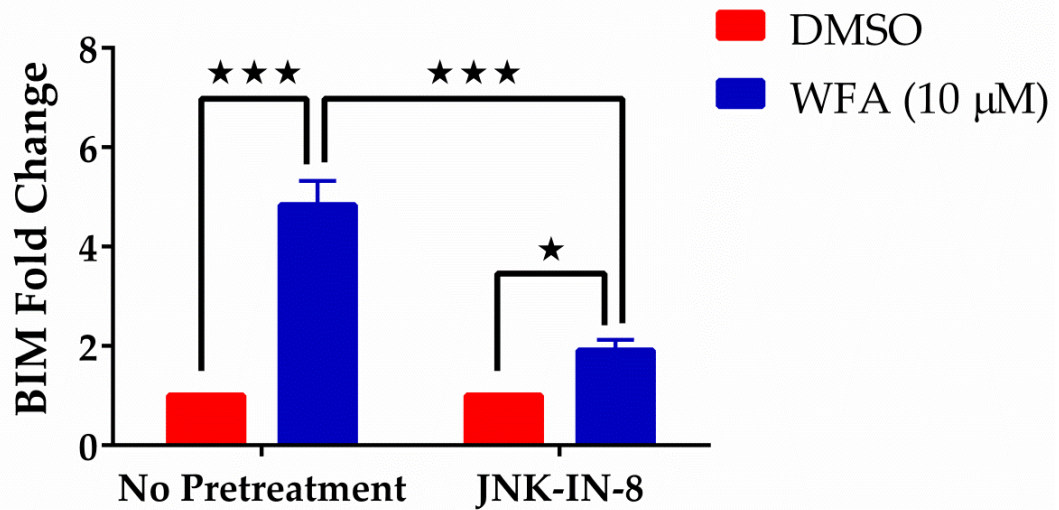
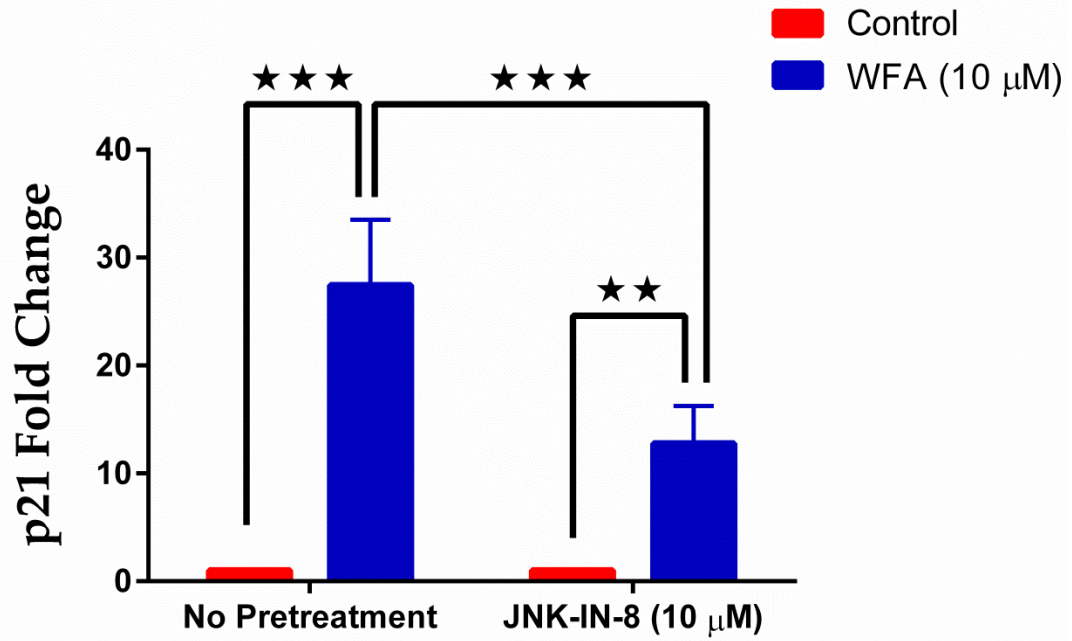


Figure 5.2: Inhibition of JNK activity suppresses transcription of BIM induced by WFA

MDS-L cells were pretreated with or without JNK-IN-8 (10 μM) for 4 h. Total RNA isolated from pretreated cells exposed to WFA for 6 h (A) or 12 h (B) was

used to determine BIM expression by qRT-PCR. BIM amplification was normalized to RPII and relative expression was determined by normalizing to DMSO control. * = $p < 0.05$, ** = $p < 0.005$, *** = $p < 0.0005$.

5.3A



5.3B

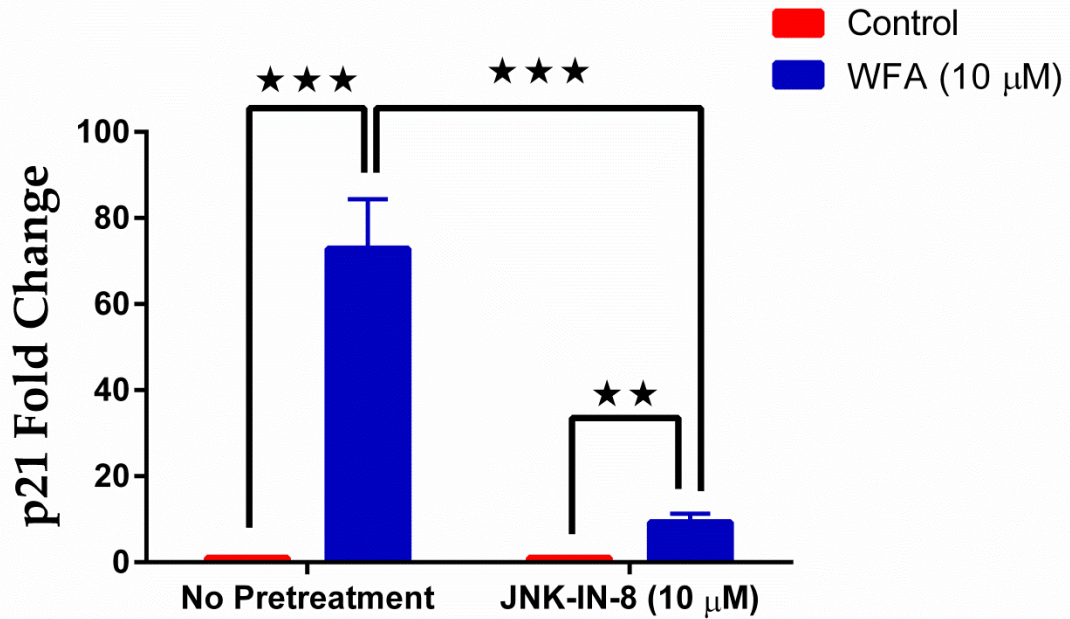
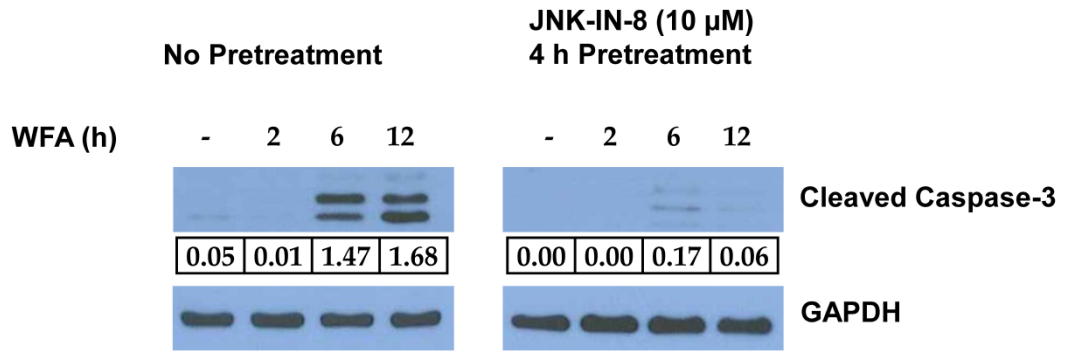


Figure 5.3: JNK activation contributes to p21 transcription in WFA-treated MDS-L cells

qRT-PCR analysis of p21 in MDS-L cells with or without JNK inhibition, treated with WFA for 6 h (A) or 12 h (B). p21 amplication was normalized to the RPII control gene and the results are presented relative to those of DMSO controls. ** = $p < 0.005$, *** = $p < 0.0005$.

5.4A



5.4B

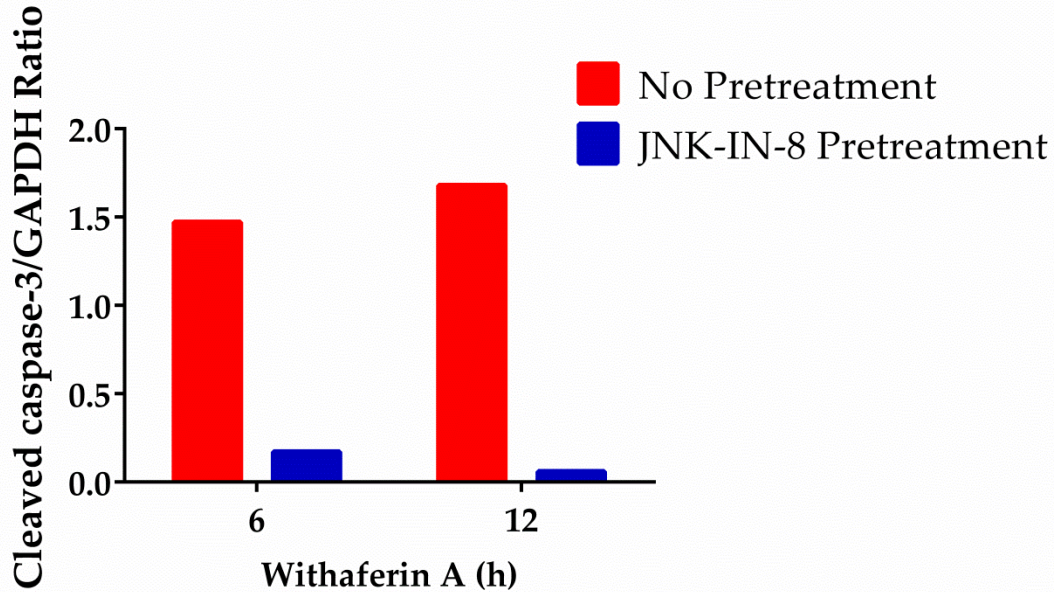
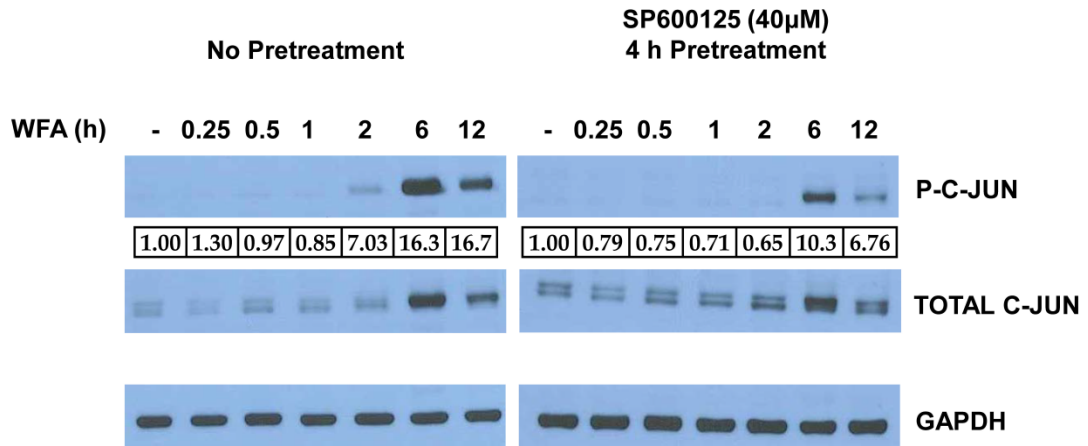


Figure 5.4: JNK-IN-8 substantially abrogates caspase-3 activation induced by WFA in MDS-L cells

(A) Western blots showing active caspase-3 (cleaved caspase-3) and GAPDH levels in MDS-L cells treated with WFA for 2, 6 or 12 h, with or without JNK blockade by JNK-IN-8. (B) Relative cleaved caspase-3 expression in (A) was normalized to GAPDH and the values expressed as densitometric ratios are shown by a bar graph.

5.5A



5.5B

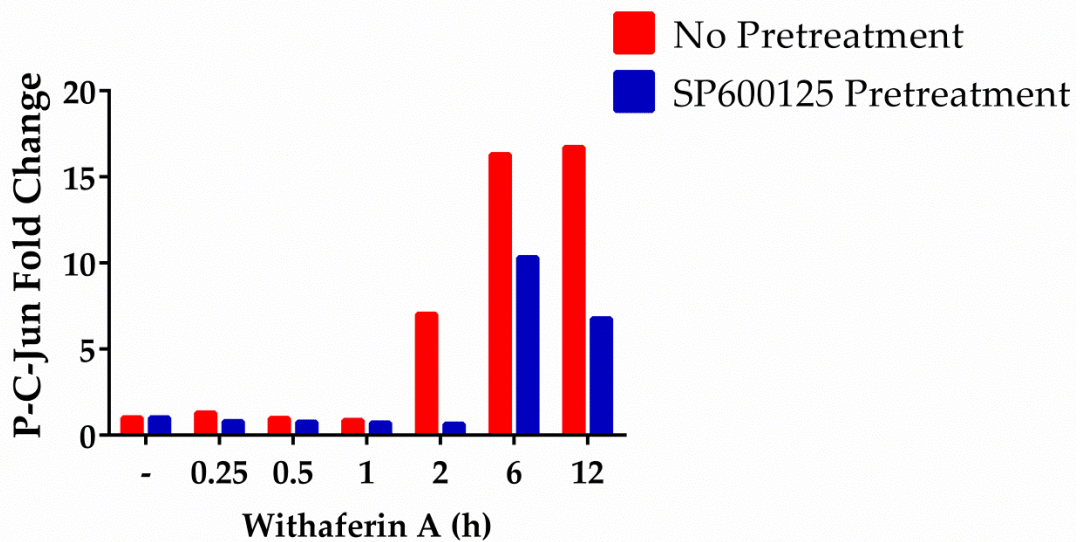
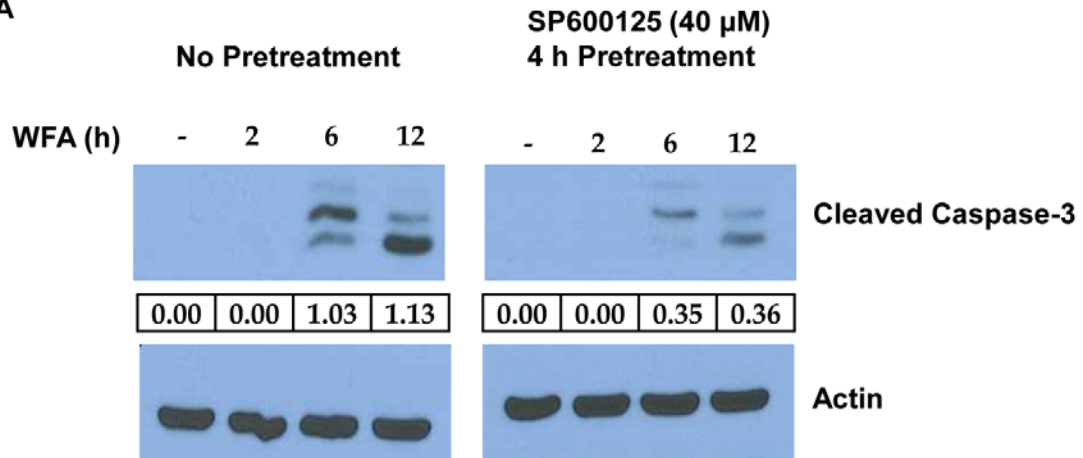


Figure 5.5: SP600125 inhibits WFA-induced JNK activity

MDS-L cells pretreated with SP600125 (40 µM) for 4 h or without pretreatment were exposed to WFA for an additional 0.25, 0.5, 1, 2, 6, or 12 h. The effect of SP600125 treatment on JNK activity was assessed by immunoblotting for P-c-Jun (A). Bar graph representation of P-c-Jun expression in (A) normalized to total c-Jun and WFA negative control (B).

5.6A



5.6B

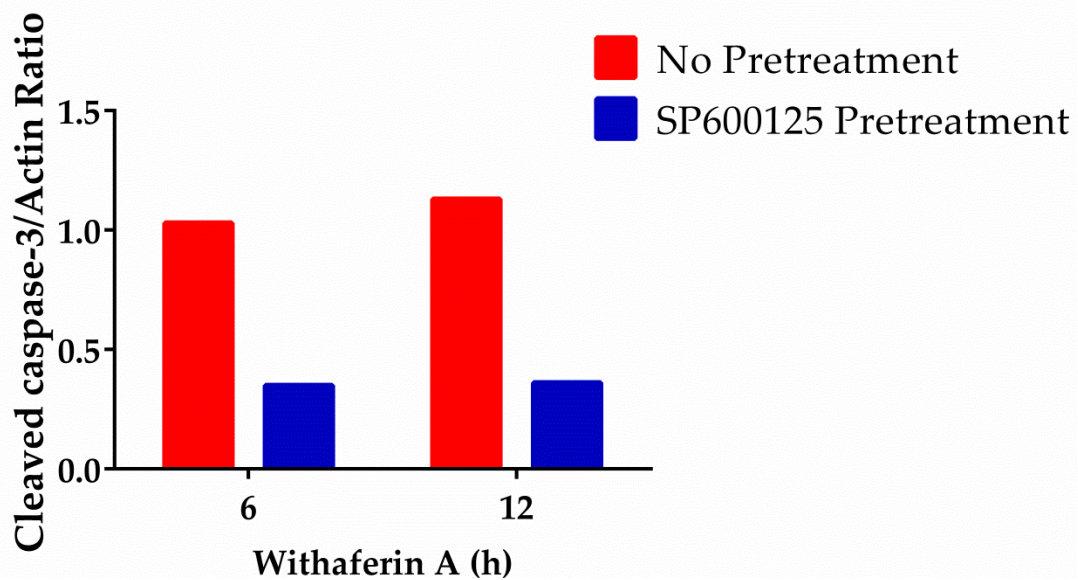
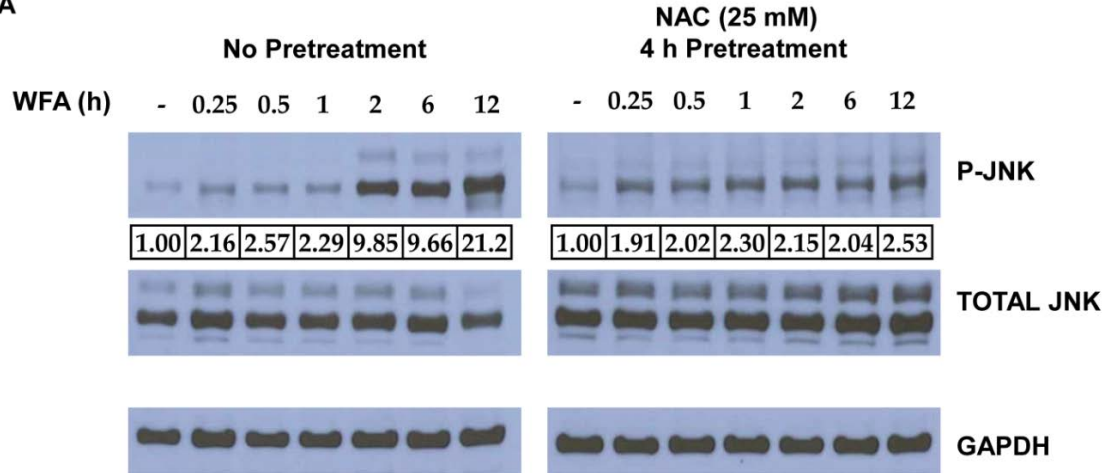


Figure 5.6: SP600125 suppresses activation of caspase-3 by WFA

MDS-L cells with or without SP600125 (40 μ M) treatment for 4 h, were treated further with WFA for 2, 6, or 12 h. Whole cell lysates from treated cells were used for immunoblot analysis of cleaved caspase-3 and β -actin (A). Cleaved caspase-3 band intensities were normalized to β -actin and relative expression by densitometric ratios is presented graphically (B).

5.7A



5.7B

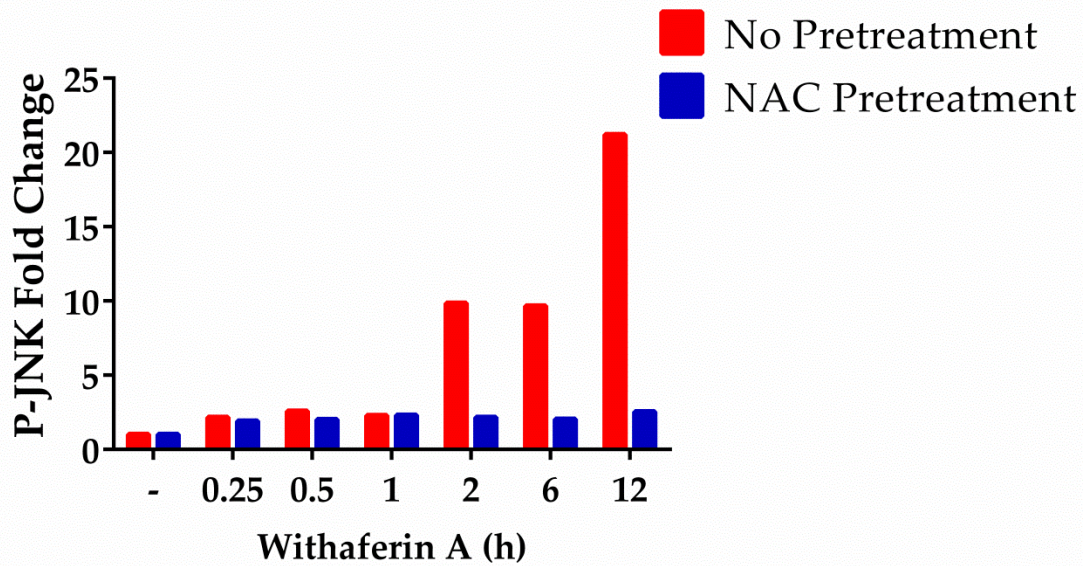
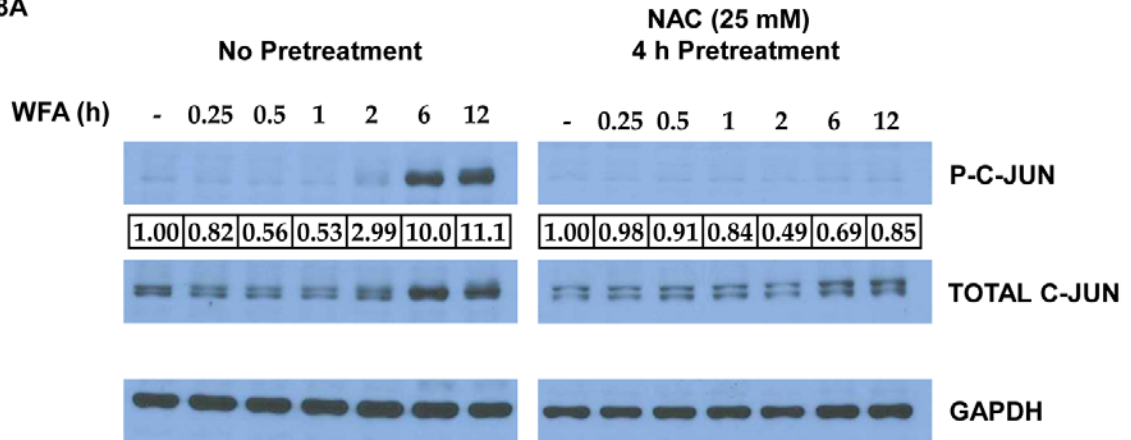


Figure 5.7: WFA-induced JNK activation is inhibited by NAC

Western blot analysis showing the effect of ROS blockade by NAC (25 mM) pretreatment for 4 h on WFA-induced JNK activation in MDS-L cells at the indicated time points (A). P-JNK expression in (A) expressed as a ratio to total JNK, with WFA negative controls set as 1 (B).

5.8A



5.8B

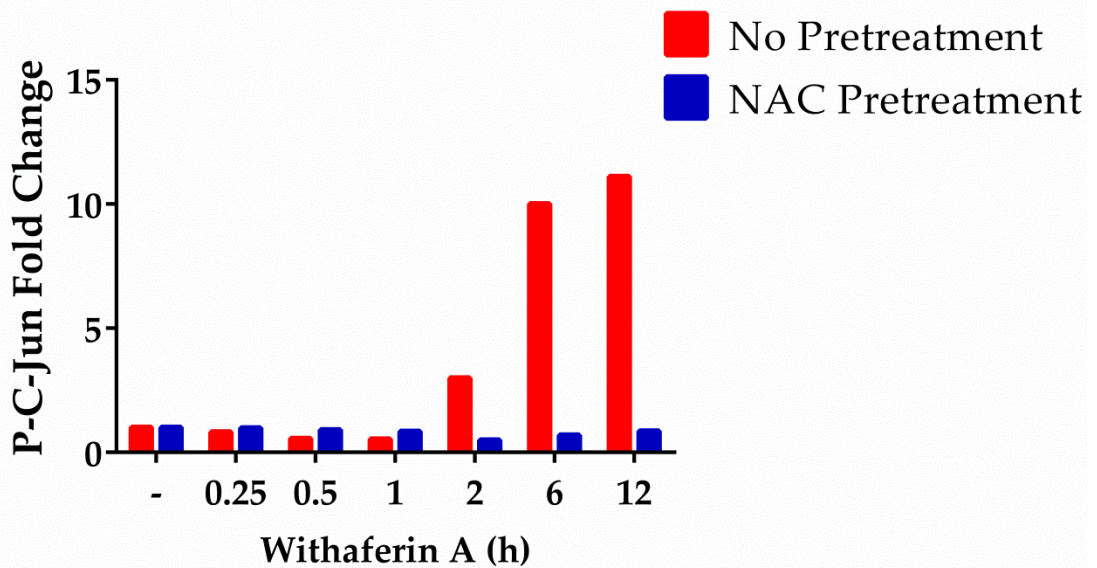


Figure 5.8: NAC inhibits JNK activity in WFA-treated MDS-L cells

(A) P-c-Jun levels measured by immunoblotting of WFA-treated MDS-L cells with or without ROS blockade by NAC (25 mM) pretreatment for 4 h. (B) P-c-Jun band intensities were normalized to those of total c-Jun and densitometric ratios of WFA negative controls set to 1.

5.9

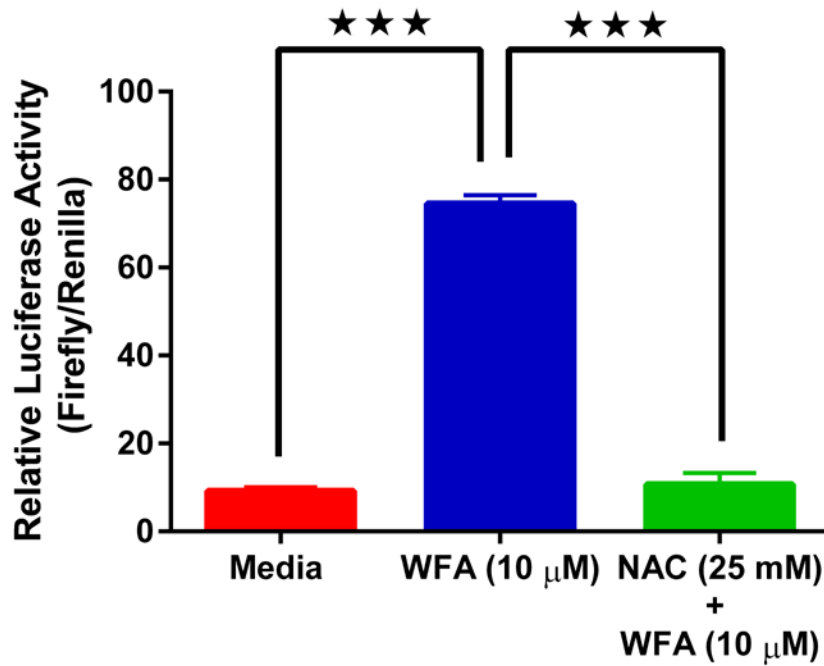
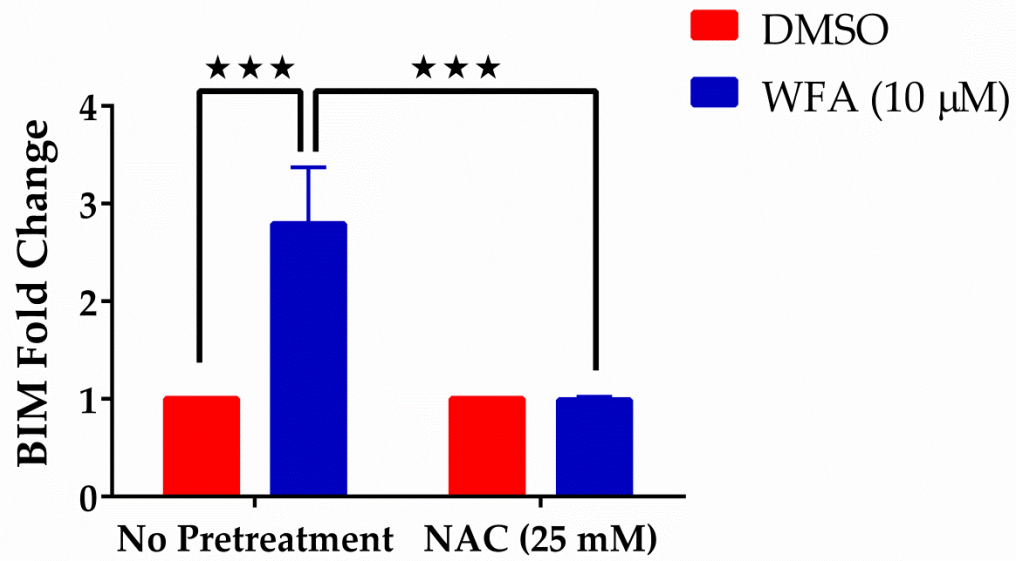


Figure 5.9: WFA-induced AP-1 dependent transcription is inhibited by NAC
MDS-L cells pretreated with or without NAC (25 mM) for 4 h were co-transfected with an AP-1 firefly luciferase expression vector and a renilla luciferase vector under the control of a constitutive promoter (2:1). Transfected cells were treated with WFA (10 μ M) for 12 h and promoter activity was assessed by the dual Glo luciferase assay. The ratios of firefly to renilla luciferase activity in relative light units are shown. Data are presented as mean \pm SD of triplicate cultures. *** = $p < 0.0005$.

5.10A



5.10B

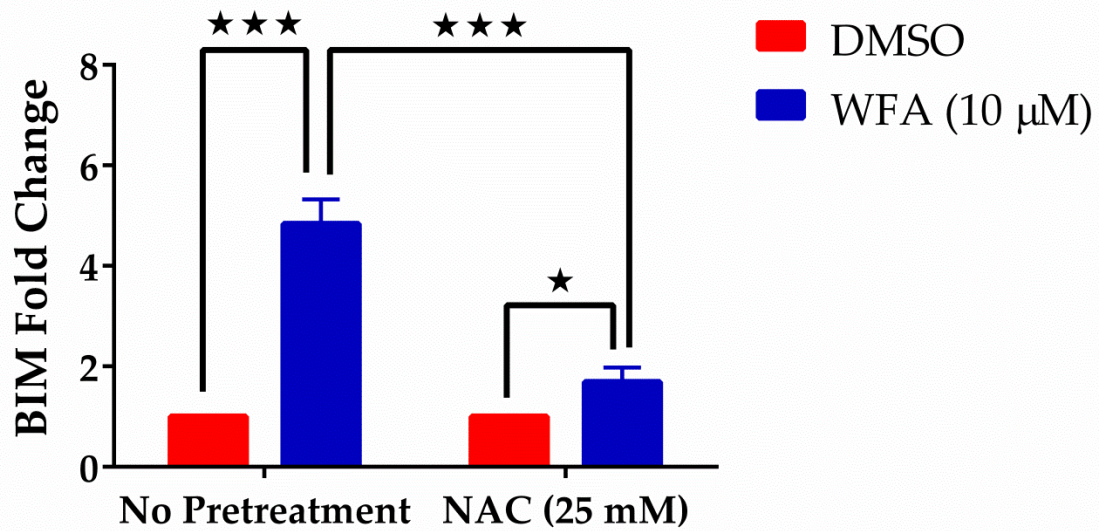
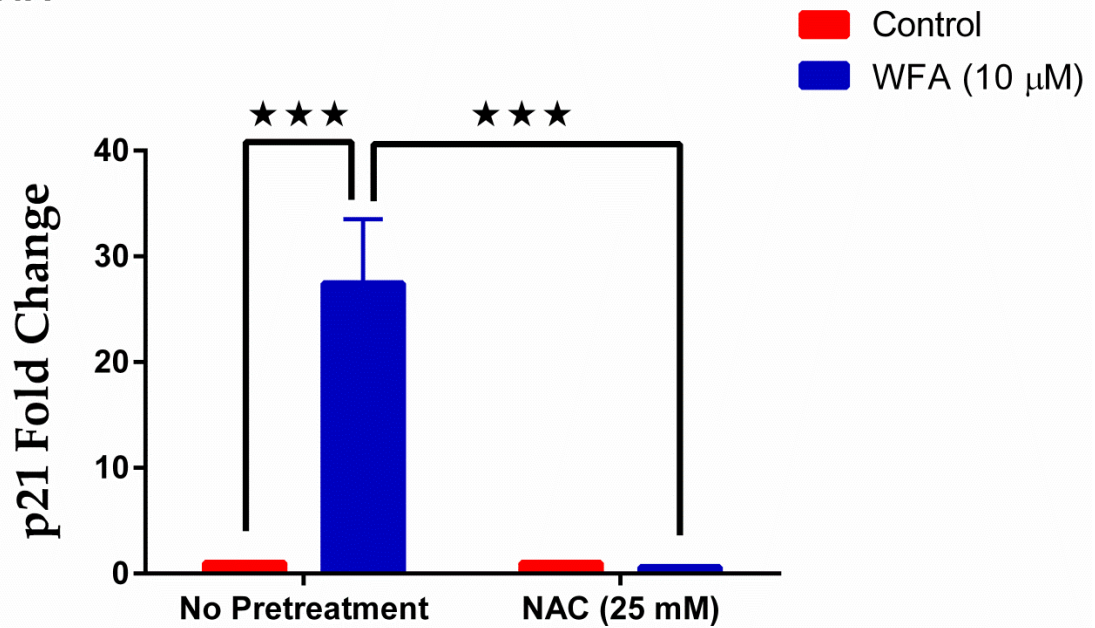


Figure 5.10: Inhibition of ROS blocked BIM transcription in WFA-treated MDS-L cells

BIM expression by qRT-PCR in MDS-L cells with or without ROS inhibition, treated with WFA for 6 h (A) or 12 h (B). BIM expression was normalized to RPII expression and the results are presented relative DMSO controls. * = $p < 0.05$, *** = $p < 0.0005$.

5.11A



5.11B

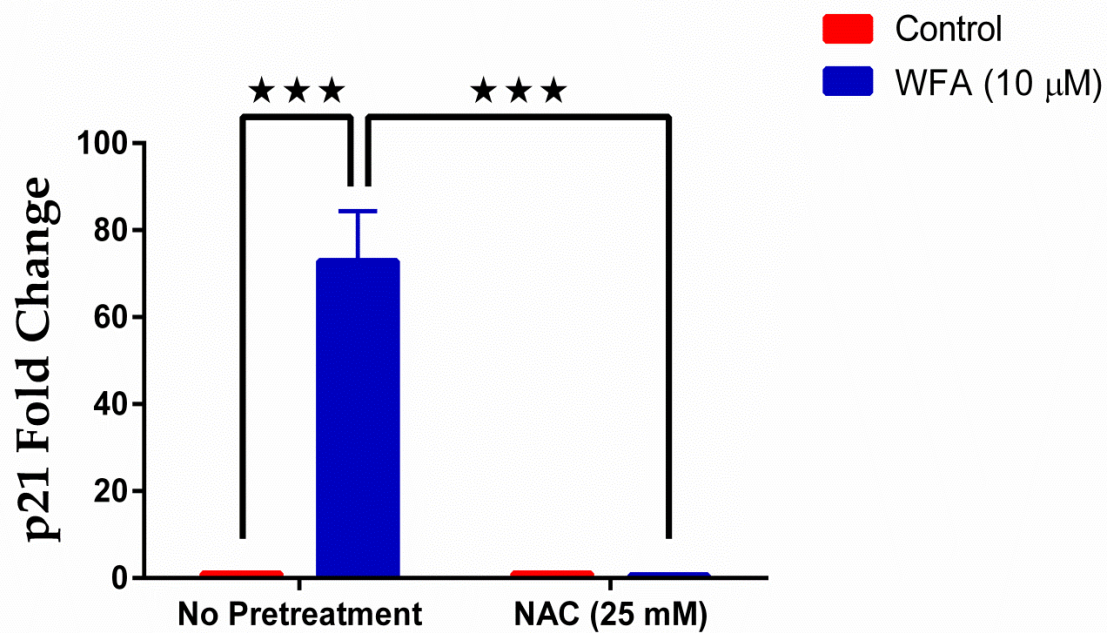


Figure 5.11: NAC abrogated WFA-induced p21 transcription

MDS-L cells were pretreated with or without NAC (25 mM) for 4 h. Total RNA isolated from pretreated cells exposed to WFA for 6 h (A) or 12 h (B) was used to determine p21 expression by qRT-PCR. p21 amplification was normalized to RPII and relative expression was determined by normalizing to DMSO control. *** = $p < 0.0005$.

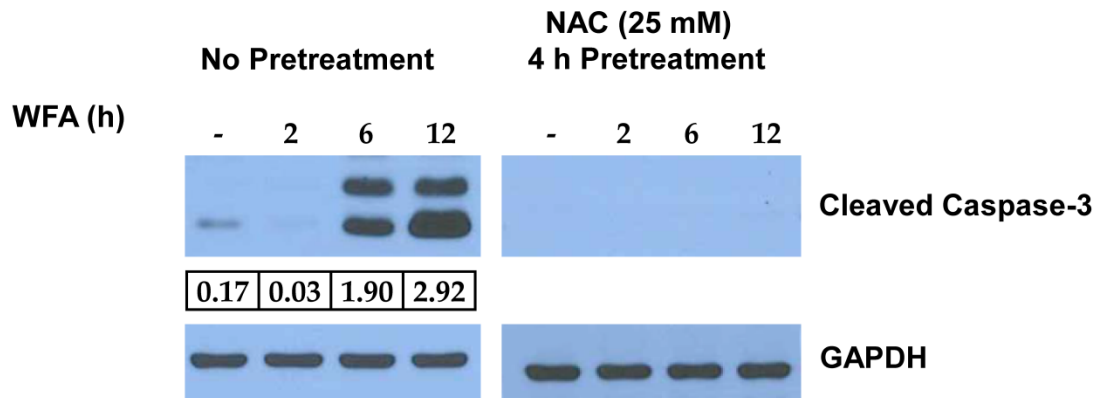
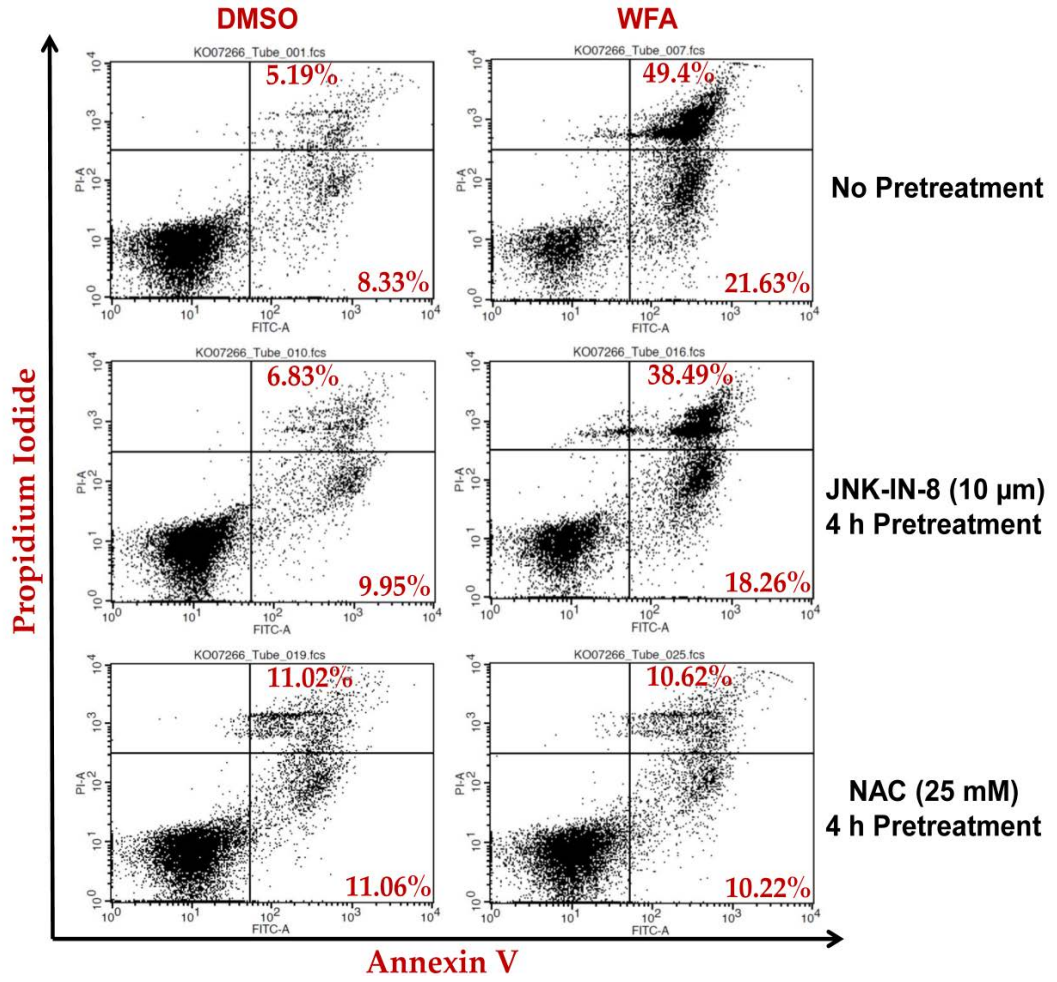


Figure 5.12: ROS inhibition completely abolished WFA-induced caspase-3 activation

Western blotting showing the effect of inhibiting ROS accumulation by NAC (25 mM) pretreatment for 4 h on WFA-induced caspase-3 activation in MDS-L cells at the indicated time points.

5.13A



5.13B

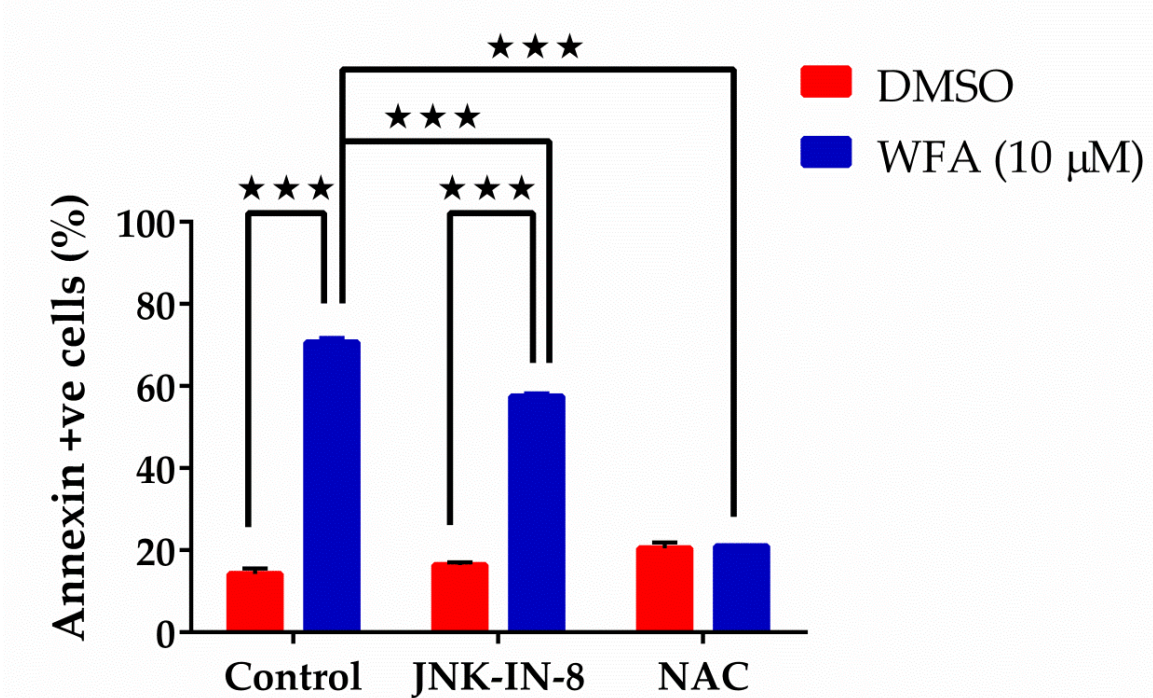


Figure 5.13: NAC protects MDS-L cells from apoptosis by WFA treatment

No pretreatment or pretreated (JNK-IN-8 or NAC for 4 h) MDS-L cells were treated with WFA (10 μM) for an additional 24 h and stained with annexin-V and PI. (A) Representative flow cytometry profiles of annexin-V/PI staining. (B) Frequency of annexin-V positive cells. Data presented as mean ± SD (n = 3). *** = p<0.0005.

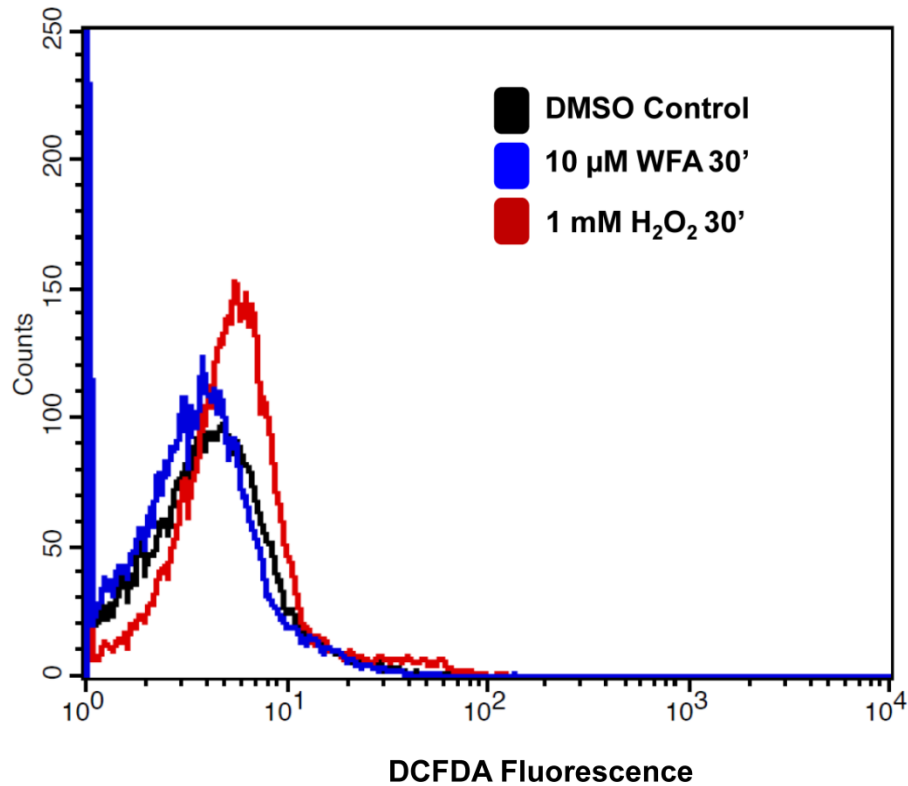


Figure 5.14: WFA does not increase ROS in normal human primary bone marrow cells

DCFH-DA assay by flow cytometry in normal human primary bone marrow cells treated with WFA or H_2O_2 for 30 min.

Summary

We previously demonstrated that WFA-induced ROS activated JNK/AP-1 signaling and apoptosis in MDS-L cells (chapter 4). Published studies have shown that JNK/AP-1 activation can lead to apoptosis in many cell types⁹³. Therefore, we investigated the significance of JNK/AP-1 activation and increased ROS production in MDS-L apoptosis by WFA. Pharmacological inhibition of JNK by JNK-IN-8 or SP600125 in WFA treated cells revealed that JNK signaling significantly contributes to WFA-induced apoptosis. We found that ROS was upstream of JNK/AP-1 activation and apoptosis in MDS-L cells, since inhibition of ROS with NAC inhibited both JNK/AP-1 signaling and apoptosis. Although JNK/AP-1 signaling plays a significant role in WFA-induced apoptosis of MDS-L cells, it was not the only pathway activated downstream of ROS because JNK inhibition significantly reduced but did not prevent apoptosis. However, ROS blockade completely prevented MDS-L apoptosis by WFA, suggesting ROS was the predominant mediator of MDS-L cytotoxicity. Consistent with these findings, WFA was not cytotoxic to normal human primary bone marrow cells in which WFA did not increase ROS levels

CHAPTER SIX

Discussion

There are three FDA approved drugs for MDS treatment, Lenalidomide, azacitidine and decitabine²⁷. Of these three, both azacitidine and decitabine are hypomethylating agents²⁹. Azacitidine and its derivative decitabine mediate DNA demethylation by inactivating the DNA methylation enzyme, DNA methyltransferase-1 (DNMT-1)²⁹. Given that mutations in DNA methylation (*DNMT3A*, *TET2*, *IDH1/2*), are recurrent in MDS⁹, it seems fitting that some MDS patients respond to hypomethylating agents. However, the response rate to these therapies is low and transient²⁷. Only about 50% of MDS patients respond to hypomethylating agents and a majority of responders relapse within 2-3 years^{27,29}. The outcome of MDS patients after hypomethylating therapy failure is very poor; - median overall survival and 2-year survival probability of 5.6 months and 15%, respectively, have been reported¹⁵². The mechanism of action of lenalidomide in MDS is not completely understood. Although it is generally thought to be an immunomodulatory agent, lenalidomide-dependent modulation of the CRL4^{CRBN} E3 ubiquitin ligase substrate specificity is critical for the activity of lenalidomide in del(5q) MDS^{134,153}. Haploinsufficiency of *csnk1a1* in hematopoietic stem cells causes an increase in β -catenin levels and survival advantage while a homozygous loss of *csnk1a1* causes p53 accumulation and ablation of hematopoietic stem cells by apoptotic cell death¹⁵⁴. Therefore, targeted degradation by lenalidomide of casein kinase 1A1 (CK1 α) in del(5q) cells which are haploinsufficient in CK1 α expression induces p53-mediated cell-

cycle arrest and cell death¹⁵³. As with hypomethylating agents, the response of MDS patients to lenalidomide is often not durable^{30,134}. The incidence of relapse with current FDA approved MDS therapies suggests these drugs are likely not targeting the disease initiating clone. HSCT is a potentially curative MDS treatment but the use of HSCT treatment for MDS is very limited^{31,32}. Less than 10% of MDS patients are referred to HSCT³¹. Underuse of HSCT treatment for MDS may be because MDS most commonly occurs in older adults and comorbidities in older patients limit tolerance to the intensive preconditioning HSCT treatments^{3,31,33}. Given the current status of MDS treatment, there is a compelling need to investigate new therapies for MDS treatment.

Toxicity is a major problem with most of the established chemotherapy drugs routinely used for cancer treatment³⁶. Hence, scientific exploration of plant-derived compounds for cancer treatment is on the rise because they are considered to have less toxic side effects^{36,37}. Withaferin A (WFA) is a plant-derived compound that has been shown to have potential in anticancer treatment³⁹. The anticancer activities of WFA have been demonstrated in several cancer models including prostate, breast, cervical and pancreatic cancers, as well as melanoma and lymphoma^{44,45}. The goal of this study was to determine if the anticancer effects of WFA extend to MDS.

Although several MDS mouse models have been developed, the heterogeneity of the disease has made it difficult to generate a mouse that models complete disease phenotype¹³³. The *NUP98-HOXD13* fusion gene transgenic mouse is one of the best of the reported MDS mouse models because

it recapitulates a majority of MDS phenotypes including peripheral cytopenias, dysplastic cell morphology and progression to AML¹⁵⁵. Nonetheless, a majority of the mice die rather from precursor T or B-cell lymphoblastic lymphoma/leukemia and not MDS¹⁵⁵. Xenotransplantation of primary MDS cells has been a challenge because engraftment of primary MDS cells into immunocompromised mice is poor and highly inefficient^{125,126}. In the present study, we utilized the MDS-L cell line model to investigate the anticancer potential and possible underlying molecular mechanisms of action of WFA in MDS. MDS-L cells represent a highly aggressive form of the disease because they have deletions in chromosomes 5 and 7¹²⁷. Deletions in chromosomes 5 and 7 are not just the most common cytogenetic abnormalities observed in MDS, but they have also been associated with a significantly worse prognosis^{12,14,16,17}. Even though the efficiency was highly variable, the engraftment of MDS-L cells in NSGS mice was reproducible.

We found that WFA significantly inhibited the proliferation of MDS-L cells both *in vitro* and *in vivo*. Similarly, WFA caused apoptosis of bone marrow cells from patients with MDS or AML which validated the clinical relevance of this study. Our findings also identified ROS signaling as a potential therapeutic target that could selectively eliminate malignant MDS cells while sparing normal cells. Importantly, WFA did not significantly change ROS levels in primary human bone marrow cells, consistent with their resistance to WFA-induced cytotoxicity. We therefore propose ROS signaling as a potential therapeutic target that could selectively target malignant MDS cells while sparing normal cells.

6a) Molecular mechanisms mediating apoptosis of MDS-L cells by WFA

The anticancer activities of WFA have been studied in several cancer models but the molecular mechanisms mediating these activities are not clearly understood. Several pathways and molecules have been implicated in the mechanism of action of WFA in cancer cells, including NF- κ B, Akt, Stat3, ER- α , endoplasmic reticulum (ER) stress response, ROS, and MAP kinases (p38, ERK and JNK)⁴⁴. It is now becoming clear that although WFA can target multiple pathways, certain pathways could be cell type specific^{44,50}. Our finding that the mechanism(s) mediating growth inhibitory effects of WFA in MDS-L cells are NF- κ B independent (Figure 4.1) support the idea of cell type specific mechanisms induced by WFA. To understand the pathways mediating cell death in MDS-L cells treated with WFA, we performed microarray gene expression analyses on cells treated with WFA or DMSO. Analyses of the microarray data led us to identify JNK/AP-1 signaling as one of the major pathways mediating WFA-induced apoptosis of MDS-L cells. Functional analysis of the differentially expressed genes revealed WFA induced cell death by apoptosis. Induction of apoptosis by WFA in MDS-L cells was confirmed by a decrease in MMP, activation of caspase-3 and an increase in the frequency of annexin-V positive cells with WFA treatment. A closer look at the top differentially regulated genes revealed c-Jun and FosB were substantially induced by WFA; 47- and 52- fold at 6 and 12 h respectively for c-Jun while FosB was up-regulated 36-fold at 6 h and 60-fold at 12 h. We focused on c-Jun and FosB because they can heterodimerize to form an AP-1 transcription factor that is activated by phosphorylation of the c-

Jun subunit by JNK and, JNK/AP-1 signaling has been demonstrated to regulate apoptosis^{93,101}. In addition, JNK cascade activation can be mediated by the ROS sensitive ASK1 and increased ROS production is one of the reported mechanisms by which WFA exerts anticancer effects^{49,62-66,98,108}. WFA treatment increased ROS and activated JNK/AP-1 signaling in MDS-L cells. Activated or phosphorylated JNK can promote apoptosis indirectly by mediating AP-1 induced expression of pro-apoptotic proteins like BIM^{111,112}. BIM induces Bax and Bad activation by inhibiting pro-apoptotic proteins such as Bcl-2 and Mcl-1, resulting in increased mitochondrial permeability and apoptosis¹⁵⁶. Our data showed that WFA induced BIM expression in MDS-L cells and we also observed a substantial decrease in MMP with WFA treatment in MDS-L cells. These results indicate that increase in BIM expression by JNK/AP-1 signaling mediates apoptosis of MDS-L cells treated with WFA. It is known that sustained p21 expression leads to cell cycle arrest and apoptosis⁸⁵. We also found that WFA induced JNK/AP-1 dependent expression of p21 and cell cycle arrest in MDS-L cells. Therefore, it is probable that cell cycle arrest by JNK/AP-1 control of p21 transcription also contributes to apoptosis of MDS-L cells by WFA.

Our studies demonstrated that increased ROS production by WFA in MDS-L cells activated JNK/AP-1 signaling and apoptosis by showing that ROS inhibition abrogated JNK/AP-1 signaling and completely protected MDS-L cells from WFA-induced apoptosis. However, JNK signaling is not the only major pathway activated by increased ROS that mediates apoptosis of MDS-L cells treated with WFA. This is because while we could completely abrogate WFA-

induced apoptosis of MDS-L cells by inhibiting ROS, inhibition of JNK significantly reduced ($p < 0.0005$) but did not completely prevent WFA-induced apoptosis of MDS-L cells. The incomplete protection by JNK inhibition by JNK inhibitors could be due to their cross-reactivity with other kinases important for cell survival. Alternatively, ROS may induce pathway(s) other than JNK that mediate apoptosis.

ROS-induced cell cycle arrest is a plausible simultaneous pathway that could promote apoptosis in parallel with JNK signaling. It is known that ROS-induced DNA damage results in cell cycle arrest⁸⁵. Cell cycle arrest allows for DNA damage repair but apoptosis is triggered if repair fails or is overwhelmed by too many DNA lesions¹⁵⁷. We observed induction of cell cycle arrest in MDS-L cells treated with WFA. Although increased expression of p21 by AP-1 via JNK activation can explain the observed cell cycle arrest, we cannot rule out a contribution from DNA damage mediated cell cycle arrest pathways. ROS-mediated DNA damage was not demonstrated in this present study but WFA has been previously shown to induce ROS-mediated DNA damage¹⁵⁸. Additionally, IPA analysis of our microarray data revealed p53 was one of the upstream regulators activated by WFA ($P = 7.58E-22$ at 6 h and $P = 1.81E-18$ at 12 h). Apoptosis is a secondary response after DNA damage. Hence, we would infer a longer kinetic for the apoptosis response triggered by prolonged cell cycle arrest. This could explain why the substantial inhibition of caspase-3 activation by WFA observed in JNK-IN-8 pretreated cells at 6 and 12 h did not strictly correlate with

the frequency of annexin-V positive cells at 24 h. Inhibition of JNK would not interfere with a ROS-induced DNA damage mediated apoptosis response.

6b) Oxidative stress is a feasible biochemical alteration that can be exploited for selective treatment in MDS

A major goal in cancer therapy is to develop drugs that would more selectively target malignant cells with minimum toxicity to normal cells. Toxic side effects routinely observed with most established chemotherapy drugs could be ameliorated by therapeutic selectivity³⁶. The idea of exploiting cancer redox biology as a basis for therapeutic selectivity is not a new concept¹⁵⁹. Most cancer cells have increased levels of ROS compared to their normal counterparts^{117,160,161}. Increased ROS levels have been associated with oncogenic transformation, tumor progression and poor prognosis¹⁶¹⁻¹⁶⁴. Redox homeostasis is an essential delicate balance under normal physiological conditions as excess ROS can result in apoptotic cell death¹⁰⁸. An antioxidant defense system has evolved to maintain ROS levels below the toxic threshold beyond which cell death is induced⁷².

It used to be a conundrum why the increased oxidative stress was insufficient to cause cell death in cancer cells. However, it is now appreciated that cancer cells adapt to this increased oxidative stress by upregulating their antioxidant capacity to keep them below the toxic threshold¹⁶⁵⁻¹⁶⁷. This adaptation suggests a delicate redox balance is also required for cancer cell function and tipping this balance may be a potential therapeutic strategy^{116,165-167}. Cancer cells

are more dependent than normal cells on the antioxidant system which would make them more vulnerable to compounds that inhibit this system^{165,166}.

Likewise, increased oxidative stress could put cancer cells closer to the toxic threshold compared to their normal counterparts¹⁵⁹. Therefore, a further increase in ROS is likely to push cancer cells but not normal cells beyond the toxic threshold^{159,165,166}. Ovarian cancer, breast cancer and AML are examples of cancer systems in which the potential of ROS inducing agents in cancer therapy has been demonstrated^{65,124,161}. The implication of increased oxidative stress in the development and prognosis of MDS¹¹⁸ is an indication that ROS inducing agents have a selective therapeutic potential in MDS.

6c) Model of cytotoxicity mechanisms of WFA in MDS

Based on our findings, we propose a model in which WFA increases ROS in MDS-L cells to induce cell death primarily by apoptosis (Figure 6.1). This is contrary to the report that WFA primarily induces autophagic cell death of MDS-L cells⁵⁵. However, it is noteworthy that the maximum drug concentration used in that study was 1 μM compared to 10 μM for this study. The difference in outcome with different WFA concentrations on the same cell line further supports the idea of a ROS threshold requirement for ROS-induced apoptotic cell death.

Nevertheless, this possibility would have to be demonstrated experimentally for a definitive conclusion. The mechanisms by which ROS inducing agents increase ROS are unclear¹²⁴. The mitochondrion is thought to be the main source of intracellular ROS in eukaryotic cells¹⁶⁸. Whether this is the site of ROS production in MDS-L cells treated with WFA was not determined in this study.

However, WFA has been shown to inhibit complex III activity within the mitochondrial respiratory chain and this inhibition induces ROS production by complex I and complex II^{49,169}. This increase in ROS by WFA in MDS-L cells results in the activation of ASK1 and subsequent activation of JNK via MKK7. Activated JNK also allows for AP-1 dependent transcription of pro-apoptotic proteins like BIM which promotes apoptosis by decreasing MMP. WFA-induced ROS also mediates cell cycle arrest which could further promote apoptosis. All pathways mediating apoptosis in MDS-L cells by WFA are ROS-dependent because pre-incubation of cells with NAC prior to WFA treatment completely prevented apoptosis. ROS and JNK have been shown, independently, to be involved in the mechanisms mediating WFA cytotoxicity in other cancer cells⁴⁴. Our studies established a link between WFA-induced ROS, JNK/AP-1 signaling and apoptosis in MDS-L cells. In addition, we demonstrated that increase in ROS production is central to the cytotoxicity of WFA in MDS-L cells. Consequently, we suggest redox biology could be exploited as the basis for therapeutic selectivity in MDS.

6d) Conclusion

The study presented here demonstrates that the plant derived compound WFA is a potential therapeutic agent for MDS treatment. Our results show that increase in ROS is central to the apoptosis of MDS-L cells treated with WFA. We identify redox biology as a potential avenue by which therapeutic selectivity can be achieved in MDS. However, several unknowns still remain to be addressed:

1. A pharmacokinetic evaluation of WFA in this study model is required to determine the optimal dose in vivo. It has been reported that the plasma concentration of WFA from a single IP injection of 4mg/kg in female BALB/c mice is 1.8 μ M with a half-life of about 1.3 h¹⁷⁰. Nonetheless, we recognize that this was a single study and mouse strain and the purity of WFA used would impact the pharmacokinetic profile.

2. Detailed analyses of the toxicity profile of WFA are also of utmost importance. We monitored toxicity in this study by weight loss and found WFA to be generally safe (Figure 3.7E). The GI tract is usually highly susceptible to chemotherapeutics because the cells in the epithelium are highly proliferative. In another study investigating the effects of WFA in a mouse lymphoma model, we found that WFA had no apparent effect on the GI tract (data not shown). Another important target of most chemotherapeutics is the bone marrow as bone marrow suppression is a major side effect of most cancer therapies¹³⁸. WFA did not suppress endogenous stem cells in this study (Figure 3.8). In fact, it rather stimulated an expansion of the stem cell population (Figure 3.8). However, the effect of WFA on the clonogenic and repopulation potential of these stem cells has to be evaluated.

3. It is clear that WFA induces ROS in MDS-L cells but the mechanism and species of ROS responsible for selective WFA toxicity remain unclear. The fact that catalase has no effect on WFA-induced ROS (data not shown) suggests H₂O₂ is not the ROS species of interest. This information will be useful to improve the efficiency of WFA and/or identify more efficient ROS-inducing agents.

4. Because the ROS threshold concept likely underlies the therapeutic selectivity of WFA in MDS, it is imperative to determine the optimal dose at which maximum killing of malignant cells occurs without pushing normal cells beyond the toxic threshold.

5. Efficacy of other ROS-inducing agents in MDS has to be evaluated.

Compounds such as 4-benzyl, 2-methyl, 1,2,4-thiadiazolidine, 3,5 dione (TDZD-8), 3-deazaneplanocin A (DZNep), and dimethylaminoparthenolide (DMAPT), which have already been demonstrated to cause killing of AML cells by inducing ROS¹²⁴ would be good candidates.

6. Combinatorial effects of WFA and current FDA approved therapies have to be evaluated. Although combining WFA and lenalidomide was neither synergistic nor additive *in vitro*, the *in vivo* outcome should be investigated. This is especially so because lenalidomide, azacitidine and decitabine all induce an erythroid response which cannot be evaluated *in vitro*.

7. We observed that the efficiency of engraftment of MDS-L cells in NSGS mice was highly variable. Therefore, it will be important to explore methods of reducing this variability such as intrafemoral injection of cells into mice and co-injection of MDS-L cells with human derived stromal cell lines.

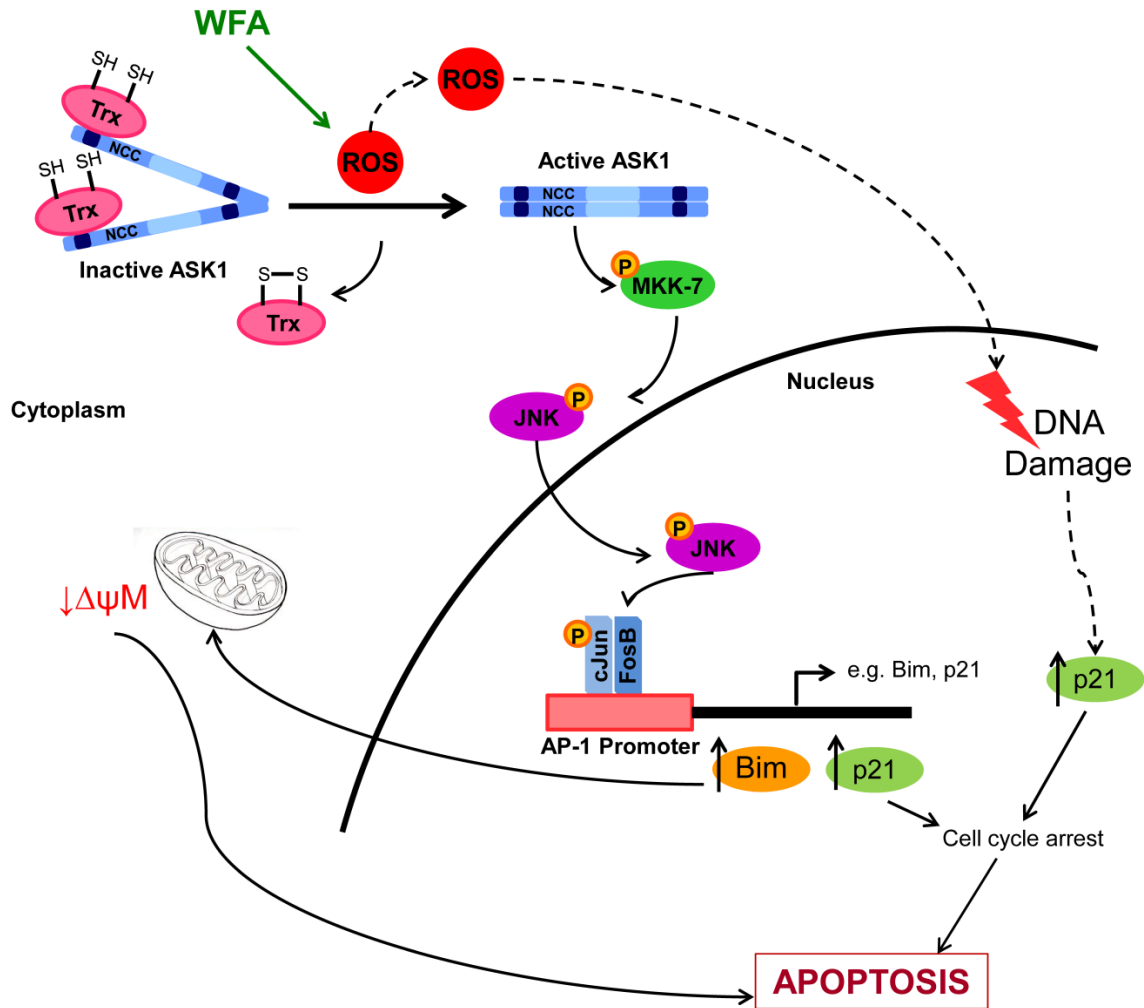


Figure 6.1: Cytotoxicity mechanisms of WFA in MDS

WFA increases ROS in the cell which activates JNK/AP-1 signaling. Increased ROS and expression of AP-1 target genes lead to cell cycle arrest and apoptosis.

APPENDIX A:

**Licence permission from Nature Publishing Group to re-use figure from
Leukemia**

NATURE PUBLISHING GROUP LICENSE TERMS AND CONDITIONS

Jan 03, 2017

This Agreement between Karine Z Oben ("You") and Nature Publishing Group ("Nature Publishing Group") consists of your license details and the terms and conditions provided by Nature Publishing Group and Copyright Clearance Center.

License Number 3991040149727
License date Nov 16, 2016

Licensed Content
Publisher
Licensed Content
Publication

Nature Publishing Group

Leukemia

Licensed Content Title Lenalidomide induces cell death in an MDS-derived cell line with deletion of chromosome 5q by inhibition of cytokinesis

Licensed Content Author A Matsuoka, A Tochigi, M Kishimoto, T Nakahara, T Kondo et al.

Licensed Content Date Feb 4, 2010

Licensed Content Volume 24
Number

Licensed Content Issue 4
Number

Type of Use reuse in a dissertation / thesis

Requestor type academic/educational Format print and electronic Portion
figures/tables/illustrations

Number of figures/tables 1

/illustrations

High-res required no Figures Figure 1a Author of this NPG article no
Your reference number

Title of your thesis /
dissertation

Therapeutic Potential of Targeting ROS Stress in MDS

Expected completion date May 2017

Estimated size (number of pages)

100

Requestor Location Karine Z Oben
800 Rose Street
317 Combs Research Building

LEXINGTON, KY 40536
United States

Attn: Karine Z Oben

Billing Type Invoice

Billing Address Karine Z Oben
800 Rose Street
317 Combs Research Building

LEXINGTON, KY 40536
United States

Attn: Karine Z Oben

Total 0.00 USD

Terms and Conditions

Terms and Conditions for Permissions

Nature Publishing Group hereby grants you a non-exclusive license to reproduce this material for this purpose, and for no other use, subject to the conditions below:

1. NPG warrants that it has, to the best of its knowledge, the rights to license reuse of this material. However, you should ensure that the material you are requesting is original to Nature Publishing Group and does not carry the copyright of another entity (as credited in the published version). If the credit line on any part of the material you have requested indicates that it was reprinted or adapted by NPG with permission from another source, then you should also seek permission from that source to reuse the material.

2. Permission granted free of charge for material in print is also usually granted for any electronic version of that work, provided that the material is incidental to the work as a whole and that the electronic version is essentially equivalent to, or substitutes for, the print version. Where print permission has been granted for a fee, separate permission must be obtained for any additional, electronic re-use (unless, as in the case of a full paper, this has already been accounted for during your initial request in the calculation of a print run). NB: In all cases, web-based use of full-text articles must be authorized separately through the 'Use on a Web Site' option when requesting permission.

3. Permission granted for a first edition does not apply to second and subsequent editions and for editions in other languages (except for signatories to the STM Permissions Guidelines, or where the first edition permission was granted for free).

4. Nature Publishing Group's permission must be acknowledged next to the figure, table or abstract in print. In electronic form, this acknowledgement must be visible at the same time as the figure/table/abstract, and must be hyperlinked to the journal's homepage.

5. The credit line should read:

Reprinted by permission from Macmillan Publishers Ltd: [JOURNAL NAME] (reference citation), copyright (year of publication)

For AOP papers, the credit line should read:

Reprinted by permission from Macmillan Publishers Ltd: [JOURNAL NAME], advance online publication, day month year (doi: 10.1038/sj.[JOURNAL ACRONYM].XXXXX)

Note: For republication from the British Journal of Cancer, the following credit lines apply.

Reprinted by permission from Macmillan Publishers Ltd on behalf of Cancer Research UK: [JOURNAL NAME] (reference citation), copyright (year of publication) For AOP papers, the credit line should read:

Reprinted by permission from Macmillan Publishers Ltd on behalf of Cancer Research UK: [JOURNAL NAME], advance online publication, day month year (doi: 10.1038/sj.[JOURNAL ACRONYM].XXXXX)

6. Adaptations of single figures do not require NPG approval. However, the adaptation should be credited as follows:

Adapted by permission from Macmillan Publishers Ltd: [JOURNAL NAME] (reference citation), copyright (year of publication)

Note: For adaptation from the British Journal of Cancer, the following credit line applies.

Adapted by permission from Macmillan Publishers Ltd on behalf of Cancer Research UK: [JOURNAL NAME] (reference citation), copyright (year of publication)

7. Translations of 401 words up to a whole article require NPG approval. Please visit <http://www.macmillanmedicalcommunications.com> for more information. Translations of up to a 400 words do not require NPG approval. The translation should be credited as follows:

Translated by permission from Macmillan Publishers Ltd: [JOURNAL NAME] (reference citation), copyright (year of publication).

Note: For translation from the British Journal of Cancer, the following credit line applies.

Translated by permission from Macmillan Publishers Ltd on behalf of Cancer Research UK: [JOURNAL NAME] (reference citation), copyright (year of publication)

We are certain that all parties will benefit from this agreement and wish you the best in the use of this material. Thank you. Special Terms:
v1.1

Questions? customercare@copyright.com or +1-855-239-3415 (toll free in the US) or +1-978-646-2777.

APPENDIX B:
COMPOSITION OF POLYACRYLAMIDE GELS

STACKING GEL (5%)	
STOCK SOLUTION	VOLUME (ml)
H ₂ O	3
1M Tris pH 6.8	1.25
40% Acrylamide	0.63
10% SDS	0.05
10% APS	0.05
TEMED	0.0005
Total volume	4.985

RESLOVING GEL			
STOCK SOLUTION	VOLUME (ml)		
	9%	10%	12%
H ₂ O	10.2	9.8	8.8
1M Tris pH 6.8	5	5	5
40% Acrylamide	4.5	5	6
10% SDS	0.2	0.2	0.2
10% APS	0.2	0.2	0.2
TEMED	0.02	0.02	0.02
Total volume	20.12	20.12	20.12

APPENDIX C:
LIST OF ABBREVIATIONS

- 2-ME - 2-Mercaptoethanol
- AML - Acute myeloid leukemia
- AP-1 - Activator protein-1
- APS - Ammonium persulfate
- ASK1 - Apoptosis signal-regulating kinase 1
- ATF2 - Activating transcription factor 2
- BAG3 - Bcl2-associated athanogene 3
- BCA - Bicinchoninic Acid
- Carboxy-DCFDA - 5-(and-6)-Carboxy-2',7'-Dichlorofluorescein Diacetate
- Carboxy-H2DCFDA - 6-Carboxy-2',7'-Dichlorodihydrofluorescein Diacetate
- CAT - Catalase
- Cdc25 - Cell division cycle 25
- Cdks - Cyclin dependent kinases
- CK1 α - casein kinase 1A1
- del 5q - Deletion in chromosome 5q
- DLAR - Division of Laboratory Animal Resources
- DMAPT - Dimethylaminoparthenolide
- DMSO - Dimethyl sulfoxide
- DNMT-1 - DNA methyltransferase-1
- DZNep - 3-deazaneplanocin A
- EDTA - Ethylenediaminetetraacetic acid

ER - Endoplasmic reticulum

FACS - Fluorescence activated cell sorter

Fas-L - Fas-ligand

FBS - Fetal bovine serum

FCCP - Carbonyl cyanide 4-(trifluoromethoxy)phenylhydrazone

FDR - False discovery rate

FWER - Family-wise error rate

GPx - Glutathione peroxidase

GSH - Glutathione

GSSG - Glutathione disulfide

H₂O₂ - Hydrogen peroxide

HSCT - Hematopoietic stem cell transplant

Hsp90 - Heat shock protein 90

IACUC - Institutional Animal Care and Use Committee

IPA - Ingenuity Pathway Analysis

IR - Irradiation

JNKs - c-Jun N-terminal kinases

LENA - Lenalidomide

LSK - Lineage negative cells double positive for both Sca-1 and c-KIT

MAPK - Mitogen-activated protein kinase

MDS - Myelodysplastic syndromes

MMP - Mitochondrial membrane potential

MSigDB - Molecular Signature Database

MTT - 4,5-Dimethylthiazol-2-yl)-2,5-diphenyltetrazolium bromide

NAC - N-acetyl-cysteine

NADPH-oxidase - Nicotinamide adenine dinucleotide phosphate-oxidase

NCC - N-terminal coiled coil

NCI - National Cancer Institute

NSG - NOD/SCID-IL2R γ

NSGS - NSG-hSCF/hGM-CSF/hIL3

OSU CCC - Ohio State University Comprehensive Cancer Center

PBS - Phosphate buffered saline

PI - Propidium Iodide

PMA - Phorbol 12-myristate-13-acetate

qRT-PCR - Quantitative Real-Time PCR

RGS-2 - Regulator of G-protein signaling 2

ROS - Reactive oxygen species

Sca-1 - Stem cell antigen

SDS - Sodium dodecyl sulfate

SOD - Superoxide dismutase

SP-1 - Specificity protein 1

TBST - Tris buffered saline Tween 20

TDZD-8 - 4-benzyl, 2-methyl, 1,2,4-thiadiazolidine, 3,5 dione

t-MDS - Therapy-related myelodysplastic syndrome

Trx - Thioredoxin

WFA - Withaferin A

WHO - World Health Organization

References

1. Heaney ML, Golde DW. Myelodysplasia. *The New England journal of medicine*. 1999;340(21):1649-1660.
2. Jaiswal S, Ebert BL. MDS is a stem cell disorder after all. *Cancer cell*. 2014;25(6):713-714.
3. Jon C Aster RMS. Clinical manifestations and diagnosis of the myelodysplastic syndromes. In: Richard A Larson AGR, ed. *UpToDate*. Online2016.
4. Santini V. Anemia as the Main Manifestation of Myelodysplastic Syndromes. *Seminars in hematology*. 2015;52(4):348-356.
5. Melchert M, List AF. Management of RBC-transfusion dependence. *Hematology / the Education Program of the American Society of Hematology. American Society of Hematology. Education Program*. 2007:398-404.
6. Janssen J, Buschle M, Layton M, et al. Clonal analysis of myelodysplastic syndromes: evidence of multipotent stem cell origin. *Blood*. 1989;73(1):248-254.
7. Woll PS, Kjallquist U, Chowdhury O, et al. Myelodysplastic syndromes are propagated by rare and distinct human cancer stem cells in vivo. *Cancer cell*. 2014;25(6):794-808.
8. Walter MJ, Shen D, Ding L, et al. Clonal architecture of secondary acute myeloid leukemia. *The New England journal of medicine*. 2012;366(12):1090-1098.
9. Papaemmanuil E, Gerstung M, Malcovati L, et al. Clinical and biological implications of driver mutations in myelodysplastic syndromes. *Blood*. 2013;122(22):3616-3627; quiz 3699.
10. Vardiman JW, Thiele J, Arber DA, et al. The 2008 revision of the World Health Organization (WHO) classification of myeloid neoplasms and acute leukemia: rationale and important changes. *Blood*. 2009;114(5):937-951.
11. Godley LA, Larson RA. Therapy-related myeloid leukemia. *Seminars in oncology*. 2008;35(4):418-429.
12. Pedersen-Bjergaard J, Pedersen M, Roulston D, Philip P. Different genetic pathways in leukemogenesis for patients presenting with therapy-related myelodysplasia and therapy-related acute myeloid leukemia. *Blood*. 1995;86(9):3542-3552.
13. Rowley JD, Olney HJ. International workshop on the relationship of prior therapy to balanced chromosome aberrations in therapy-related myelodysplastic syndromes and acute leukemia: Overview report. *Genes, Chromosomes and Cancer*. 2002;33(4):331-345.
14. Smith SM, Le Beau MM, Huo D, et al. Clinical-cytogenetic associations in 306 patients with therapy-related myelodysplasia and myeloid leukemia: the University of Chicago series. *Blood*. 2003;102(1):43-52.
15. Singh ZN, Huo D, Anastasi J, et al. Therapy-related myelodysplastic syndrome: morphologic subclassification may not be clinically relevant. *American journal of clinical pathology*. 2007;127(2):197-205.
16. Pedersen-Bjergaard J, Andersen MT, Andersen MK. Genetic pathways in the pathogenesis of therapy-related myelodysplasia and acute myeloid leukemia. *Hematology / the Education Program of the American Society of Hematology. American Society of Hematology. Education Program*. 2007:392-397.
17. Malmgren JA, Calip GS, Pyott SM, Atwood MK, Kaplan HG. Therapy-related myelodysplastic syndrome following primary breast cancer. *Leukemia research*. 2016;47:178-184.
18. Ma X, Does M, Raza A, Mayne ST. Myelodysplastic syndromes: incidence and survival in the United States. *Cancer*. 2007;109(8):1536-1542.

19. Goldberg SL, Chen E, Corral M, et al. Incidence and clinical complications of myelodysplastic syndromes among United States Medicare beneficiaries. *Journal of clinical oncology : official journal of the American Society of Clinical Oncology*. 2010;28(17):2847-2852.
20. Sekeres MA, Schoonen WM, Kantarjian H, et al. Characteristics of US patients with myelodysplastic syndromes: results of six cross-sectional physician surveys. *Journal of the National Cancer Institute*. 2008;100(21):1542-1551.
21. Michels SD, McKenna RW, Arthur DC, Brunning RD. Therapy-related acute myeloid leukemia and myelodysplastic syndrome: a clinical and morphologic study of 65 cases. *Blood*. 1985;65(6):1364-1372.
22. Passmore SJ, Hann IM, Stiller CA, et al. Pediatric myelodysplasia: a study of 68 children and a new prognostic scoring system. *Blood*. 1995;85(7):1742-1750.
23. Hasle H. Myelodysplastic syndromes in childhood--classification, epidemiology, and treatment. *Leukemia & lymphoma*. 1994;13(1-2):11-26.
24. Cogle CR, Craig BM, Rollison DE, List AF. Incidence of the myelodysplastic syndromes using a novel claims-based algorithm: high number of uncaptured cases by cancer registries. *Blood*. 2011;117(26):7121-7125.
25. McQuilten ZK, Wood EM, Polizzotto MN, et al. Underestimation of myelodysplastic syndrome incidence by cancer registries: Results from a population-based data linkage study. *Cancer*. 2014;120(11):1686-1694.
26. De Roos AJ, Deeg HJ, Onstad L, et al. Incidence of myelodysplastic syndromes within a nonprofit healthcare system in western Washington state, 2005-2006. *American journal of hematology*. 2010;85(10):765-770.
27. Bejar R, Steensma DP. Recent developments in myelodysplastic syndromes. *Blood*. 2014;124(18):2793-2803.
28. Hankey BF, Ries LA, Edwards BK. The surveillance, epidemiology, and end results program: a national resource. *Cancer epidemiology, biomarkers & prevention : a publication of the American Association for Cancer Research, cosponsored by the American Society of Preventive Oncology*. 1999;8(12):1117-1121.
29. Derissen EJ, Beijnen JH, Schellens JH. Concise drug review: azacitidine and decitabine. *The oncologist*. 2013;18(5):619-624.
30. Gohring G, Giagounidis A, Busche G, et al. Patients with del(5q) MDS who fail to achieve sustained erythroid or cytogenetic remission after treatment with lenalidomide have an increased risk for clonal evolution and AML progression. *Annals of hematology*. 2010;89(4):365-374.
31. Bhatt VR, Steensma DP. Hematopoietic Cell Transplantation for Myelodysplastic Syndromes. *Journal of oncology practice / American Society of Clinical Oncology*. 2016;12(9):786-792.
32. Ballen KK, Gilliland DG, Guinan EC, et al. Bone marrow transplantation for therapy-related myelodysplasia: comparison with primary myelodysplasia. *Bone marrow transplantation*. 1997;20(9):737-743.
33. Yakoub-Agha I, de La Salmoniere P, Ribaud P, et al. Allogeneic bone marrow transplantation for therapy-related myelodysplastic syndrome and acute myeloid leukemia: a long-term study of 70 patients-report of the French society of bone marrow transplantation. *Journal of clinical oncology : official journal of the American Society of Clinical Oncology*. 2000;18(5):963-971.

34. Armand P, Kim HT, Mayer E, et al. Outcome of allo-SCT for women with MDS or AML occurring after breast cancer therapy. *Bone marrow transplantation*. 2010;45(11):1611-1617.
35. Miller CB, Piantadosi S, Vogelsang GB, et al. Impact of age on outcome of patients with cancer undergoing autologous bone marrow transplant. *Journal of clinical oncology : official journal of the American Society of Clinical Oncology*. 1996;14(4):1327-1332.
36. Desai AG, Qazi GN, Ganju RK, et al. Medicinal plants and cancer chemoprevention. *Current drug metabolism*. 2008;9(7):581-591.
37. Greenwell M, Rahman PK. Medicinal Plants: Their Use in Anticancer Treatment. *International journal of pharmaceutical sciences and research*. 2015;6(10):4103-4112.
38. Tavakoli J, Miar S, Majid Zadehzare M, Akbari H. Evaluation of Effectiveness of Herbal Medication in Cancer Care: A Review Study. *Iranian Journal of Cancer Prevention*. 2012;5(3):144-156.
39. Prakash O, Kumar A, Kumar P, Ajeet A. Anticancer Potential of Plants and Natural Products: A Review. *American Journal of Pharmacological Sciences*. 2013;1(6):104-115.
40. Mirjalili MH, Moyano E, Bonfill M, Cusido RM, Palazon J. Steroidal lactones from *Withania somnifera*, an ancient plant for novel medicine. *Molecules (Basel, Switzerland)*. 2009;14(7):2373-2393.
41. Vanden Berghe W, Sabbe L, Kaileh M, Haegeman G, Heyninck K. Molecular insight in the multifunctional activities of Withaferin A. *Biochemical pharmacology*. 2012;84(10):1282-1291.
42. Winters M. Ancient medicine, modern use: *Withania somnifera* and its potential role in integrative oncology. *Alternative medicine review : a journal of clinical therapeutic*. 2006;11(4):269-277.
43. NCCIH. Ayurvedic Medicine: In Depth 2005; NCCIH Fact sheet. Available at: nccih.nih.gov.
44. Vyas AR, Singh SV. Molecular targets and mechanisms of cancer prevention and treatment by withaferin a, a naturally occurring steroidal lactone. *The AAPS journal*. 2014;16(1):1-10.
45. McKenna MK, Gachuki BW, Alhakeem SS, et al. Anti-cancer activity of withaferin A in B-cell lymphoma. *Cancer biology & therapy*. 2015;16(7):1088-1098.
46. Bargagna-Mohan P, Keshipeddy S, Wright DL, Mohan R. Imaging Withaferin A-Vimentin Interactions in Live Cells and Fibrotic Tissues. *The FASEB Journal*. 2016;30(1 Supplement):612.617.
47. Heyninck K, Lahtela-Kakkonen M, Van der Veken P, Haegeman G, Vanden Berghe W. Withaferin A inhibits NF-kappaB activation by targeting cysteine 179 in IKKbeta. *Biochemical pharmacology*. 2014;91(4):501-509.
48. Yu Y, Hamza A, Zhang T, et al. Withaferin A targets heat shock protein 90 in pancreatic cancer cells. *Biochemical pharmacology*. 2010;79(4):542-551.
49. Hahm ER, Moura MB, Kelley EE, Van Houten B, Shiva S, Singh SV. Withaferin A-induced apoptosis in human breast cancer cells is mediated by reactive oxygen species. *PLoS one*. 2011;6(8):e23354.
50. Lee IC, Choi BY. Withaferin-A--A Natural Anticancer Agent with Pleiotropic Mechanisms of Action. *International journal of molecular sciences*. 2016;17(3):290.
51. Stan SD, Zeng Y, Singh SV. Ayurvedic medicine constituent withaferin a causes G2 and M phase cell cycle arrest in human breast cancer cells. *Nutrition and cancer*. 2008;60 Suppl 1:51-60.

52. Munagala R, Kausar H, Munjal C, Gupta RC. Withaferin A induces p53-dependent apoptosis by repression of HPV oncogenes and upregulation of tumor suppressor proteins in human cervical cancer cells. *Carcinogenesis*. 2011;32(11):1697-1705.
53. Shah N, Kataria H, Kaul SC, Ishii T, Kaur G, Wadhwa R. Effect of the alcoholic extract of Ashwagandha leaves and its components on proliferation, migration, and differentiation of glioblastoma cells: combinational approach for enhanced differentiation. *Cancer science*. 2009;100(9):1740-1747.
54. Samadi AK, Cohen SM, Mukerji R, et al. Natural withanolide withaferin A induces apoptosis in uveal melanoma cells by suppression of Akt and c-MET activation. *Tumour biology : the journal of the International Society for Oncodevelopmental Biology and Medicine*. 2012;33(4):1179-1189.
55. Okamoto S, Tsujioka T, Suemori S, et al. Withaferin A suppresses the growth of myelodysplasia and leukemia cell lines by inhibiting cell cycle progression. *Cancer science*. 2016;107(9):1302-1314.
56. Grogan PT, Sleder KD, Samadi AK, Zhang H, Timmermann BN, Cohen MS. Cytotoxicity of withaferin A in glioblastomas involves induction of an oxidative stress-mediated heat shock response while altering Akt/mTOR and MAPK signaling pathways. *Investigational new drugs*. 2013;31(3):545-557.
57. Zhang X, Samadi AK, Roby KF, Timmermann B, Cohen MS. Inhibition of cell growth and induction of apoptosis in ovarian carcinoma cell lines CaOV3 and SKOV3 by natural withanolide Withaferin A. *Gynecologic oncology*. 2012;124(3):606-612.
58. Yang H, Shi G, Dou QP. The tumor proteasome is a primary target for the natural anticancer compound Withaferin A isolated from "Indian winter cherry". *Molecular pharmacology*. 2007;71(2):426-437.
59. Srinivasan S, Ranga RS, Burikhanov R, Han SS, Chendil D. Par-4-dependent apoptosis by the dietary compound withaferin A in prostate cancer cells. *Cancer research*. 2007;67(1):246-253.
60. Lahat G, Zhu QS, Huang KL, et al. Vimentin is a novel anti-cancer therapeutic target; insights from in vitro and in vivo mice xenograft studies. *PloS one*. 2010;5(4):e10105.
61. Gambhir L, Checker R, Sharma D, et al. Thiol dependent NF-kappaB suppression and inhibition of T-cell mediated adaptive immune responses by a naturally occurring steroidal lactone Withaferin A. *Toxicology and applied pharmacology*. 2015;289(2):297-312.
62. Malik F, Kumar A, Bhushan S, et al. Reactive oxygen species generation and mitochondrial dysfunction in the apoptotic cell death of human myeloid leukemia HL-60 cells by a dietary compound withaferin A with concomitant protection by N-acetyl cysteine. *Apoptosis : an international journal on programmed cell death*. 2007;12(11):2115-2133.
63. Lee TJ, Um HJ, Min do S, Park JW, Choi KS, Kwon TK. Withaferin A sensitizes TRAIL-induced apoptosis through reactive oxygen species-mediated up-regulation of death receptor 5 and down-regulation of c-FLIP. *Free radical biology & medicine*. 2009;46(12):1639-1649.
64. Mayola E, Gallerne C, Esposti DD, et al. Withaferin A induces apoptosis in human melanoma cells through generation of reactive oxygen species and down-regulation of Bcl-2. *Apoptosis : an international journal on programmed cell death*. 2011;16(10):1014-1027.

65. Widodo N, Priyandoko D, Shah N, Wadhwa R, Kaul SC. Selective killing of cancer cells by Ashwagandha leaf extract and its component Withanone involves ROS signaling. *PLoS one*. 2010;5(10):e13536.
66. Yang ES, Choi MJ, Kim JH, Choi KS, Kwon TK. Withaferin A enhances radiation-induced apoptosis in Caki cells through induction of reactive oxygen species, Bcl-2 downregulation and Akt inhibition. *Chemico-biological interactions*. 2011;190(1):9-15.
67. Pelicano H, Carney D, Huang P. ROS stress in cancer cells and therapeutic implications. *Drug resistance updates : reviews and commentaries in antimicrobial and anticancer chemotherapy*. 2004;7(2):97-110.
68. Trachootham D, Alexandre J, Huang P. Targeting cancer cells by ROS-mediated mechanisms: a radical therapeutic approach? *Nature reviews. Drug discovery*. 2009;8(7):579-591.
69. Kohen R, Nyska A. Oxidation of biological systems: oxidative stress phenomena, antioxidants, redox reactions, and methods for their quantification. *Toxicologic pathology*. 2002;30(6):620-650.
70. Valko M, Leibfritz D, Moncol J, Cronin MT, Mazur M, Telser J. Free radicals and antioxidants in normal physiological functions and human disease. *The international journal of biochemistry & cell biology*. 2007;39(1):44-84.
71. Decoursey TE, Ligeti E. Regulation and termination of NADPH oxidase activity. *Cellular and molecular life sciences : CMLS*. 2005;62(19-20):2173-2193.
72. Poljsak B, Suput D, Milisav I. Achieving the balance between ROS and antioxidants: when to use the synthetic antioxidants. *Oxidative medicine and cellular longevity*. 2013;2013:956792.
73. Sies H. Strategies of antioxidant defense. *European journal of biochemistry / FEBS*. 1993;215(2):213-219.
74. Pastore A, Federici G, Bertini E, Piemonte F. Analysis of glutathione: implication in redox and detoxification. *Clinica chimica acta; international journal of clinical chemistry*. 2003;333(1):19-39.
75. Masella R, Di Benedetto R, Vari R, Filesi C, Giovannini C. Novel mechanisms of natural antioxidant compounds in biological systems: involvement of glutathione and glutathione-related enzymes. *The Journal of nutritional biochemistry*. 2005;16(10):577-586.
76. Jones DP, Carlson JL, Mody VC, Cai J, Lynn MJ, Sternberg P. Redox state of glutathione in human plasma. *Free radical biology & medicine*. 2000;28(4):625-635.
77. Droge W. Free radicals in the physiological control of cell function. *Physiological reviews*. 2002;82(1):47-95.
78. Halliwell B. Free radicals and antioxidants - quo vadis? *Trends in pharmacological sciences*. 2011;32(3):125-130.
79. Paiva CN, Bozza MT. Are reactive oxygen species always detrimental to pathogens? *Antioxidants & redox signaling*. 2014;20(6):1000-1037.
80. Hultqvist M, Olsson LM, Gelderman KA, Holmdahl R. The protective role of ROS in autoimmune disease. *Trends in immunology*. 2009;30(5):201-208.
81. Ray PD, Huang BW, Tsuji Y. Reactive oxygen species (ROS) homeostasis and redox regulation in cellular signaling. *Cellular signalling*. 2012;24(5):981-990.
82. Schreck R, Rieber P, Baeuerle PA. Reactive oxygen intermediates as apparently widely used messengers in the activation of the NF-kappa B transcription factor and HIV-1. *The EMBO journal*. 1991;10(8):2247-2258.

83. Waypa GB, Guzy R, Mungai PT, et al. Increases in mitochondrial reactive oxygen species trigger hypoxia-induced calcium responses in pulmonary artery smooth muscle cells. *Circulation research*. 2006;99(9):970-978.
84. Fleury C, Mignotte B, Vayssiere JL. Mitochondrial reactive oxygen species in cell death signaling. *Biochimie*. 2002;84(2-3):131-141.
85. Boonstra J, Post JA. Molecular events associated with reactive oxygen species and cell cycle progression in mammalian cells. *Gene*. 2004;337:1-13.
86. Sarsour EH, Kumar MG, Chaudhuri L, Kalen AL, Goswami PC. Redox control of the cell cycle in health and disease. *Antioxidants & redox signaling*. 2009;11(12):2985-3011.
87. Verbon EH, Post JA, Boonstra J. The influence of reactive oxygen species on cell cycle progression in mammalian cells. *Gene*. 2012;511(1):1-6.
88. Lim S, Kaldis P. Cdks, cyclins and CKIs: roles beyond cell cycle regulation. *Development*. 2013;140(15):3079-3093.
89. Li Y, Zhang LP, Dai F, et al. Hexamethoxylated Monocarbonyl Analogues of Curcumin Cause G2/M Cell Cycle Arrest in NCI-H460 Cells via Michael Acceptor-Dependent Redox Intervention. *Journal of agricultural and food chemistry*. 2015;63(35):7731-7742.
90. Brooks CL, Gu W. p53 ubiquitination: Mdm2 and beyond. *Molecular cell*. 2006;21(3):307-315.
91. Fischer M, Steiner L, Engeland K. The transcription factor p53: not a repressor, solely an activator. *Cell cycle (Georgetown, Tex.)*. 2014;13(19):3037-3058.
92. Johnson GL, Lapadat R. Mitogen-activated protein kinase pathways mediated by ERK, JNK, and p38 protein kinases. *Science (New York, N.Y.)*. 2002;298(5600):1911-1912.
93. Dhanasekaran DN, Reddy EP. JNK signaling in apoptosis. *Oncogene*. 2008;27(48):6245-6251.
94. Manning G, Whyte DB, Martinez R, Hunter T, Sudarsanam S. The protein kinase complement of the human genome. *Science (New York, N.Y.)*. 2002;298(5600):1912-1934.
95. Davis RJ. Signal transduction by the JNK group of MAP kinases. *Cell*. 2000;103(2):239-252.
96. Gupta S, Barrett T, Whitmarsh AJ, et al. Selective interaction of JNK protein kinase isoforms with transcription factors. *The EMBO journal*. 1996;15(11):2760-2770.
97. Dhanasekaran N, Premkumar Reddy E. Signaling by dual specificity kinases. *Oncogene*. 1998;17(11 Reviews):1447-1455.
98. Wu Z, Wu J, Jacinto E, Karin M. Molecular cloning and characterization of human JNKK2, a novel Jun NH2-terminal kinase-specific kinase. *Molecular and cellular biology*. 1997;17(12):7407-7416.
99. Raman M, Chen W, Cobb MH. Differential regulation and properties of MAPKs. *Oncogene*. 2007;26(22):3100-3112.
100. Bogoyevitch MA, Kobe B. Uses for JNK: the many and varied substrates of the c-Jun N-terminal kinases. *Microbiology and molecular biology reviews : MMBR*. 2006;70(4):1061-1095.
101. Karin M, Liu Z, Zandi E. AP-1 function and regulation. *Current opinion in cell biology*. 1997;9(2):240-246.
102. Pulverer BJ, Kyriakis JM, Avruch J, Nikolakaki E, Woodgett JR. Phosphorylation of c-jun mediated by MAP kinases. *Nature*. 1991;353(6345):670-674.
103. Kyriakis JM, Banerjee P, Nikolakaki E, et al. The stress-activated protein kinase subfamily of c-Jun kinases. *Nature*. 1994;369(6476):156-160.

104. Johnson GL, Nakamura K. The c-jun kinase/stress-activated pathway: regulation, function and role in human disease. *Biochimica et biophysica acta*. 2007;1773(8):1341-1348.
105. Bubici C, Papa S. JNK signalling in cancer: in need of new, smarter therapeutic targets. *British journal of pharmacology*. 2014;171(1):24-37.
106. Kriehuber E, Bauer W, Charbonnier AS, et al. Balance between NF-kappaB and JNK/AP-1 activity controls dendritic cell life and death. *Blood*. 2005;106(1):175-183.
107. Tournier C. The 2 Faces of JNK Signaling in Cancer. *Genes & cancer*. 2013;4(9-10):397-400.
108. Circu ML, Aw TY. Reactive oxygen species, cellular redox systems, and apoptosis. *Free radical biology & medicine*. 2010;48(6):749-762.
109. Fujino G, Noguchi T, Matsuzawa A, et al. Thioredoxin and TRAF family proteins regulate reactive oxygen species-dependent activation of ASK1 through reciprocal modulation of the N-terminal homophilic interaction of ASK1. *Molecular and cellular biology*. 2007;27(23):8152-8163.
110. Saitoh M, Nishitoh H, Fujii M, et al. Mammalian thioredoxin is a direct inhibitor of apoptosis signal-regulating kinase (ASK) 1. *The EMBO journal*. 1998;17(9):2596-2606.
111. Whitfield J, Neame SJ, Paquet L, Bernard O, Ham J. Dominant-negative c-Jun promotes neuronal survival by reducing BIM expression and inhibiting mitochondrial cytochrome c release. *Neuron*. 2001;29(3):629-643.
112. Putcha GV, Le S, Frank S, et al. JNK-mediated BIM phosphorylation potentiates BAX-dependent apoptosis. *Neuron*. 2003;38(6):899-914.
113. Shaulian E, Karin M. AP-1 as a regulator of cell life and death. *Nature cell biology*. 2002;4(5):E131-136.
114. Aoki H, Kang PM, Hampe J, et al. Direct activation of mitochondrial apoptosis machinery by c-Jun N-terminal kinase in adult cardiac myocytes. *The Journal of biological chemistry*. 2002;277(12):10244-10250.
115. Schroeter H, Boyd CS, Ahmed R, et al. c-Jun N-terminal kinase (JNK)-mediated modulation of brain mitochondria function: new target proteins for JNK signalling in mitochondrion-dependent apoptosis. *The Biochemical journal*. 2003;372(Pt 2):359-369.
116. Schumacker PT. Reactive oxygen species in cancer cells: live by the sword, die by the sword. *Cancer cell*. 2006;10(3):175-176.
117. Szatrowski TP, Nathan CF. Production of large amounts of hydrogen peroxide by human tumor cells. *Cancer research*. 1991;51(3):794-798.
118. Goncalves AC, Cortesao E, Oliveiros B, et al. Oxidative stress and mitochondrial dysfunction play a role in myelodysplastic syndrome development, diagnosis, and prognosis: A pilot study. *Free radical research*. 2015;49(9):1081-1094.
119. Trachootham D, Zhang H, Zhang W, et al. Effective elimination of fludarabine-resistant CLL cells by PEITC through a redox-mediated mechanism. *Blood*. 2008;112(5):1912-1922.
120. Guzman ML, Li X, Corbett CA, et al. Rapid and selective death of leukemia stem and progenitor cells induced by the compound 4-benzyl, 2-methyl, 1,2,4-thiadiazolidine, 3,5 dione (TDZD-8). *Blood*. 2007;110(13):4436-4444.
121. Zhang H, Mi JQ, Fang H, et al. Preferential eradication of acute myelogenous leukemia stem cells by fenretinide. *Proceedings of the National Academy of Sciences of the United States of America*. 2013;110(14):5606-5611.
122. Jin Y, Lu Z, Ding K, et al. Antineoplastic mechanisms of niclosamide in acute myelogenous leukemia stem cells: inactivation of the NF-kappaB pathway and generation of reactive oxygen species. *Cancer research*. 2010;70(6):2516-2527.

123. Guzman ML, Rossi RM, Karnischky L, et al. The sesquiterpene lactone parthenolide induces apoptosis of human acute myelogenous leukemia stem and progenitor cells. *Blood*. 2005;105(11):4163-4169.
124. Zhang H, Fang H, Wang K. Reactive oxygen species in eradicating acute myeloid leukemic stem cells. *Stem cell investigation*. 2014;1:13.
125. Thanopoulou E, Cashman J, Kakagianni T, Eaves A, Zoumbos N, Eaves C. Engraftment of NOD/SCID-beta2 microglobulin null mice with multilineage neoplastic cells from patients with myelodysplastic syndrome. *Blood*. 2004;103(11):4285-4293.
126. Benito AI, Bryant E, Loken MR, et al. NOD/SCID mice transplanted with marrow from patients with myelodysplastic syndrome (MDS) show long-term propagation of normal but not clonal human precursors. *Leukemia research*. 2003;27(5):425-436.
127. Matsuoka A, Tochigi A, Kishimoto M, et al. Lenalidomide induces cell death in an MDS-derived cell line with deletion of chromosome 5q by inhibition of cytokinesis. *Leukemia*. 2010;24(4):748-755.
128. Tohyama K, Tsutani H, Ueda T, Nakamura T, Yoshida Y. Establishment and characterization of a novel myeloid cell line from the bone marrow of a patient with the myelodysplastic syndrome. *British journal of haematology*. 1994;87(2):235-242.
129. Drexler HG, Dirks WG, Macleod RA. Many are called MDS cell lines: one is chosen. *Leukemia research*. 2009;33(8):1011-1016.
130. Rhyasen GW, Wunderlich M, Tohyama K, Garcia-Manero G, Mulloy JC, Starczynowski DT. An MDS xenograft model utilizing a patient-derived cell line. *Leukemia*. 2014;28(5):1142-1145.
131. Subramanian A, Tamayo P, Mootha VK, et al. Gene set enrichment analysis: A knowledge-based approach for interpreting genome-wide expression profiles. *Proceedings of the National Academy of Sciences*. 2005;102(43):15545-15550.
132. Perelman A, Wachtel C, Cohen M, Haupt S, Shapiro H, Tzur A. JC-1: alternative excitation wavelengths facilitate mitochondrial membrane potential cytometry. *Cell death & disease*. 2012;3:e430.
133. Wegrzyn J, Lam JC, Karsan A. Mouse models of myelodysplastic syndromes. *Leukemia research*. 2011;35(7):853-862.
134. Duong VH, Komrokji RS, List AF. Efficacy and safety of lenalidomide in patients with myelodysplastic syndrome with chromosome 5q deletion. *Therapeutic advances in hematology*. 2012;3(2):105-116.
135. Pellagatti A, Jadersten M, Forsblom AM, et al. Lenalidomide inhibits the malignant clone and up-regulates the SPARC gene mapping to the commonly deleted region in 5q-syndrome patients. *Proceedings of the National Academy of Sciences of the United States of America*. 2007;104(27):11406-11411.
136. Greenberg AJ, Walters DK, Kumar SK, Vincent Rajkumar S, Jelinek DF. Responsiveness of cytogenetically discrete human myeloma cell lines to lenalidomide: lack of correlation with cereblon and interferon regulatory factor 4 expression levels. *European journal of haematology*. 2013;91(6):504-513.
137. Biedermann KA, Sun JR, Giaccia AJ, Tosto LM, Brown JM. scid mutation in mice confers hypersensitivity to ionizing radiation and a deficiency in DNA double-strand break repair. *Proceedings of the National Academy of Sciences of the United States of America*. 1991;88(4):1394-1397.
138. Wang Y, Probin V, Zhou D. Cancer therapy-induced residual bone marrow injury- Mechanisms of induction and implication for therapy. *Current cancer therapy reviews*. 2006;2(3):271-279.

139. Breccia M, Alimena G. NF-kappaB as a potential therapeutic target in myelodysplastic syndromes and acute myeloid leukemia. *Expert opinion on therapeutic targets*. 2010;14(11):1157-1176.
140. Karin M. NF-kappaB as a critical link between inflammation and cancer. *Cold Spring Harbor perspectives in biology*. 2009;1(5):a000141.
141. Gottlieb E, Armour SM, Harris MH, Thompson CB. Mitochondrial membrane potential regulates matrix configuration and cytochrome c release during apoptosis. *Cell death and differentiation*. 2003;10(6):709-717.
142. Porter AG, Janicke RU. Emerging roles of caspase-3 in apoptosis. *Cell death and differentiation*. 1999;6(2):99-104.
143. Rosati A, Graziano V, De Laurenzi V, Pascale M, Turco MC. BAG3: a multifaceted protein that regulates major cell pathways. *Cell death & disease*. 2011;2:e141.
144. Endale M, Kim SD, Lee WM, et al. Ischemia induces regulator of G protein signaling 2 (RGS2) protein upregulation and enhances apoptosis in astrocytes. *American journal of physiology. Cell physiology*. 2010;298(3):C611-623.
145. Lyu JH, Park DW, Huang B, et al. RGS2 suppresses breast cancer cell growth via a MCP1P1-dependent pathway. *Journal of cellular biochemistry*. 2015;116(2):260-267.
146. Wolff DW, Xie Y, Deng C, et al. Epigenetic repression of regulator of G-protein signaling 2 promotes androgen-independent prostate cancer cell growth. *Int J Cancer*. 2012;130(7):1521-1531.
147. Sharma SC, Richards JS. Regulation of AP1 (Jun/Fos) factor expression and activation in ovarian granulosa cells. Relation of JunD and Fra2 to terminal differentiation. *The Journal of biological chemistry*. 2000;275(43):33718-33728.
148. Abbas T, Dutta A. p21 in cancer: intricate networks and multiple activities. *Nature reviews. Cancer*. 2009;9(6):400-414.
149. Chang BD, Watanabe K, Broude EV, et al. Effects of p21Waf1/Cip1/Sdi1 on cellular gene expression: implications for carcinogenesis, senescence, and age-related diseases. *Proceedings of the National Academy of Sciences of the United States of America*. 2000;97(8):4291-4296.
150. Zhang T, Inesta-Vaquera F, Niepel M, et al. Discovery of potent and selective covalent inhibitors of JNK. *Chemistry & biology*. 2012;19(1):140-154.
151. Bennett BL, Sasaki DT, Murray BW, et al. SP600125, an anthrapyrazolone inhibitor of Jun N-terminal kinase. *Proceedings of the National Academy of Sciences of the United States of America*. 2001;98(24):13681-13686.
152. Prebet T, Gore SD, Esterni B, et al. Outcome of high-risk myelodysplastic syndrome after azacitidine treatment failure. *Journal of clinical oncology : official journal of the American Society of Clinical Oncology*. 2011;29(24):3322-3327.
153. Kronke J, Fink EC, Hollenbach PW, et al. Lenalidomide induces ubiquitination and degradation of CK1alpha in del(5q) MDS. *Nature*. 2015;523(7559):183-188.
154. Schneider Rebekka K, Ademà V, Heckl D, et al. Role of Casein Kinase 1A1 in the Biology and Targeted Therapy of del(5q) MDS. *Cancer cell*.26(4):509-520.
155. Lin YW, Slape C, Zhang Z, Aplan PD. NUP98-HOXD13 transgenic mice develop a highly penetrant, severe myelodysplastic syndrome that progresses to acute leukemia. *Blood*. 2005;106(1):287-295.
156. Aguilo N, Uranga S, Marinova D, Martin C, Pardo J. Bim is a crucial regulator of apoptosis induced by Mycobacterium tuberculosis. *Cell death & disease*. 2014;5:e1343.
157. Roos WP, Kaina B. DNA damage-induced cell death: from specific DNA lesions to the DNA damage response and apoptosis. *Cancer letters*. 2013;332(2):237-248.

158. Sen N, Banerjee B, Das BB, et al. Apoptosis is induced in leishmanial cells by a novel protein kinase inhibitor withaferin A and is facilitated by apoptotic topoisomerase I-DNA complex. *Cell death and differentiation*. 2007;14(2):358-367.
159. Kong Q, Beel JA, Lillehei KO. A threshold concept for cancer therapy. *Medical hypotheses*. 2000;55(1):29-35.
160. Toyokuni S, Okamoto K, Yodoi J, Hiai H. Persistent oxidative stress in cancer. *FEBS letters*. 1995;358(1):1-3.
161. Trachootham D, Zhou Y, Zhang H, et al. Selective killing of oncogenically transformed cells through a ROS-mediated mechanism by β -phenylethyl isothiocyanate. *Cancer cell*. 10(3):241-252.
162. Patel BP, Rawal UM, Dave TK, et al. Lipid peroxidation, total antioxidant status, and total thiol levels predict overall survival in patients with oral squamous cell carcinoma. *Integrative cancer therapies*. 2007;6(4):365-372.
163. Behrend L, Henderson G, Zwacka RM. Reactive oxygen species in oncogenic transformation. *Biochemical Society transactions*. 2003;31(Pt 6):1441-1444.
164. Wu WS. The signaling mechanism of ROS in tumor progression. *Cancer metastasis reviews*. 2006;25(4):695-705.
165. Liou GY, Storz P. Reactive oxygen species in cancer. *Free radical research*. 2010;44(5):479-496.
166. Trachootham D, Alexandre J, Huang P. Targeting cancer cells by ROS-mediated mechanisms: a radical therapeutic approach? *Nature reviews. Drug discovery*. 2009;8(7):579-591.
167. Miao L, Holley AK, Zhao Y, St Clair WH, St Clair DK. Redox-mediated and ionizing-radiation-induced inflammatory mediators in prostate cancer development and treatment. *Antioxidants & redox signaling*. 2014;20(9):1481-1500.
168. Turrens JF. Mitochondrial formation of reactive oxygen species. *The Journal of physiology*. 2003;552(Pt 2):335-344.
169. Bleier L, Droese S. Superoxide generation by complex III: from mechanistic rationales to functional consequences. *Biochimica et biophysica acta*. 2013;1827(11-12):1320-1331.
170. Thaiparambil JT, Bender L, Ganesh T, et al. Withaferin A inhibits breast cancer invasion and metastasis at sub-cytotoxic doses by inducing vimentin disassembly and serine 56 phosphorylation. *International Journal of Cancer*. 2011;129(11):2744-2755.

VITA

KARINE Z. OBEN

Education

- 08/11 - Present PhD., Department of Microbiology, Immunology and
Molecular Genetics
- 08/08 - 08/10 MS, Agricultural and Environmental Sciences
- 10/03 - 08/06 BS, Biochemistry; Minor in Medical Laboratory Technology

Professional Experiences

- 08/11 - Present Graduate Research Assistant, University of Kentucky,
Lexington, KY
- 06/08 - 05/10 Graduate Research Assistant, University of Tuskegee,
Tuskegee, AL
- 02/08 - 06/08 Research Assistant, University of Buea, Buea Cameroon
- 09/06 - 06/07 Teacher, Salvation Bilingual High School, Buea Cameroon
- 10/05 - 10/06 Laboratory Technician Intern, Health for All Foundation,
Buea, Cameroon

Awards and/or Scholarships

- 08/11 - Present Graduate research assistant scholarship, University of
Kentucky
- 06/08 - 05/10 Graduate research assistant scholarship, University of
Tuskegee
- 08/06 BS, Biochemistry; Minor in Medical Laboratory Technology,
with second class honors

Publications

Oben KZ et al., (2017) Radiation Induced Apoptosis of Murine Bone Marrow Cells is Independent of Early Growth Response 1 (EGR1). PLoS ONE 12(1):e0169767.

McKenna MK, Gachuki BW, Alhakeem SS, **Oben KN**, Rangnekar VM, Gupta RC, Bondada S. Anti-cancer activity of Withaferin A in B cell lymphoma. Cancer Biol Ther. 2015; 16(7): 1088-98

Nyiauwung, KZ et al., (2012). Sweetpotato. In C. Kole, C.P. Joshi & D.R. Shonnard (Eds.), Handbook of bioenergy crop plants (pp. 737-747). Boca Raton, FL: CRC Press

Nyiauwung, K.Z et al., Evaluation of ten sweetpotato cultivars as potential feedstock for biofuel production. Journal of Root Crops. 2010; 63(2): 242-249

Abstracts and Lectures

05/16 Anti-cancer potential of Withaferin A in a model of human 5q Myelodysplastic Syndrome

Markey Cancer Center Research Day

05/16 Growth inhibitory effects of Withaferin A on MDS-L cells – A human 5q Myelodysplastic Syndrome (MDS) cell line

AAI Annual Meeting

05/16 Investigating the therapeutic potential of Withaferin A in a model of human 5q Myelodysplastic Syndrome

Departmental Retreat

05/15 Role of EGR1 in radiation induced apoptosis of bone marrow cells

Conference on normal tissue radiation effects and counter measures (CONTREC)

05/14 Investigation of Withaferin A as a novel therapy for the treatment of 5q Myelodysplastic syndrome (MDS)

Markey Cancer Center Research Day

05/14 Effect of Withaferin A on MDS-L – A 5q Myelodysplastic Syndrome (MDS) Cell Line

Departmental Retreat

05/13 Early growth response 1 (Egr1) knock out hematopoietic stem cells are more sensitive to radiation

Departmental Retreat

03/13 Role of Egr1 family members in MDS/t-MDS (Co-author)

Edward P Evans Foundation annual Retreat

02/10 Screening Sweetpotato Cultivars as a Potential Source of Feedstock for Bio-ethanol Production

Sweetpotato Collaborators Meeting

04/11 Sweetpotato as potential source of feedstock for bio-fuel production

Association of research directors, 16th Biennial Research Symposium